**POLITECNICO DI MILANO**

School of Industrial and Information Engineering

Master of Science Course in Aeronautical Engineering


# Hybrid-electric aircraft powertrain modelling and simulation

Supervisor:
Prof. Lorenzo Trainelli

Co-Supervisors:
Prof. Carlo E.D. Riboldi
Prof. Alberto Rolando

Author:
Gabriele Poiana
Id. 863096

Academic Year 2016 - 2017

# Contents

# List of Figures

# List of Tables

# Nomenclature

| | |
|---|---|
| AC | Alternate Current |
| ACARE | Advisory Council for Aeronautics Research in Europe |
| AIAA | American Institute of Aeronautics and Astronautics |
| ATM | Air Traffic Management |
| Batt | Battery |
| BP | Battery Pack |
| BSFC | Brake Specific Fuel Consumption |
| CI | Compression Ignition |
| Cmd | Commanded |
| CPT | Cockpit |
| DC | Direct Current |
| ED | Electric Drive |
| FADEC | Full Authority Digital Engine Control |
| FC | Fuel Cell |
| FMS | Flight Management System |
| GBX | Gearbox |
| HEV | Hybrid Electric Vehicle |
| HMI | Human Machine Interface |
| ICE | Internal Combustion Engine |
| ISA | International Standard Atmosphere |
| PEM | Proton-Exchange Membrane |
| PMCD | Power Management, Control and Delivery |
| Pwr | Power |
| RAeS | Royal Aeronautical Society |

| | |
|---|---|
| RAT | Ram Air Turbine |
| SI | Spark Ignition |
| SOC | State Of Charge |
| SOFC | Solid Oxide Fuel Cell |
| TAS | True Airspeed |
| TGM | Thrust Generation Module |
| Trq | Torque |
| UAV | Unmanned Aerial Vehicle |

# Introduction

The aeronautical sector is experiencing a phenomenal growth in the development of new hybrid powertrain configurations and other associated technologies for different applications. The interest is driven by new technological enhancements that allow to employ other energy and power sources different from traditional engines. This introduces an increment in complexity of new propulsion systems and dependence on embedded controllers. The results are in an increased difficulty in predicting interactions among various vehicle components and a modification to the classic approach to aircraft design.

The motivation of this work is to allow an accurate prediction of the behaviour of a hybrid-electric powertrain with respect to the exploited configuration and its components. This can be achieved providing a specific tool that can be used in aircraft design to model and simulate a hybrid-electric powertrain. In this way, it is possible to study different configuration alternatives, highlighting advantages and disadvantages for a given architecture, in order to find the best solution for a particular aircraft. Moreover, the possibility to investigate effects in changing system parameters on aircraft performance could be of interest, since classic design approaches cannot be applied as such to hybrid-electric airplane sizing.

The main practical objective of this activity is to develop a tool that allows to simulate hybrid-electric powertrains, considering different configurations and parametric studies. In particular, given a few parameters related to aircraft design, such as flight profile and characteristics of subsystem components, the target is to simulate each sub-part of the considered aircraft power-plant to provide an assessment about aircraft design or to find the best configuration for a specific mission. Starting from required power during each flight phase, the simulator provides an estimate of output power and consumptions of the system, from take-off to landing. Since several system configurations can be exploited, the tool has to be developed considering a large variety of sub-cases and applications. For this reason a modular arrangement has to be considered in order to give the model the possibility to adapt to different situations. Finally, the tool could be inserted in a design process: the opportunity to interface this work with preliminary sizing and other simulation tools, related to overall aircraft parametric analyses, has to be taken into account during its development.

Several attempts to model an entire system in a development environment can be found in the literature, both in the aeronautical and automotive fields. For example, in [1] the goal of the project is to determine the feasibility of hybrid-electric propulsion over a wide range of aircraft scales and to build a hybrid-electric demonstrator aircraft. The theoretical assessment of analysing hybrid-electric powertrains for the mid-scale aviation sector is conducted within a real-time simulation environment consisting of several linked software packages, including the well known X-Plane, Matlab Simulink, and JavaProp. X-Plane provides a realistic flight model, JavaProp models the propeller performance while Matlab Simulink represents the core of the simulation. However, even if a detailed flight model is considered, the simulator is not easily applicable to other aircraft. The proposed tool, instead, aims to provide a general configuration capable of including different aircraft architectures and subsystems that can be changed according to the system to be modelled. Another example of an already existing project

is the one presented in [2], in which the best flight performance of a specific hybrid aircraft is evaluated varying the relevant mission parameters, such as range, cruise altitude, speed and the amount of available energy, in terms of batteries and fuel. Then, in the second part, a hybrid airplane simulator, conceived to implement different mission profiles and to include pilot effects on power management by adopting a human-in-the-loop approach, is presented. Even in this case a very specific application is considered. Power management of a UAV hybrid-electric system is described in [3]. In particular, three electric propulsion systems with different power sources, such as solar cells, fuel cells, and batteries, are considered. Interestingly this article shows a comparison between different control logics and models used for simulating the systems. However, the presence of an internal combustion engine is not considered and a general configuration that can be exploited in every case is not given.

Also the automotive sector is focusing its research in hybrid-electric propulsion: different control logics that can be used in a parallel hybrid-electric truck are presented in [4] in order to find an optimal control strategy. Even in this case the proposed model is related only to a specific configuration. Another industrial vehicle is discussed in [5]: a model for a series hybrid configuration is shown alongside with control strategy to maintain engine in its high efficiency operating region. In Simulink *Powertrain Blockset* examples about hybrid-electric vehicles have been recently introduced [6]: in this case very detailed models are used but no generalities about the systems are provided. Moreover, the proposed models are quite difficult to modify and to introduce additional features.

The proposed model aims to provide the possibility to explore different vehicle configurations, thanks to an interface that can be dynamically modified basing on user input. Also, the possibility to introduce different models and additional features in the future is provided by a clear arrangement and standardised input/output relations. In addition to this, the opportunity to exploit different control logics has to be considered: the model has to be developed with in mind the possibility to add several controllers to investigate alternative solutions.

## Structure of the work

**Chapter 1: Overview to hybrid-electric vehicles** An overview about hybrid-electric vehicles is presented, particularly focused on aircraft. Different aspects of each possible hybrid configuration are detailed, followed by a short review of hybrid-electric and all-electric aircraft and UAVs.

**Chapter 2: Powertrain configurations** After the general overview presented in the previous chapter, in this part a possible scheme of the system model is proposed. In particular, a general structure that can group, with minimal changes, all the possible hybrid configurations is researched. Then, different applications of the general architecture are presented to show relations between subsystems in each configuration.

**Chapter 3: Powertrain modelling** The proposed model of the whole system, developed in Simulink, is presented first in a general overview and later in a detailed view of each component, discussing about models, issues and implementations. This section can be considered as an user guide that can be useful in understanding exploited models and simulation results.

**Chapter 4: Applications** Three applications, based on conceptual aircraft designs developed during Politecnico di Milano Aircraft Design Course over the years, are implemented in order to prove usability and to show features of the tool. In particular, a series hybrid-electric

four seat aircraft, named Hybris, a parallel configuration, Flybrid, and also an all-electric system, Project A, are presented and implemented to provide an estimate of their power-plant characteristics. Of particular interest is that a tool designed to investigate hybrid-electric aircraft can be exploited in all-electric aircraft design.

**Chapter 5: Conclusions** After a summary of the whole work, conclusions in the form of a critical analysis, faced problems and possible future developments of this tool are discussed in the final part.

# Chapter 1

# Overview to hybrid-electric vehicles

In recent years, the interest of the aviation community for the application of novel propulsion technologies to aircraft of any size has significantly grown [7]. This has been built up by several issues encountered with most widespread combustion engines.

Fuel economy is the primary issue for both owners of smaller private aircraft and for airlines, due to the unpredictability of fuel prices and the fact that combustion efficiency appears to be difficult to improve without a major technological breakthrough. More in detail, considering a projection period from 2017 to 2050, jet fuel consumption is expected to grow more than any other transportation fuel, rising 64%, against a background of rising fossil fuel prices. This is due to air travels that will double from 0.9 trillion revenue passenger miles to 1.9 trillion revenue passenger miles [8]. Gas turbines and internal combustion engines are employed as prime movers for aviation applications and are usually fed with hydrocarbon fuels because of their superior energy density with respect to other solutions. However, thermal engines have a lower efficiency and power-to-weight ratio when compared to electric motors [9]. In this context, the rekindling of interests in electric vehicles, and more in general in hybrid-electric vehicles, started at the outbreak of the energy crisis and oil shortage in the 1970's [10] and it is continuously growing.

Secondarily, noise pollution around airports is generally still too high. For smaller General Aviation airfields, this results in difficult negotiations with the local communities, often producing heavy traffic limitations and which constitute an obstacle to the development of Sport Aviation [11]. Furthermore, on-board comfort, especially for smaller aircraft, is usually lower due to high level of noise mainly produced by engine [12]. Noise emissions represent a cost for airlines, as most municipalities around larger airports apply fees proportionate to the noise footprint of aircraft operations on the ground and during first phases of flight [13].

Another important issue is environmental pollution. Earth's global surface temperatures in 2017 ranked as the second warmest, after 2016, since 1880 [14], continuing the planet long-term warming trend. Globally averaged temperatures in 2017 were 1.62 degrees Fahrenheit (0.90 degrees Celsius) warmer than the 1951 to 1980 mean, according to scientists at NASA's Goddard Institute for Space Studies (GISS) in New York. In a separate, independent analysis, scientists at the National Oceanic and Atmospheric Administration (NOAA) concluded that 2017 was the third-warmest year in their record. The minor difference in rankings is due to different methods used by the two agencies to analyse global temperatures, although over the long-term the agencies records remain in strong agreement: both analyses show that the five warmest years on record all have taken place since 2010. This phenomenon has led agencies, such as ACARE (Advisory Council for Aviation Research and Innovation in Europe) and European Commission, to work in order to reduce emissions, that are accused to be one of the main actors involved in global warming. In aeronautical field several possibilities are given

in order to achieve this target, as presented in Flightpath 2050 [15], in which the following main topics are presented in the following list:

- Strong reduction of gas emissions and noise pollution with respect to levels computed in the year 2000.
- To allow 90% of passengers in EU borders to travel 4-hours-door-to-door.
- To transform Europe in a centre of excellence for what concern alternative and sustainable fuels, research and development.
- To develop a new ATM system that can operate 25 millions of flights per year using more efficient routes.

Also NASA has set aggressive fuel burnt, noise, and emission reduction goals for a new generation (N+3) of aircraft targeting concepts that could be achievable in the 2035 time frame. Several N+3 concepts have been formulated, where the term "N+3" indicate aircraft three generations later than current state-of-the-art aircraft, "N". Dramatic improvements need to be made in the airframe, propulsion systems, mission design, and air transportation system in order to meet these N+3 goals [16].

It is clear that these targets can not be achieved through marginal improvements in turbine technology or aircraft design. Rather, disruptive technologies and more innovative aircraft must be considered. In this context new powertrain solutions such as hybrid-electric or all-electric systems can be appealing. Avoiding greenhouse gas emissions translates back into reducing fuel combustion as much as possible: the most promising road toward this goal is the electrification of transport. Electric motors, which are not subjected to Carnot limit, are much more efficient than combustion engines, and instantly reduce local emissions down to zero in the case the vehicle is entirely battery-powered [17]. An hybrid-electric solution allows to reduce environmental pollution with the possibility of travelling longer ranges with respect to all-electric aircraft, using two kind of different propulsive systems in the same power-plant: combustion engines and electric motors. For this reason nowadays hybrid-electric vehicles are recognized as one the most promising technologies in significantly reducing the petroleum fuel consumption, toxic and greenhouse gases emissions.

As proposed by Technical Committee 69 (Electric Road Vehicles) of the International Electrotechnical Commission, an Hybrid Electric Vehicle (HEV) is a vehicle in which propulsion energy is available from two or more kinds or types of energy stores, sources or converters, and at least one of them can deliver electrical energy [10]. Traditionally, HEVs were classified into two basic kinds: series and parallel. The key feature of the series hybrid is to couple the engine with the generator to produce electricity for pure electric propulsion, whereas the key feature of the parallel hybrid is to couple both the engine and the electric motor with the transmission via the same drive shaft. So, in a serial hybrid the node is electrical, while in a parallel hybrid the node is mechanical [17]. These architectures give more flexibility in terms of power management and they can provide a significant reduction of environmental impact, increasing safety at the same time, with respect to a traditional powertrain. In fact, the presence of two independent energy sources introduces a redundancy and, in addition, an electric motor is more reliable than a piston engine [2]. The integration of actuators with power electronics not only can improve the overall system reliability but also reduces costs and sizes [18]. Recently, with the introduction of some HEVs offering the features of both the series and parallel hybrids, the classification has been extended to four kinds: series, parallel, series–parallel and complex hybrid, as discussed in the following.

Significant improvement have been made in electric propulsion: performance of electric motors and batteries are quickly increasing, as one can see in everyday life, accelerating the progress and the usability of this technology also in aeronautic segment. This led in a massive investments in more-electric aircraft in the last years [19], which main purpose is to improve engine overall fuel efficiency by minimizing the amount of bleed air taken from other subsystems, such as de-icing, through their electrification, and the possibility to have all-electric aircraft serially-built [20]. However, electric energy storage systems still do not allow the same performance of traditional power-plants, even if an all-electric solution, thanks also to the powerful characteristics of electric motors, allows to achieve zero emissions during flight and a very high reduction in noise produced by aircraft. However in this case an evident limit of electric propulsion is given by energy storage: the specific energy of batteries is much lower than the one provided by fossil fuel, and so a shorter range is reached considering the same weight. Actual batteries used in automotive applications can reach up to 150 Wh/kg [21], while standard fuel has a specific energy equal to 13000 Wh/kg. Moreover, batteries, differently from fuel, do not reduce the weight during consumption, providing additional weight along mission profile, influencing aircraft performance and design in terms of centre of gravity balance. Finally, reduced battery life cycle can be an important problem of exploiting all-electric aircraft in terms of operational costs and refuses.

The hybrid-electric powertrain has been introduced as an interim solution before the full implementation of electric-vehicles and can be considered as a trade-off between all-electric and traditional systems. Although recently established in the automotive sector, hybrid-electric propulsion systems are still in early stages of development for the aviation field, with the potential for improved performance over current propulsion systems, applicable from small to larger-scale aircraft, increasing aircraft fuel economy, lowering emissions, reducing take-off and landing noise, increasing system reliability, and improving operational capabilities [22] by combining an electric motor and an internal combustion engine in such a way that the most desirable characteristics of each can be utilised. An important plus of these systems is that they require only little changes in the energy supply infrastructure: it exists the possibility to convert a traditional aircraft into a hybrid-electric system. The key drawbacks of these new powertrains are loss of the zero emission concept and increased complexity. Nevertheless, these systems are vastly less polluting and have lower fuel consumption than traditional power-plants that allow the same range. These merits are due to the fact that the engine of the HEV can always operate in its most efficient mode, yielding lower emissions and lower fuel consumption. Moreover, hybrid-vehicles can operate as a pure electric aircraft in a zero emission operative condition, possibly during take-off and landing. It is becoming a consensus that hybrid-electric vehicles are not only an interim solution for implementation of zero emission vehicles, but also a practical solution for commercialization of super-ultra-low-emission vehicles [10].

In the near future this technology could be also applied to unmanned aerial vehicles (UAVs) used for military, homeland security, and disaster-monitoring missions involving intelligence, surveillance, and reconnaissance (ISR) [3]. Thanks to hybrid and electric-only modes, the potential benefits in this field include increased time on station, longer range, and reduced signature. Moreover, electric-only operation eliminates exhaust emissions that could interfere with chemical-detecting sensors [23].

A generic hybrid-electric powertrain can be composed by several components disposed in different configurations. The generalised system can include:

- An engine and its fuel.
- Electrical energy storage system, e.g. battery pack.
- Electric drives (EDs) that behave as motors and/or generators.

- Electrical bus to route electrical power.
- Mechanical bus, e.g. a transmission, to route power between the propeller and other mechanical sources and sinks.

These components and their reciprocal connections are similar to the one employed in automotive applications. However, due to the sensitivity to size and weight and different reference missions introduced in aircraft applications, the benefits and drawbacks of each configuration are magnified [24].

Finally, it is possible to classify a hybrid system under two aspects: the first one is related to the configuration type, such as series and parallel architectures, as detailed in the following sections, while the second one is related to how much of the power required for propulsion is provided by which component. So it is possible to define the degree of hybridisation as:

$$H_P = \frac{P_{el}}{P_{tot}},$$

where $P_{em}$ is the maximum installed electric power at drive shaft while $P_{tot}$ is the total power installed. However this parameter doesn't provide information about energy storage. For this reason a second hybridisation parameter is here introduced and defined as:

$$H_E = \frac{E_{el}}{E_{tot}},$$

in which $E_{el}$ is the electric energy onboard while $E_{tot}$ is the total available energy. In this way it is possible to identify hybrid-electric power systems in a two-dimensional parameter space presented in Figure 1.1. The origin corresponds to traditional powertrain, in which shaft power is provided by ICE and the energy is stored only in the form of fuel. On the other side, in the point (1,1) are located purely electrically-powered vehicles with only batteries as onboard energy carriers. Considering the previous definitions of degree of hybridisation, it is possible to conclude that pure serial hybrid powertrains are placed in the point (0,1): in this case the propeller is driven by an electric motor that is fed only from electricity provided by fuel through an engine and a generator. In general, series hybrid power systems lie in the line between points (0,1) and (1,1). In the diagram it is possible to note an unfeasible region of the parameters space in the context of transport systems: it has no sense to carry more energy in the electrical form than the system is able to convert into power to the drive shaft with an electric motor [17]. The rest of the diagram is populated by parallel hybrid-electric systems. A detailed differentiation between configurations is provided in the following.

## 1.1 Series hybrid

The series hybrid powertrain, Figure 1.2a, has its foremost advantage in the fact that the engine is mechanically decoupled from the load and it can operate in its high efficiency speed and torque region, while its main disadvantage is that mechanical power from the engine is transformed twice, from mechanical to electrical in the generator and from electrical to mechanical again in the electric motor [5]. The converted electricity either charges the battery or can be directly used as input of the electric motor to move the propeller. Because of the absence of clutches throughout the mechanical link, this configuration has the definite advantage to locate the engine-generator set in a flexible way, since only electrical links are needed from generator to batteries or other electric devices. Although it has an added advantage of simplicity of its

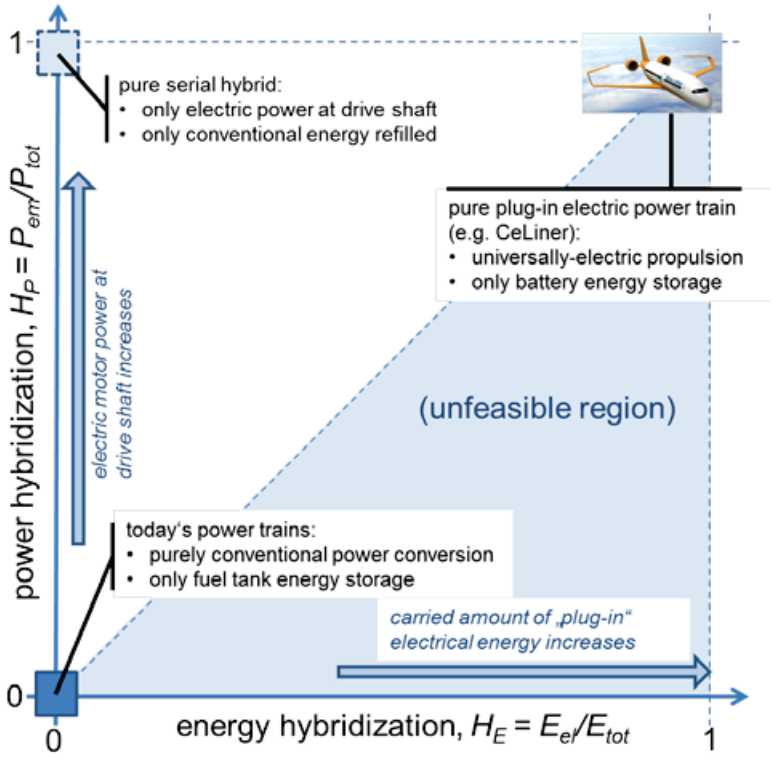


Figure 1.1: Power vs energy degree of hybridisation, [17]

drive train, it needs three propulsion devices: the engine, the generator and the electric motor that have to be sized for the maximum sustained power [10].

During high energy demanding phases, both the engine (through the generator) and battery deliver electrical energy to a power management device, which then drives the electric motor. At light load, the engine output could be greater than the one required and so the surplus generated electrical energy can be used to charge batteries. Batteries can be charged by the engine even when the aircraft comes to a complete stop. This strategy can be used as backup power source of energy for the batteries if no charging station or fully charged batteries are available when the aircraft has landed. However, this feature has no sense considering that the aim is to reduce pollution when the aircraft is near the field

Summarising, a general strategy consists in battery packs that provide additional energy during the most power demanding flight segments (take-off and climb), while during cruise the generator, coupled with the engine, can give sufficient power for both powering the electric motor and charging batteries [2]. The basic power electronic components for a typical series hybrid vehicle system are a converter, needed to condition the alternator output to DC for charging the batteries, and an inverter, used for converting the DC to AC in order to power the electric motor, if it is not a DC motor. Other DC–DC converters and inverters are required according to other aircraft systems requirements [18].

## 1.2 Parallel hybrid

In a parallel hybrid-electric powertrain the engine can deliver torque directly to the propeller without energy transformations. The major disadvantage of a parallel configuration is that in general the engine can not always work in its high efficiency operating region because it is still mechanically coupled to the load. The gearbox, in this case, plays a fundamental role. A

scheme of this type of hybrid-electric configuration can be found in Figure 1.2b.

The parallel HEV allows both the engine and electric motor to deliver power to the power shaft: the two components are coupled to the shaft via two clutches. In this way the propeller torque may be supplied by the engine alone, by the electric motor or by both, depending on the situation. Better than series, parallel hybrid needs only two propulsion devices: the engine and the electric motor. Another advantage over the series case is that a smaller engine and a smaller electric motor can be used to get the same performance until the battery has charge [10]: during high load flight conditions, both the engine and electric motor proportionally share the required power, while during lower load conditions, such as cruise, the engine solely supplies the necessary power to propel the vehicle. In this way lower emissions and noise pollution are produced during take-off and climb thanks to the lower power that the engine has to perform. Also, since both the engine and electric motor are coupled to the same drive shaft, the batteries can be charged by the engine via the electric motor that acts as generator when the aircraft is at light load. As in all the other configurations, batteries can be recharged when the propeller is in a wind-milling operational condition, decoupling the engine from the shaft. The mechanical bus generally consists of a transmission having a changeable gear ratio with output connected to the propeller and inputs from the engine and electric motor. Further, there is either a clutch in these power flow paths to couple/decouple them from the transmission [22]. The basic power electronics required are the same of the series hybrid.

## 1.3 Series-parallel hybrid

This configuration incorporates the features of both the series and parallel HEVs, involving an additional mechanical link compared with the series hybrid and also an additional generator, and its related mechanical and electrical link, with respect to parallel hybrid, as one can see in Figure 1.2c. Although possessing the advantageous features of both the series and parallel systems, the series-parallel HEV is relatively more complicated and costly. Similar to a series hybrid, this configuration is installed with two electric drives, one primarily for motoring, connected to propeller shaft, and one primarily for generating. In contrast to series configuration, and similar to the parallel architecture, both the engine and the electric motor can supply power to the propeller. The motoring ED can receive power directly from the generating one, driven by the engine, thus avoiding battery usage [22].

In this configuration there are many possible operating modes to perform its power flow control [10]. At very light load, for example while taxiing, the battery solely provides the necessary power to propel the aircraft, while engine is switched off. During full throttle, both the engine and electric motor proportionally share the required power. During cruise, the engine provides the necessary power to fly, while the motoring electric motor, connected to the shaft, can provide power, can be switched off or can act as generator, depending on the situation. The presence of a second generator that directly links engine and batteries through a power management device can be exploited to charge the batteries avoiding using the other ED as generator, leaving all the shaft power available for the propeller. Alternatively, it is possible to employ the electric motor to propel the shaft while the other electric drive recharges batteries and produce electricity to move the first one, if this strategy is considered convenient. Usually a planetary gear is employed to split the engine output, hence to move the propeller and to drive the generator. As the series hybrid, when the aircraft is at standstill, the engine can maintain driving the generator to charge the battery.

## 1.4 Complex hybrid

The key difference, referring to 1.2d, with respect to the series-parallel configuration is due to the bidirectional power flow between ED and engine, differently from the unidirectional link related to the generator in the series-parallel hybrid. Bidirectional power flow allows for more versatile operating modes, such as the three propulsion power (due to the engine and two electric motors) [10], exploiting all the series-parallel features and adding the possibility of supporting the engine with an electric motor directly connected to it through a planetary gear, while the second electric motor is coupled to the shaft. In this way it is possible to sub-size all the motors. However this leads to an increase in weights and in complexity of the system that brings this configuration impractical for aviation purposes.

## 1.5 Configuration summary

Each hybrid-electric powertrain configuration has advantages and disadvantages in terms of mass, cost, and power management complexity.

The series and series-parallel architectures normally have greater mass than the parallel one for the same propeller power. This is because the former two configuration have multiple EDs versus the single one used in a parallel arrangement. However the increasing in complexity of the parallel gearbox could reduce this advantage. Also, both the motoring and generating devices in the series configuration must be sized to provide the maximum propelling power, including efficiency losses in the numerous power conversions needed, while in the parallel configuration the ED is required to provide the difference in power between nominal engine output and maximum required power. Finally both series-parallel and complex systems require a power split device unlike the parallel configuration.

As for cost analysis can follow from the mass comparison: additional components as well as larger sized components will normally lead to greater powertrain costs. Thus, it is expected that the parallel configuration will be less costly than other architectures. Furthermore, power management complexity increases with the number of potential power flow paths. The series configuration has the least number of these paths, while the most number of potential flows can be found in the series-parallel and complex systems. Hence, power management complexity, in increasing order is expected to be series, parallel, series-parallel and complex configuration.

System mass, cost, and power management complexity are a few of the considerations for hybrid propulsion sizing and implementation. Terrestrial vehicles, which are not as mass-sensitive as aircraft, are currently trending towards a series-parallel architecture, while aircraft applications are trending toward the parallel one [22].

## 1.6 State of the art

Hybrid-electric or all-electric aircraft that can be found nowadays are usually prototypes. In particular, an aircraft that uses only batteries is very limited because of actual technologies, even if this category of airplane presents zero-emissions during flight and a very reduced noise pollution.

Hybrid-electric powertrains for UAVs are under development at the University of Colorado [25], in cooperation with TIGON EnerTEC, at the Queensland University of Technology [26] and at the U.S. Air Force Research Laboratory [27]. Each research group considers a different mechanical layout for the hybrid-electric powertrain, covering a range of engine types and different clutches [9].

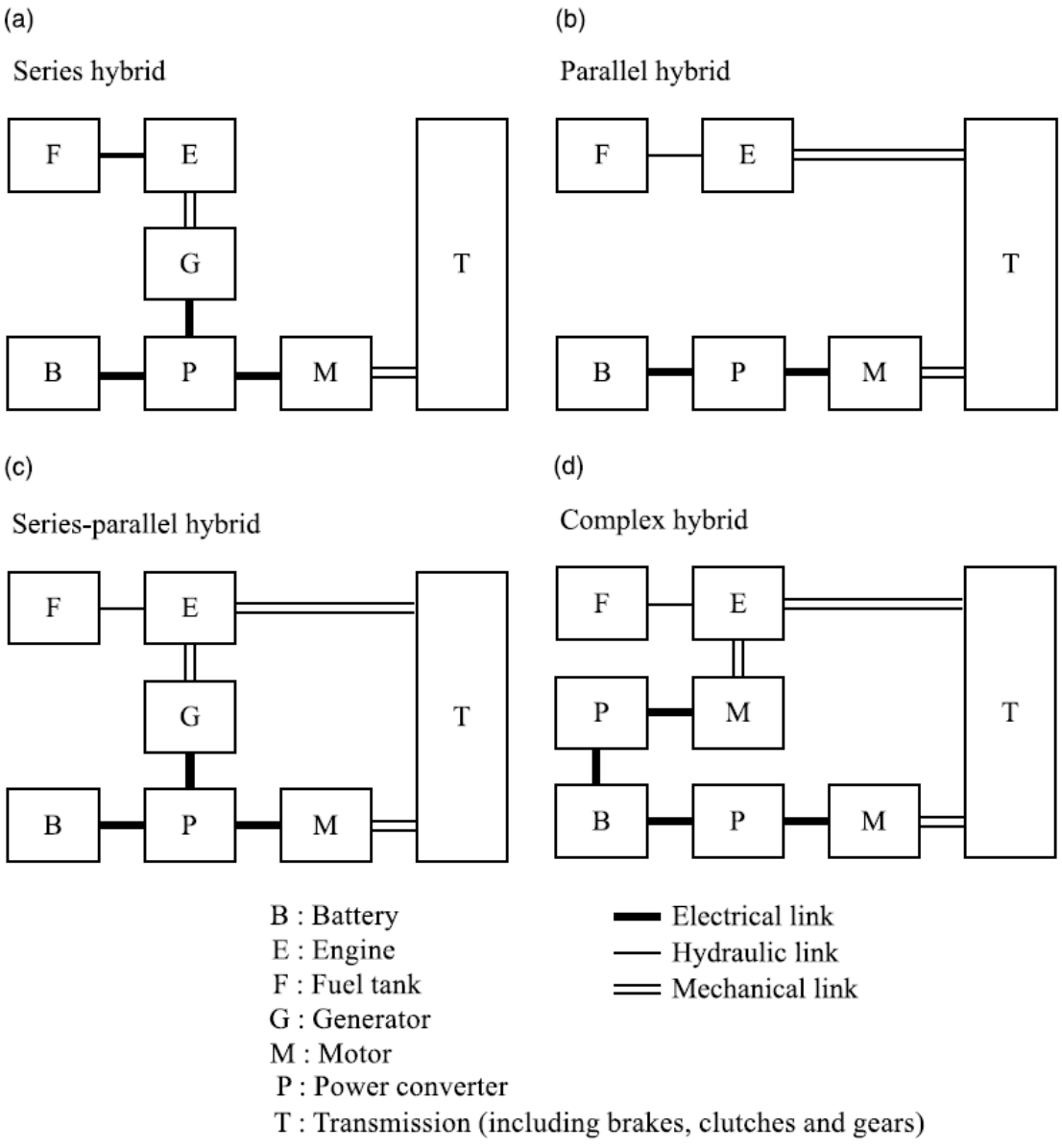


Figure 1.2: Classifications of hybrid-electric powertrains, [10]

In terms of hybrid-electric midscale demonstrators, the aircraft population is constantly growing. In Paris Air Show Le Bourget 2011, DA-36 E-Star made its debut as world's first series hybrid-electric aircraft. It is realized by a collaboration between Diamond Aircraft, European Aeronautic Defence and Space Company (EADS), and Siemens AG, using a series configuration to investigate the scaling potential of hybrid powertrains from the midscale to the large-scale sector. The airplane propeller is powered by a 70 kW electric motor produced by Siemens. Electricity is supplied by a small Wankel engine from Austro Engine through a generator. A Siemens converter supplies the electric motor with power from the battery and the generator. Fuel consumption is very low since the combustion engine always runs with a constant low output of 30 kW: the aircraft, which was modelled off of the HK36 Super Dimona, relies on a battery to provide the extra power needed for take-off and climb, while recharges it during cruise. The intended aim of the partnership is to cut fuel consumption and emissions by 25%, compared to today's most efficient technologies, making air travel more sustainable [28]. A second generation of this aircraft has been presented in 2013. The same airplane has been used in the Boeing fuel cell demonstrator shown in Figure 1.3a. The aircraft flew at an altitude of 1000 m above sea level for 20 minutes at a speed of around 100 km/h powered solely by fuel cells, becoming then the first manned aircraft to do so in history.

Parallel powertrains are used in the hybrid Alatus and in the EcoEagle, but neither of these has the capability to recharge batteries during flight. The hybrid Alatus was the first hybrid-electric demonstrator and was developed by Robertson at the University of Cambridge in 2010. This demonstrator used a 2.8 kW four-stroke ICE, a 12 kW brushless motor, and lithium-polymer (LiPo) batteries with a capacity of 2.3 kWh. The EcoEagle used a 74.5 kW four-stroke ICE and a 29.8 kW electric motor and conducted its first maiden flight in 2011 [9].

At the larger scale, hybrid-electric or purely electric concepts for airliners are rarely discussed in the literature and represent new propulsion concepts in the aviation sector. However in recent times several studies are in progress: NASA supported a comprehensive study led by Boeing called the Subsonic Ultra Green Aircraft Research (SUGAR) to design new concepts that would meet the N+3 goals discussed before. After studying different concepts with advanced propulsion systems, aerodynamics and structures, it was shown that an aircraft with hybrid propulsion would come close to meeting NASA N+3 goals. An outcome from the study is a concept named SUGAR Volt, shown in Figure 1.3c, which integrates a next generation gas turbine engine with an electric motor powered by batteries. It was concluded that a parallel hybrid system of electric motor and gas turbine engine would provide the greatest reduction in fuel burn. The team estimates that fuel savings for commercial aviation can reach 70% through hybrid systems. The project also included versions that utilized pure electric power or fuel cells for its propulsion system.

Distributed electric propulsion is another strategy that has been studied by EADS and Rolls-Royce: this concept, named E-Thrust [29], has several electrically powered fans distributed along the wing span and one advanced gas turbine unit to provide electrical power to the fans. Another example of distributed propulsion is NASA X-57, presented in Figure 1.3b.

After the partnership between Airbus and Siemens that led in 2014 to E-Fan project, an all-electric prototype two-seater which target market was intended to be pilot training, until its production was cancelled in April 2017 [30], Airbus, Rolls-Royce, and Siemens have formed a new partnership which aims at developing a near-term flight demonstrator which will be a significant step forward in hybrid-electric propulsion for commercial aircraft. The E-Fan X hybrid-electric technology demonstrator is anticipated to fly in 2020 following a comprehensive ground test campaign, provisionally on a BAe 146 flying test-bed, with one of the aircraft four gas turbine engines replaced by a two megawatt electric motor. Provisions will be made to replace a second gas turbine with an electric motor once system maturity has been proven [31].

In 2016, the HYPSTAIR project, based on the four-seater Pipistrel Panthera airframe, became the most powerful hybrid-electric aircraft in its category by delivering 200 kW in ground testing [2]. Batteries allow Hypstair to take-off and climb in all-electric mode, being very silent and emission free in the proximity of airports.

Of course batteries are not the sole system that can be used to provide electric power: other technologies such as fuel cells and solar arrays can be used as well. The Georgia Institute of Technology demonstrated the feasibility of a small fuel-cell-powered UAV through fabrication, flight testing, and ground testing of a 500 W PEM fuel-cell powered aircraft [32]. KAIST investigated the current and voltage behaviours of an NaBH4 fuel cell through a flight test of a UAV containing a 100 W fuel cell combined with a battery [3]. Michigan State University and Adaptive Materials recorded 10 hours of flight with a SOFC fuel cell that uses propane, a hydrocarbon fuel. Recent applications of solar cells in both manned and unmanned vehicles show remarkable progress in endurance. Solar Impulse, a manned aircraft, recorded 27 hours of flight endurance, while Zephyr, a UAV from QinetiQ, recorded 2 weeks in the air. In cases involving such long endurance flights, aircraft is equipped with secondary high capacity batteries for overnight operation [3].

Zunum Aerospace, a start-up company set in Seattle, is proposing hybrid-electric powertrain technology for different sized transports. This project, sponsored by Boeing and JetBlue, aims to introduce this technology to the commercial market in the next three years with the goal of eliminating aviation emissions in twenty years with their 'hybrid-to-electric' proposal: as technology improves, the Zunum system will rely less on fuel and more on electric, with the final goal of an all-electric aircraft [33].

Thanks to recent technology enhancement, hybrid-electric and all-electric aircraft are reality for Pipistrel, a Slovenian manufacturer that can show in its portfolio three different serially-built aircraft: the Alpha Electro, shown in Figure 1.3d, a two-seat electric trainer, the Taurus Electro, the first electric two-seat motor-glider in serial production available on the market, and the Panthera, available with either electric motor, hybrid propulsion or petrol engine [34], represented in Figure 1.3e. Pipistrel, in consortium with DLR, H2Fly, University of Ulm and Stuttgart Airport, produced HY4 in 2016, the world's first four-seater passenger aircraft powered solely by hydrogen fuel cell system and electric propulsion. The aircraft, depicted in Figure 1.3f, was built connecting two fuselages of the Pipistrel Taurus. It has a maximum speed of 200 km/h and can fly up to 1500 km.

Pipistrel is currently leading an European project alongside Politecnico di Milano and other industries and universities named Modular Approach to Hybrid-Electric Propulsion Architecture (MAHEPA). The project goal is developing propulsion technology for future small and regional passenger airplane, capable of exploiting the existing small local airports to provide micro-feeder service to larger hubs and eliminating gaseous emission impact on surrounding communities. The project will develop new components in a modular way to power two four-passenger hybrid electric airplane scheduled to fly in 2020. The main result of MAHEPA project will be novel, modular and scalable hybrid-electric powertrains capable of running on alternative fuels or on hydrogen with zero emissions [35].

Also Politecnico di Milano students, thanks to Aircraft Design Course, are facing to hybrid-electric and all-electric airplane: Flybrid, Flynk [36], Hybris [37], Project A are conceptual projects of these types of aircraft.


(a) Boeing fuel cell demonstrator

(b) NASA X-57

(c) Boeing Sugar Volt

(d) Pipistrel Alpha Electro

(e) Pipistrel Panthera

(f) HY4

Figure 1.3: Examples of hybrid or all-electric aircraft

# Chapter 2

# Powertrain configurations

## 2.1 General configuration

After an overview of possible architectures that can be exploited in an hybrid-electric powertrain of an aircraft, presented in the previous chapter, a generic block scheme is developed in order to reproduce it in a computational environment. The specialisation in hybrid series, parallel and other configurations are shown in the following, to prove that one basic architecture can be exploited easily and with minimal changes over each configuration. Considering the differences between configurations presented in Chapter 1, a possible representation of a generic powertrain, in the form of block diagram, can be found in Figure 2.1. In the scheme, blocks are depicted and linked together to point out mechanical (black), hydraulic (blue), electric (red) and logical (green) relations. Possible linkage are shown by arrows: some of them present a two-way link, meaning that the considered flow is bidirectional, while others represent only a single-way connection. Links are purely representative of relations between blocks: in this phase detailed input/output relations are not considered. Blocks related to energy reservoirs are highlighted in orange.

The diagram proposed in Figure 2.1 is composed by several blocks that are detailed in the following. It is important to note that the list presented below is not a description of features of the developed model, that instead it is presented in Chapter 3. This section can be considered as a compendium of suggestions, ideas and intentions that are pointed out in a very first stage of this work, to provide a global idea of this tool and its potentialities. This led the development of the simulator and could also be used in future improvements.

**HMI: Human Machine Interface** This block represents all the Human Machine Interface (HMI) and so it consists in pilot control actions and interactions between pilot and aircraft. If needed, it is possible to consider not only the requests by the pilot but all the pilot-in-the-loop model. In general the set of required power during flight, the control of operating temperatures of the systems, the selection of power sources to use in the case pilot has authority on the power controller, and so on can be defined within this block. In general a model of avionic systems is not useful since it is out of scope of this work, however their power consumption can be considered.

**FMS: Flight Management System** Here, the pilot input is filtered in order not to exceed manoeuvrability limits, loads, etc. Also the request of thrust from the pilot is modified to the one admissible by the engine, keeping it inside design and safe operating conditions. This block represents the presence of the FMS and FADEC in a traditional aircraft, providing required power needed for a safe flight to the Power Management, Control and Delivery module. Inside

this block a flight mechanics model can be considered in order to assess that the system can provide enough power to perform manoeuvrers and more in general to be compliant with the proposed flight profile. Quantities related to flight, such as density that depends on the altitude, can be computed in this block and then distributed to other blocks of interest.

**PMCD: Power Management, Control and Delivery** The PMCD is the system that controls and manages the powertrain. It basically controls power and energy sources, requiring the amount of power/energy that they have to provide. It is composed by switches and electronics that are commanded possibly by a controller based on required power, available power, power source data, future request of power (future flight profile, that comes from FMS), and so on. It has an implemented logic of operations built in order to decide what and when to do it. In addition, this device is responsible for batteries State Of Charge (SOC), e.g. requiring more power to other sources if recharging batteries is needed. Another role of PMCD is to collect and manage all the sources of voltage and current in order to distribute them to move the electric motor or dually, if the electric drive is acting as generator, to charge batteries. An inverter is used to convert direct current from batteries and fuel cell to AC to power electric motors, otherwise if a DC motor is considered, a DC-DC converter is needed. Several control strategies can be implemented in PMCD: examples can be found in Section 3.9. A possible improvement of the whole model could consist in an optimising algorithm in order to find the best control logic for the considered case.

**F: Fuel Tank** It represents the tank that contains the fuel, considering also the metering system for the residual fuel and valves, pipes and pumps needed to feed the engine, depending on the engine type. Fuel tanks are hydraulically connected to the engine, in order to feed it with fuel. Of course data communications to the cockpit, giving the pilot the possibility to check the residual fuel, to the Flight Management System, in order to make range estimates and flight profile forecasts, and to the PMCD, so that it can compute the best power management strategy based on available fuel, are considered but not displayed with the intention of providing a better readability of the block diagram, focusing only on basic and primary links.

**ICE: Internal Combustion Engine** With the term ICE it is considered whatever combustion engine is accounted for in the HEV, doesn't matter it consists in a piston engine or in a gas turbine. Depending of the configuration used, ICE provides power to the propeller and/or to the generator. Even if in the scheme is not graphically represented, the engine is linked directly also to FMS/FADEC, in order to protect its operating condition, and also to cockpit, to inform the pilot about its parameters of interest. If a planetary gear or similar device is needed to split the output power to feed both mechanical shaft to propeller and the generator, it is modelled within this block. The ICE is connected mechanically to the power shaft and to one electric drive, that can be exploited as generator in the series and series-parallel scheme or as motor in case of complex hybrid. In general, more than one engine can be considered, depending on the configuration used. Of particular interest is the possibility of considering different types of ICE, reciprocating engine or gas turbine, to find the best solution for a given powertrain.

**ACP: AC Plug-In** This subsystem models the presence of an external AC source of electric power that can be used to charge aircraft batteries. Considering the plug-in for charging batteries when the aircraft is on ground, an AC–DC converter with power factor correction and a programmable digital controller with a proper voltage–current profile are needed. This

block could be useful for example in case it is of interest to investigate about time required to charge batteries.

**BP: Battery Pack** In this block batteries are modelled. The state of charge is continuously updated depending on the situation and the voltage/current profiles are computed. Depending on the flight phase, the battery pack can discharge or charge, following one of the possible logical flows exposed in Chapter 1. It is possible to model also energy and power losses due to batteries life cycle and efficiencies. A DC-DC converter is considered in order to couple battery voltage to the electrical bus one. Batteries are connected directly with PMCD that is responsible of their SOC. Data-link to HMI and FMS to present battery SOC are prominent but not visualized in order to simplify the diagram.

**H2, O2: Fuel Cell Tank** This box represents the tanks needed for the fuel cell: the hydrogen tank and the oxygen one. In this blocks are also contained all the systems needed to provide the fuel cell the correct quantities of reagents through an hydraulic link. In the same way as the fuel tank, links with HMI, FMS and PMCD to provide status and request to supply fuel to FC are not shown. Of course, if needed, other combination between oxidizer and fuel can be considered.

**FC: Fuel Cell** The fuel cell is modelled inside this block. If the FC is not present in the considered powertrain it is possible to switch off this box. The fuel cell provides current and voltage that could be used to move directly the electric motor or to recharge batteries, depending on the control logic implemented in PMCD. An electrical bus connects fuel cell to PMCD. Fuel cell stack output voltage is conditioned to be compatible with the battery one using a power conditioner, which could be a step-up or step-down converter, depending on the voltage levels of the fuel cell and of the battery [18]. The FC status can be displayed in HMI and be available to FMS through a proper data-link. It is important to note these devices in general are characterised by a slow dynamic and so a system with a faster dynamic to be placed in parallel to fuel cell, such as a capacitor, is required to cover fast transients.

**C: Capacitor** Capacitors are widely used in electric devices and in electric power transmission systems because they stabilize voltage and power flow. Also, an ultra-capacitor is generally connected across the fuel cell system to provide supplemental power and for starting the system [18]. It can be used as an accumulator of power that can be exploited during transients and temporary power losses since it is connected directly to PMCD.

**AP: Auxiliary Power** Other power/energy sources, such as solar arrays and emergency devices (RAT), can be modelled inside this block. Solar arrays are considered as an auxiliary power source since they can not provide enough power, for the actual technologies, to be employed as primary power source. Moreover, the provided power is subjected to several external factors such as solar irradiation, panels orientation, ambient temperature and so on, as detailed in [38, 39]. For these reasons, solar arrays can not be considered as a primary power source. All electronics and utilities needed to the considered system to perform correctly take place in this block. An electrical connection links up AP to PMCD, while a data bus relates AP to FMS and HMI.

**OS: Other Systems** Other aircraft systems that are not considered in the powertrain model are represented in this block. The aim is to take into account voltage and current transfor-

mations, considering power losses, and the power consumption of these systems, such as air conditioning and pressurization, that in general can not be considered negligible. Electrical and data links connect this block to PMCD and FMS/HMI even if they are not displayed. In this block DC-DC converters and inverters needed to power the considered electric systems are considered.

**ED: Electric Drive** This module represents both an electric motor or a generator, depending on the situation. When ED acts as motor, it receives voltage and current as inputs from PMCD and produces a torque. On the other side, when it is acting as generator, this device is moved in order to produce a current. On one side there is an electrical connection between PMCD and ED, while on the other one there is a mechanical link, necessary to move a shaft or to be moved by the shaft. This component can be a DC or AC system, synchronous or asynchronous, mono-phase or multi-phase, depending on the powertrain considered. The proposed model for this block has to take into account the differences between these components.

**GBX: Gearbox** All the equipment used to connect the propeller shaft to ICE and/or ED are modelled in this block. Depending on the architecture used, it can be simply a speed reducer/multiplier or a direct link in the case of series hybrid. It is composed by clutches in order to couple ICE with the ED in case of parallel hybrid. A correct model of power losses in gearbox is crucial if a choice between different architectures has to be made.

**TGM: Thrust Generation Module** In this block systems used by the aircraft to generate thrust are modelled. The thrust device can be a propeller or a ducted fan as well and all its parameters, e.g. efficiency, are computed within this module. The presence of only one box doesn't mean that only one propeller is available in the overall scheme: depending on the situation, this block can contain multiple propeller, even if a connection one to one between propellers and motors/engines is considered. Also distributed propulsion, concept related to a purely serial architectural arrangement [40], can be considered in this tool.

## 2.2 Exploiting configurations

Starting from the general system configuration of Figure 2.1, it is possible to specialise the block diagram in currently exploited configurations such as series, parallel, series-parallel and complex hybrid.

By eliminating the link between the combustion engine and the gearbox and considering only the connection from ICE to PMCD, it is possible to obtain a series hybrid powertrain, presented in Figure 2.2. In the figure a two-way link between ICE and PMCD is depicted: this represent the possibility of using the ED in the middle as starter for the engine. In the series hybrid case the gearbox is simply a rotating speed reducer or multiplier, if needed: electric motors can also directly drive the propeller. Of course the presence of capacitors, auxiliary power sources and fuel cells can be added or eliminated depending of the considered system.

On the other side, removing links between ICE and PMCD, and so the ED in between, it is possible to obtain a pure parallel system, as presented in Figure 2.3. In this case the gearbox is more complicated than in the previous configuration since a system of clutches and other components are needed to couple the rotating speed of the combustion engine to the one of the electric motor, since a single shaft is connected to the propeller. The possibility to use the ED to move the shaft and so starting the engine could be considered. If more than one propeller is considered, more than one engine and electric motor have to be taken into account

in the system: in general, in a parallel architecture the number of propellers is equal to the number of engines and electric motors.

Considering an one-way link from ICE to PMCD, and the electric drive in the middle acting as a generator, it is possible to modify the general scheme into a series-parallel configuration, shown in Figure 2.4. This architecture gives the system the possibility of an enormous improvement of the energy and power flow controls and possibilities. However a much more complexity in the system is added with respect to other configurations. An influence in costs and weights is expected, as already discussed in Section 1.4. Of course the possibility of using the generator as starting motor for ICE, in the same fashion of series configuration, can be exploited for this task, instead of using the other ED, through the shaft, as in the case of the parallel system.

The last possible configuration is the so called complex hybrid [10], in which a two-way link between ICE and PMCD is considered and the ED acts as generator or motor depending on the situation. The configuration is the same of the series-parallel hybrid, presented in Figure 2.4, but in this case the ED placed in between PMCD and ICE not only can be used at starting but also can provide power, supporting the ICE at high loads, exploiting the so called three propulsion power. Only a single-way link between ICE and gearbox is considered because using the shaft to start the engine is considered less efficient than using the previously mentioned system.

In all the configurations presented before, connection between propeller and PMCD has been considered always two-way, giving the possibility to charge batteries when propeller is in the wind-milling operating phase [41]. If this feature is not to be taken into account, it just possible to switch the link into a one-way connection.

## 2.3 Input/output relations

Before starting to develop the model, it has been useful to focus on input/output relations between each block. This was achieved using another block scheme, presented in Figure 2.5, that shows, without going into deep details, in a graphical and intuitive way, possible links between each component in a generic powertrain. Some of the connections presented are already exposed in Section 2.1. After focusing on the power flow in the system, in this case the attention goes to what kind of information has to be released by each block and which subsystems are interested in it. It is possible to note that blocks that are reached by a larger number of connections are the FMS and PMCD: this is due to the fact that these systems provide and retrieve data for and from all the other system that are present in the architecture.

In the powertrain model, that will be discussed in the following chapter, not all this connections are present for several reasons: some blocks are not already modelled due to different factors, such as lack of data e time constraints, also links between components that are not of interest in the simulation, such as data representation in the cockpit, as discussed above, have not be considered in the model. The input/output relations diagram could be considered as a good practice in order to start modelling the overall system with in mind all the possible connections between blocks and so organising the model plant in a correct way.

Thus, after a first look at different configurations that can be exploited using a general architecture and related connections between blocks, it is possible to use a computational environment to model and simulate an aircraft powertrain.

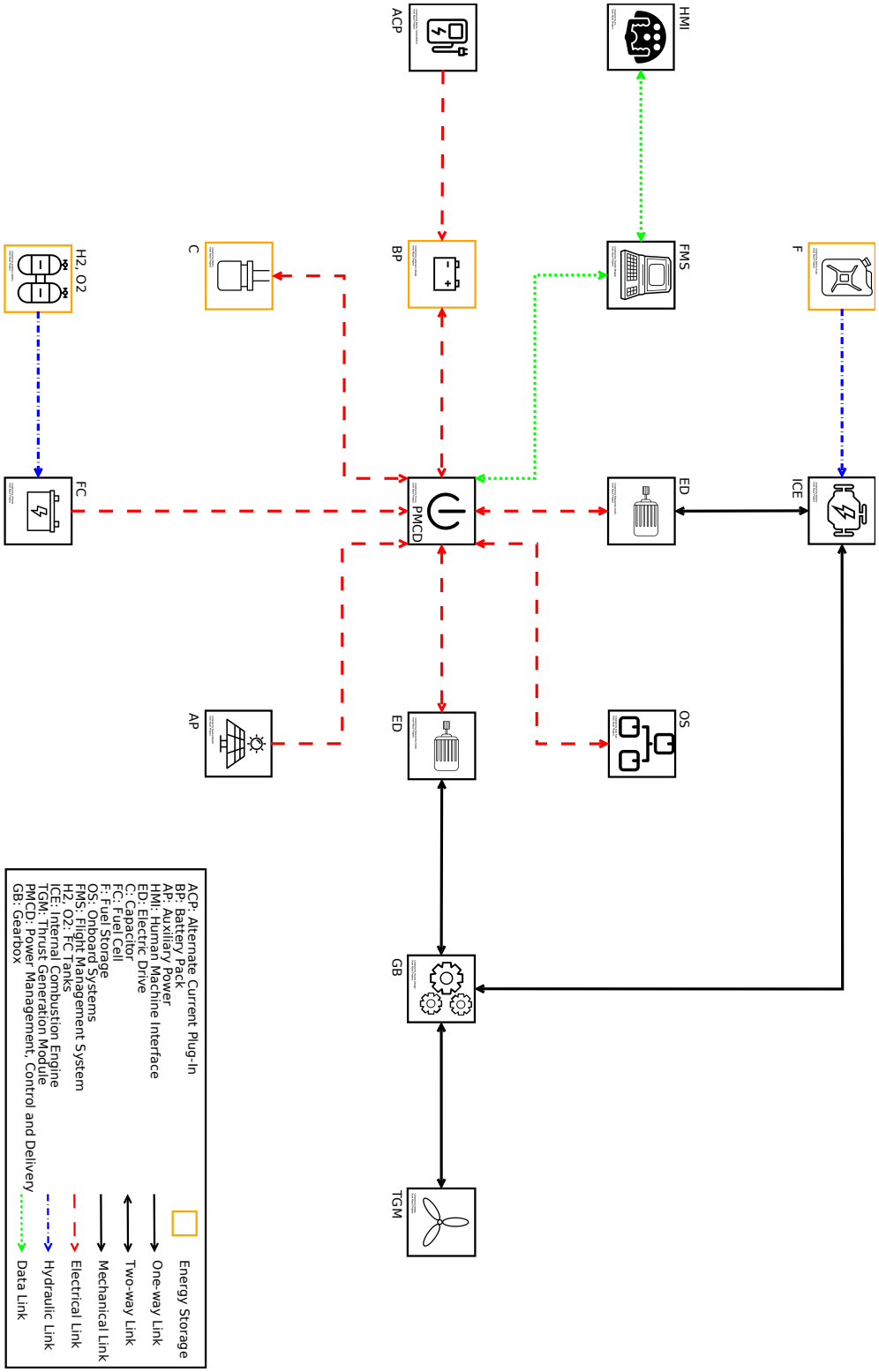


Figure 2.1: Generic system configuration

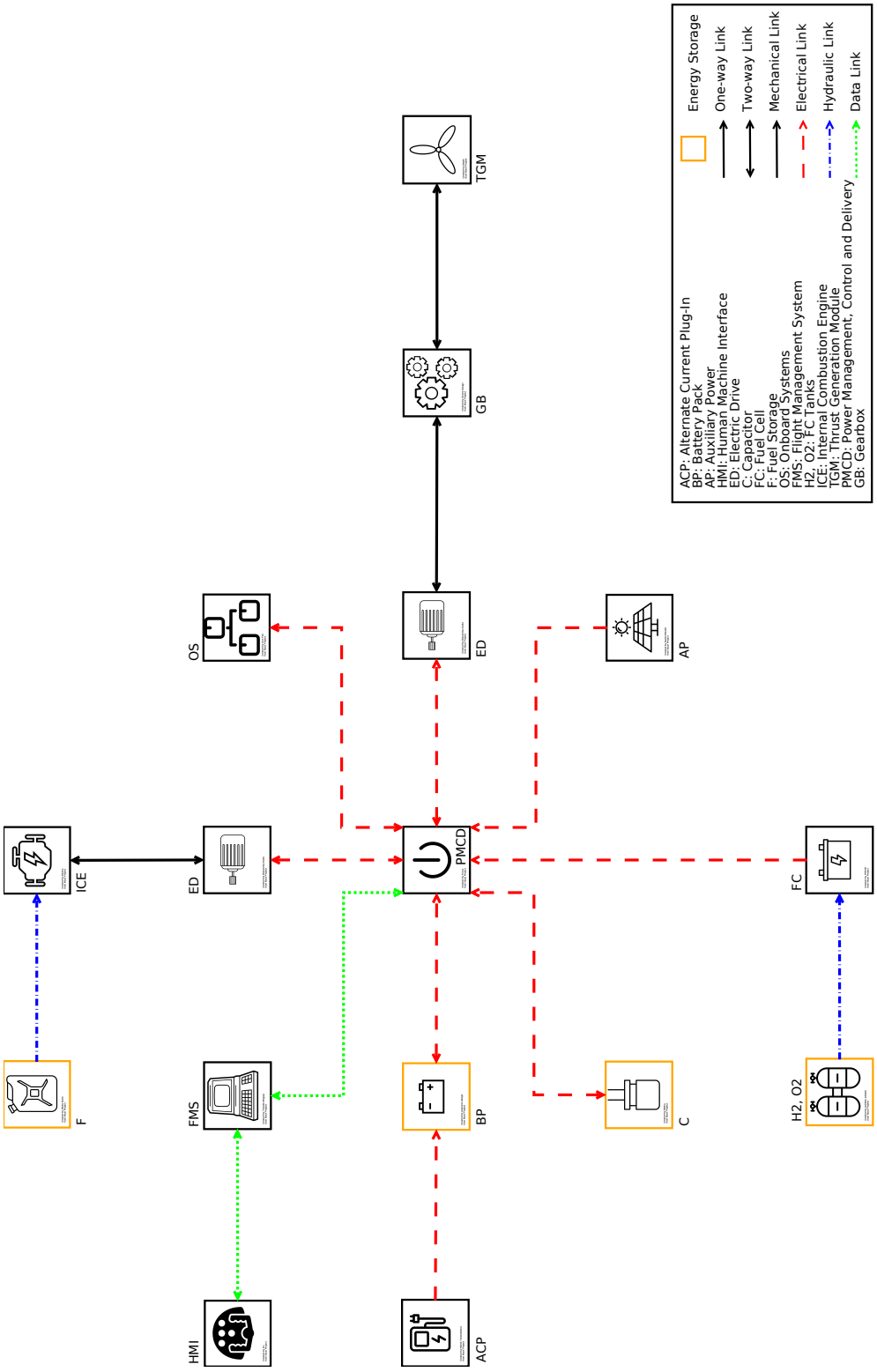


Figure 2.2: Series hybrid configuration

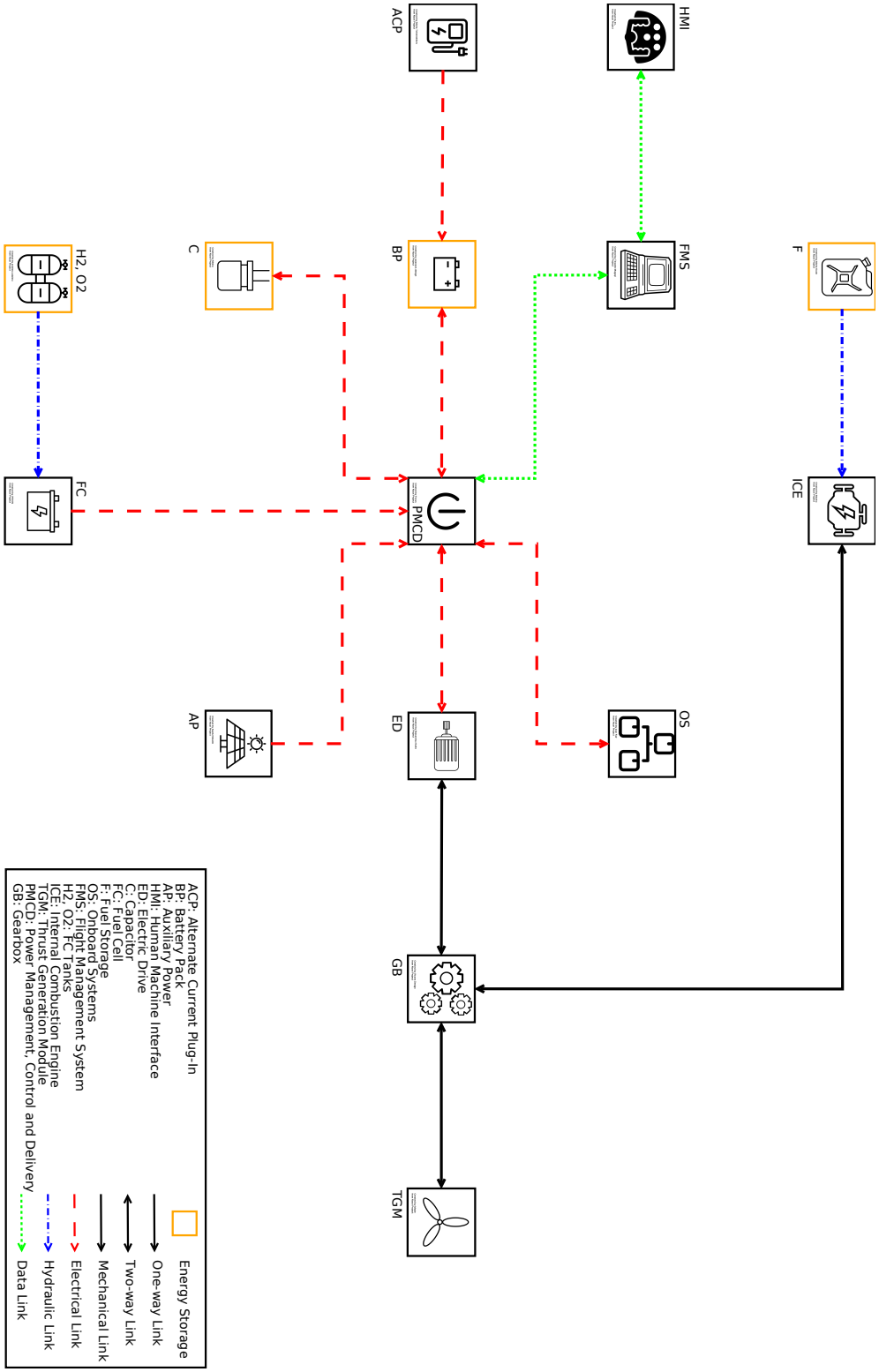


Figure 2.3: Parallel hybrid configuration

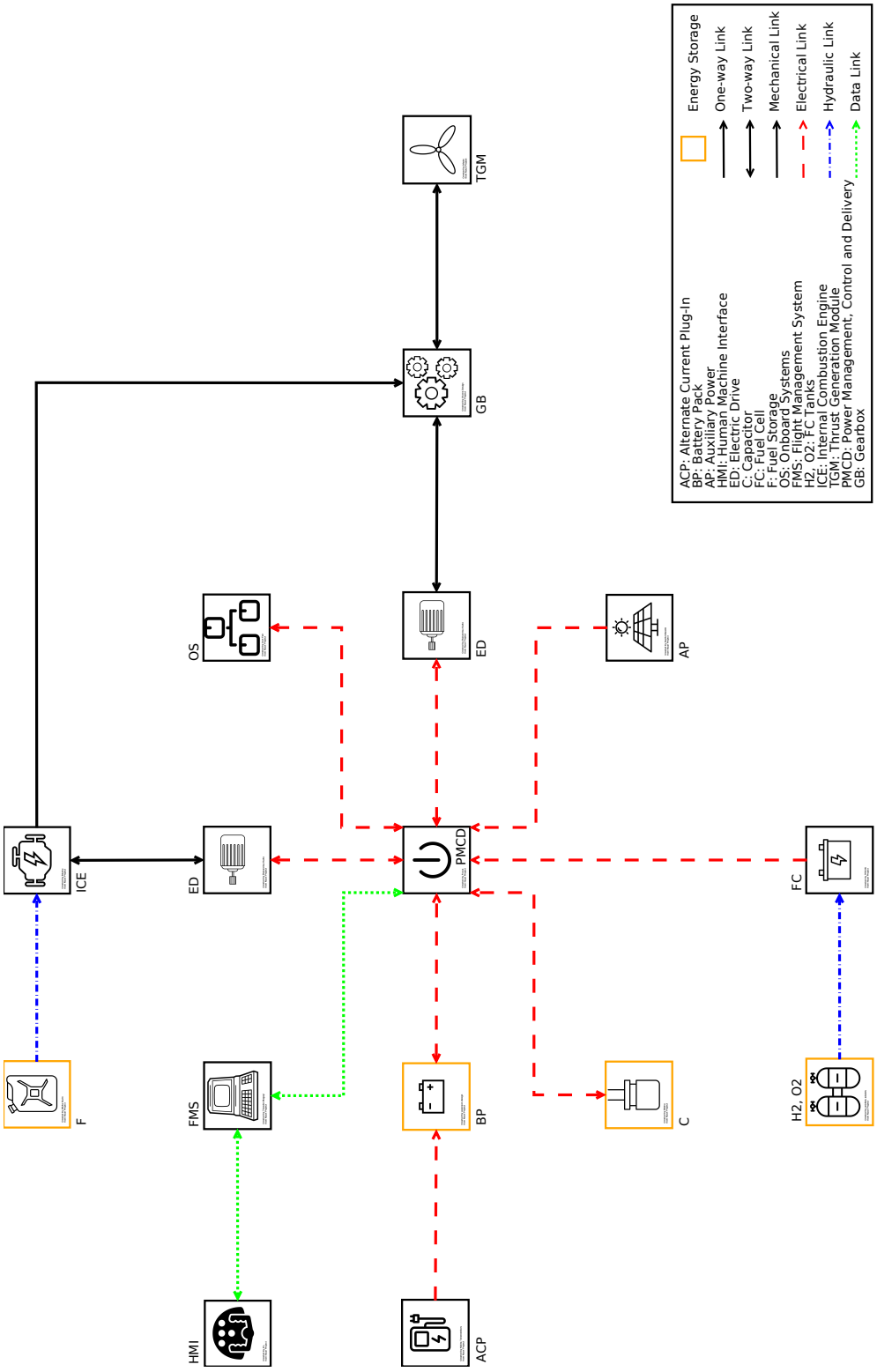


Figure 2.4: Series-parallel hybrid configuration

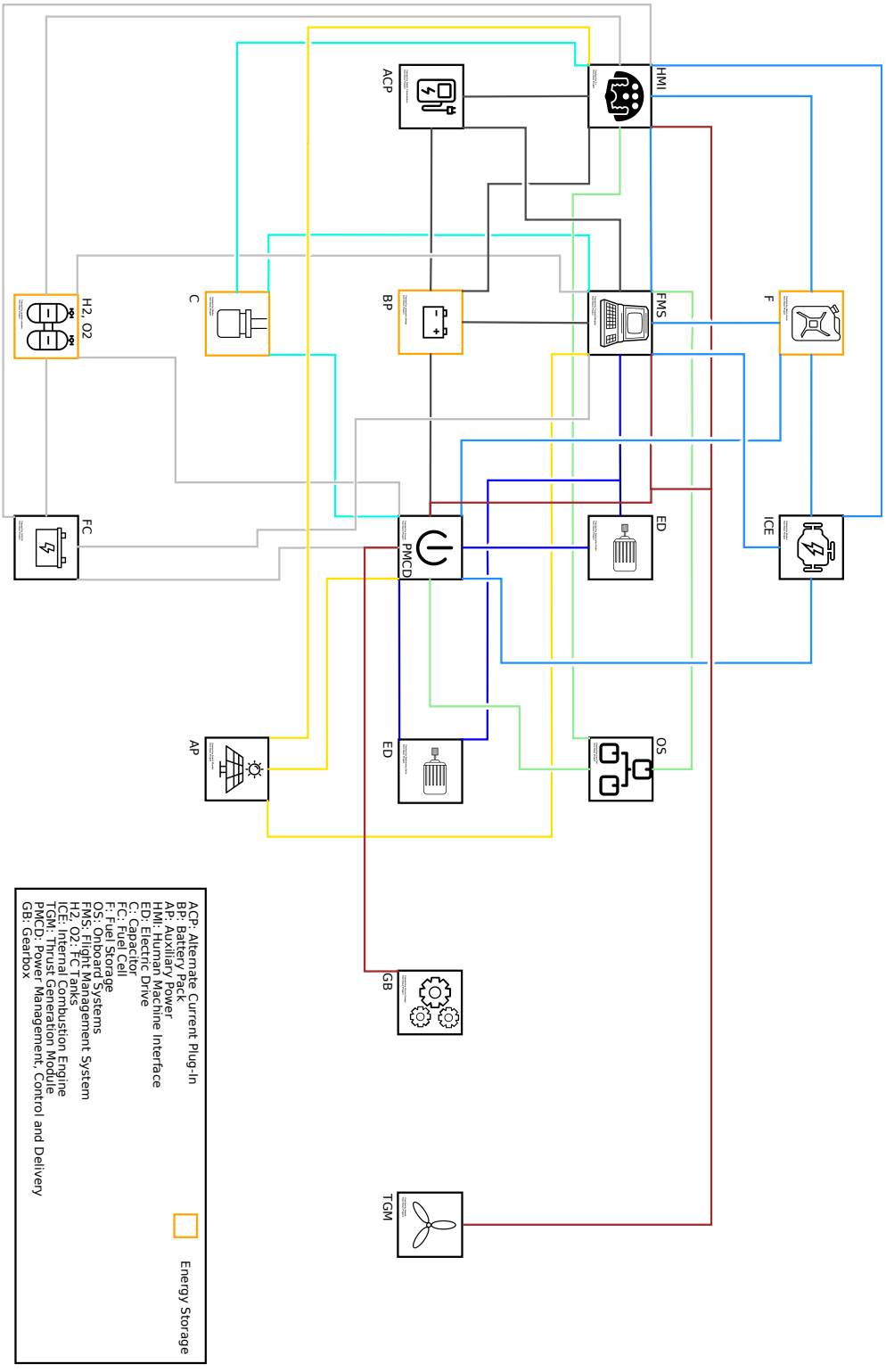


Figure 2.5: Input/output relations

# Chapter 3

# Powertrain modelling

After an overview of different powertrain configurations and links between components, a quite large amount of time has been dedicated to look for an appropriate mathematical model for each subsystem. The features of the models and how they are built into Simulink and Matlab are described in the following pages. An overview of the entire system developed in Simulink is displayed in Figure 3.1. It is important to remark that the model has been developed with in mind the possibility to add parts or modify current subsystems in the near future.

From the simulation point of view each block is organized as follows: in general only one output signal, in the form of data bus, is present out of each block. In this way a quite good readability of the scheme is achieved. In the data bus are collected all the signals of interest that have to reach PMCD and other subsystems. In case one block depends on another without the interaction of PMCD, for example ICE and generator, more outputs are considered. The number of inputs of each block of course depends on what signals are necessary to it to work. A *Bus Selector* [42] is used to take from data-bus signals of interest. From Figure 3.1 it is possible to notice that in some blocks an input port coming from high is present: this is necessary to have an Enabled Subsystem [43], that allows to switch on and off the entire subsystem during the simulation. In order to give the tool a user-friendly interface, model parameters and other variables, that are detailed in the following, are set in Matlab. Each system has a dedicated script. In this way the user can just modify variables of interest and update the *Workspace* directly from the code and then run the simulation in Simulink. Variables are stored into Struct [44]: each struct in general refers to a particular subsystem and so in the *Workspace* are visible *Structs* called `Battery`, `DCDC`, `ICE` and so on, making quantities stored in a tidy way. It is important to note that if a physical quantity is needed for computation in more than one block, it is not calculated twice: the variable is computed or provided only in the block that ideally is correlated to it and then, in order to not recompute it several times and to make the simulation more efficient, it is distributed to all necessary blocks. An example of this can be shown for atmospheric quantities such as pressure, temperature and air density: these variables are computed in FMS block and then signals reach other blocks of interest.

In Figure 3.1 it is possible to note that there are few differences between this scheme and the ones presented in Figure 2.1 and in Section 2.3. In particular, this work focuses on how batteries and internal combustion engines can be coupled in different configurations. Other energy sources such as solar arrays and fuel cells have been investigated but not reproduced in the system. The block related to other aircraft systems (OS) is not taken into account because data about power consumption is not available. However the introduction of this block could be done without effort in the future. Instead, for what concern the system downstream the PMCD, all its parts have been modelled in the computational environment. Considering input/output relations it is possible to note that Figure 3.1 shows less links than Figure 2.5: this is caused,

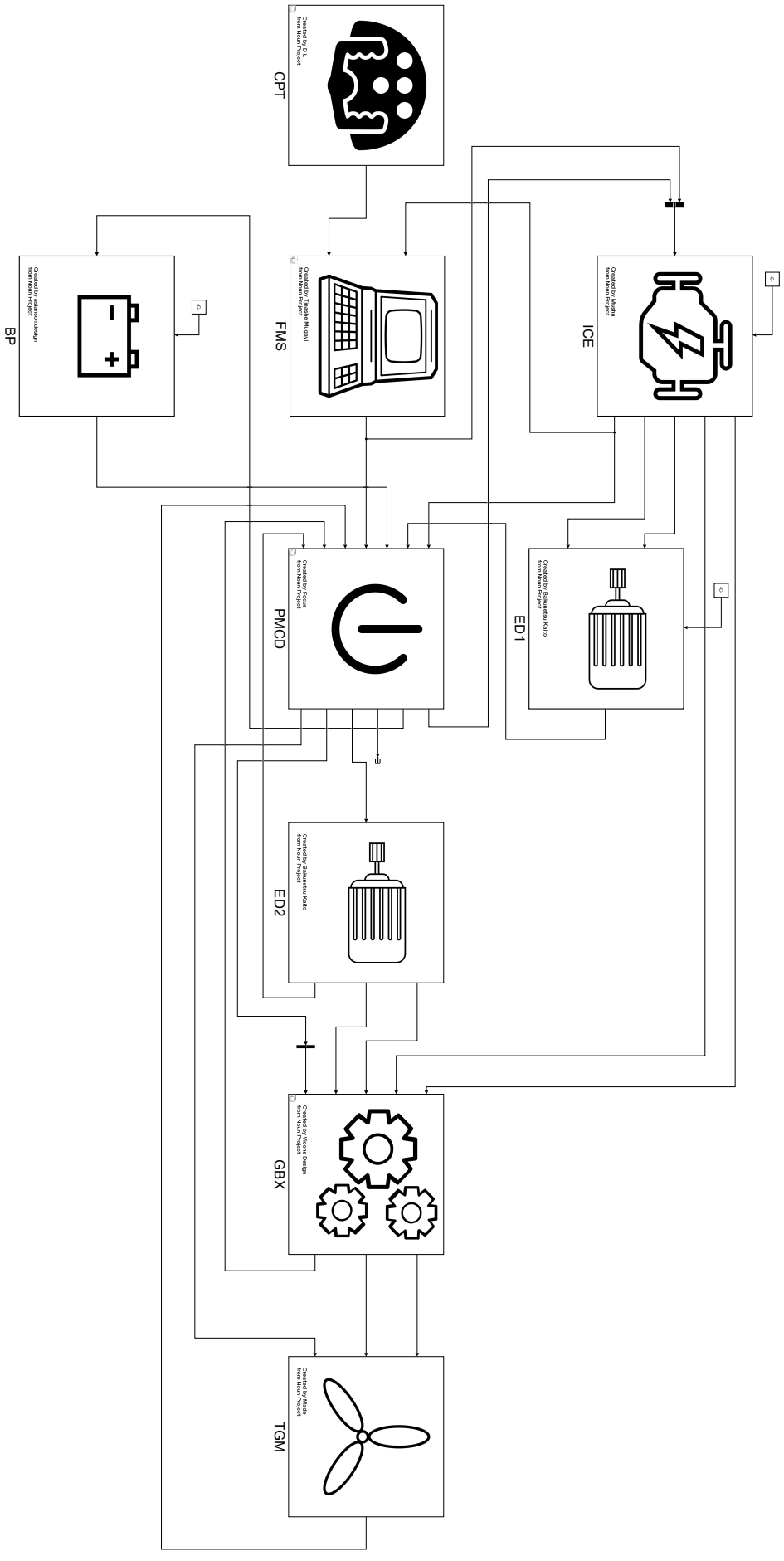


Figure 3.1: Powertrain model

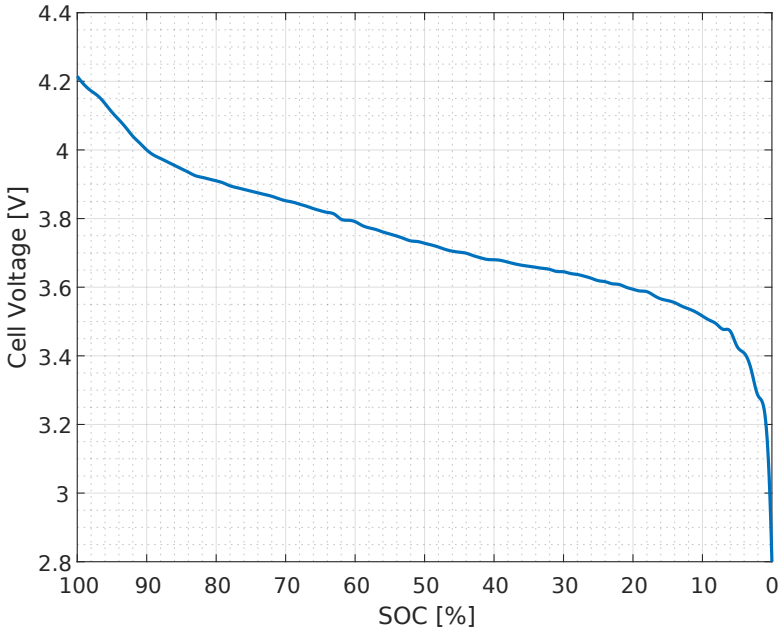


Figure 3.2: Typical discharge curve

as already mentioned, by avoiding to introduce in the model connections that are not useful for the simulation.

## 3.1 Battery pack (BP)

The first item investigated during this work is the battery because of its importance in an hybrid-electric vehicle. This is also the central element of all-electric vehicles, that are an aircraft category of interest for this work. Batteries store a great amount of energy to be released when necessary and they are also useful when coupled with slow dynamic energy source such as fuel cells. The typical discharge curve of a battery can be found in Figure 3.2, in which three different trend of discharge can be seen: the first one is the so called exponential zone and occurs in the first times of discharge, then a nominal area, with a constant and small rate of discharge, can be seen, up to the final operative condition of the battery, in which the state of charge is too low and the cell voltage drops.

The corresponding block in the Simulink model should have as input the power required to the battery and as output the power provided by the battery and other quantities about its status. The aim for the model of interest is to link the physical characteristics of the battery such as the number of cell in series and in parallel to its charge/discharge dynamics and capacity. This can be achieved with different models that can be found in literature, however the ability of the model to be easy to use and its simplicity to extract the model parameters from battery data-sheets are of prominence importance. There are basically three types of battery models reported in the literature, specifically: experimental, electrochemical and electric circuit-based. Experimental and electrochemical models are not well suited to represent cell dynamics for the purpose of state of charge estimations of battery packs. However, electric circuit-based models can be useful to represent electrical characteristics of batteries [45]. The most simple electric model consists in an ideal voltage source in series with an internal resistance [46]. This model, however, does not take into account the battery SOC. Very detailed battery models can be found easily in literature, however their parameter identification are based on a rather

complicated techniques: an example can be found in [47]. Another model, presented in [48], uses only the battery SOC as state variable to represent the voltage behaviour. This is valid in steady state (constant current) condition but this model produces unreliable results when the current varies with time. Finally, in [45] only three points on the manufacturer steady state discharge curve are required to obtain parameters of an easy-to-use battery dynamic model. This last model has been considered for the very first developments of the system in Simulink, as it can be seen in Figure 3.3. This represent accurately the voltage dynamics when the current varies and takes into account the open circuit voltage as a function of SOC. The particularity of this model is in the use of a filtered current flowing through the polarisation resistance. In fact, experimental results show a voltage slow dynamic behaviour for a current step response. Assumptions and limitations of the considered model, detailed in [45], may affect the behaviour of the battery model. However, since the aim of this work is to model, simulate and investigate the overall power-plant, and so investigating the system at an high level point of view, the limitations, that could appear evident in the case of working specifically on the battery, can be neglected since only the discharge trend is of interest for the considered point of view.

The user, after parameters and battery type have been selected into Matlab, is able to simulate the model of the battery in Simulink. An example in finding the parameters from the battery characteristic curve can be found in [45]. From the model represented in Figure 3.3, it is possible to note that the entire block is an *Enabled Subsystem*, that is a conditionally executed subsystem controlled by a signal. In this way an important feature is introduced in the model: the possibility to switch on or off each subsystem depending, for the sake of an example, on the flight condition or the control strategy.

The research of a suitable model for the simulator turned out to be a time consuming activity: it has taken more than two weeks to find an appropriate model. A possible solution came from the Simulink *Powertrain Blockset* introduced in Matlab version 2017b, which provides fully assembled reference application models of automotive powertrains, including gasoline, diesel, hybrid, and electric systems [49]. In this way it is possible to use built-in models, without spending time to find and reproduce them in Simulink, with the only task to validate them in the aftermath in order to check if models agree with the level of accuracy of the entire system. In particular, battery, DC-DC converters and combustion engine blocks used to simulate the powertrain are taken from this blockset.

A more detailed description on how the battery subsystem works can be provided starting from Figure 3.4. From the data-bus that links PMCD to battery block input port 1 named *Batt Cmd*, two signals are selected: *Batt Cmd Pwr [W]*, that is the power required by the PMCD to battery, and the Bus Voltage, that is the overall output voltage of this subsystem. In order to avoid Algebraic Loops [50], these signals are conditioned by *Unit Delay* blocks [51]: its parameter are defined in a specific script, detailed in Appendix A.1. After *Unit Delay* block, signals go into *DC-DC converter* block. Useful information, that are included into the output bus of this subsystem, and output battery current are provided by this last block. The computed current is then used as input in *Datasheet Battery* block, together with battery temperature, considered as constant during the simulation and defined in the *Workspace* by the user. As previously seen, the battery block provides several information, included in the bus, and battery voltage, used as input in DC-DC converter. It is clear that in this case a loop composed by battery and converter is present unless a *Unit Delay* is placed in between. All the relevant quantities are included in a bus that through the output port 1 named *Batt Out* reaches PMCD block. Input and output relations of this block are detailed in Table 3.1.

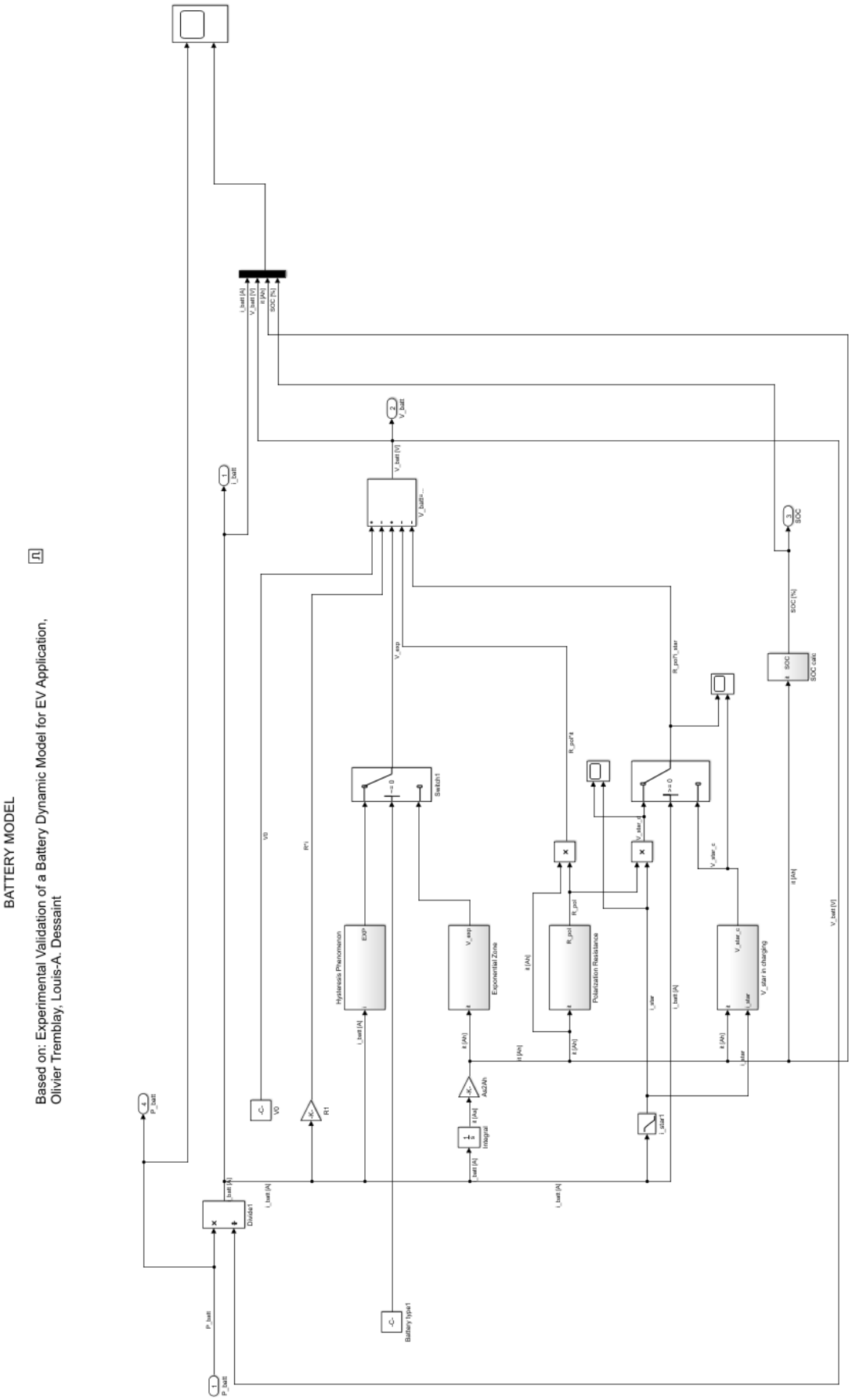


Figure 3.3: Battery model

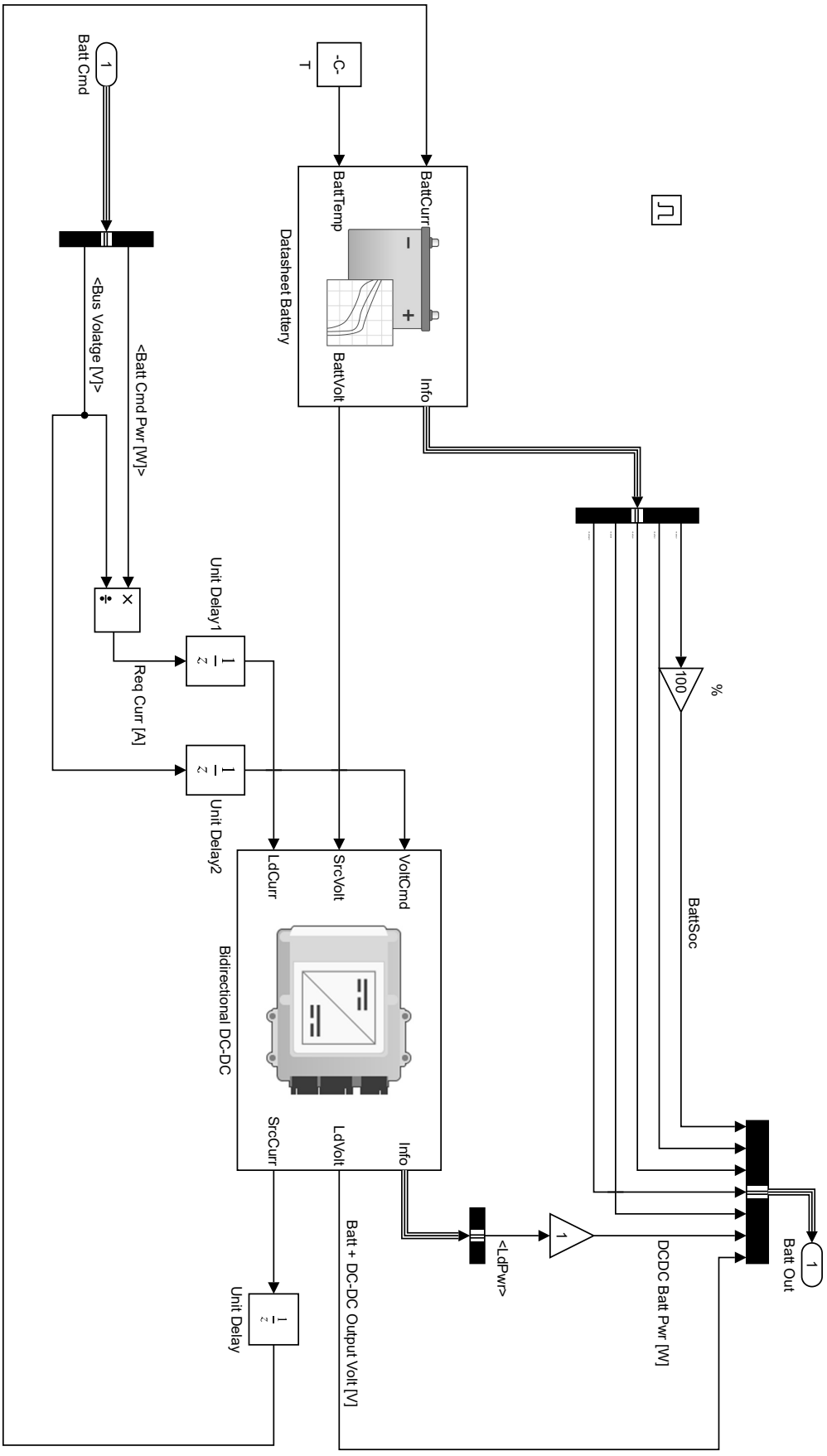


Figure 3.4: BP model

| Input | Description | Source |
|---|---|---|
| Batt Cmd Pwr [W] | Power required to battery block from controller | PMCD |
| Bus Voltage [V] | Voltage of the electric system | PMCD |

| Output | Description | Destination |
|---|---|---|
| BattSoc | Battery state of charge | PMCD |
| Batt Pwr [W] | Power provided by the battery | PMCD |
| Batt Curr [A] | Actual battery current | PMCD |
| Batt Volt [V] | Actual battery voltage | PMCD |
| Batt AmpH | Actual battery charge | PMCD |
| DCDC Batt Pwr [W] | Effective power provided by the block | PMCD |
| Batt + DC-DC Output Volt [V] | Output voltage of the block | PMCD |

Table 3.1: BP input and output

### 3.1.1 Datasheet battery

For what concerns the battery, it has been used the *Datasheet Battery* block [52], that implements a lithium-ion, lithium-polymer, or lead-acid battery model that can be parametrised using manufacturer data. To compute the open-circuit voltage and internal resistance parameters needed for the block, it is possible to use discharge characteristics that can be found in data-sheets. To determine the battery output voltage, the block takes into account lookup tables for the battery open-circuit voltage and the internal resistance. Lookup tables are functions of state of charge and battery temperature, characterizing the battery performance at various operating points. In this way through simple relations it is possible to compute the output quantities of interest referring only to manufacturer data-sheet. The mask of this block can be seen in Figure A.1 and the description of each variable is listed below.

- Input:
  - *BattCurr*: load current in Ampere. From another point of view it is the output current of the battery.
  - *BattTemp*: battery temperature in K. This value is set by user and it is considered constant.
- Output:
  - *Info*: it is a bus signal containing block calculations such as state of charge.
  - *BattVolt*: it is the output voltage of the battery in Volt.
- Parameters:
  - *Rated capacity at nominal temperature*: the maximum capacity of the battery expressed in Ah at nominal temperature of 15°.

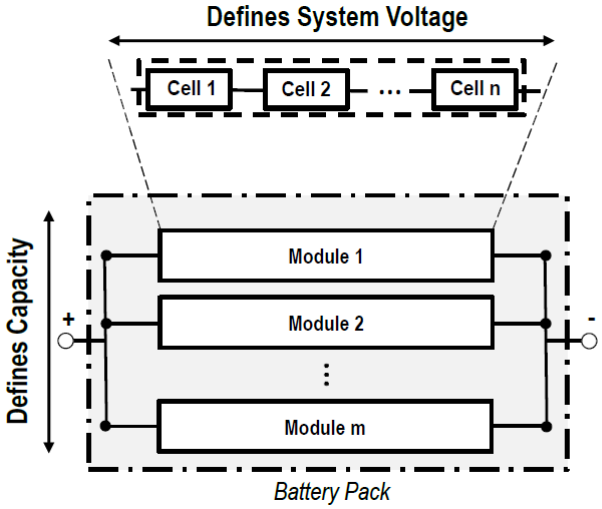


Figure 3.5: Generic battery architecture, [53]

- *Open circuit voltage table data*: it is an array of N values of open circuit voltage, expressed in Volt, in function of the state of charge of the battery. These values can be taken from the discharge curve present in data-sheets. The representation of this data with respect to battery SOC gives Figure 3.2.
- *Open circuit voltage breakpoints 1*: it is an array of N values of state of charge, defined between 0 and 1, at which open circuit voltage table data are evaluated. From another point of view, they are the values on x-axis of Figure 3.2.
- *Internal resistance table data*: it is an M x L matrix that represents internal resistance map, in Ohm, as a function of M temperature and L SOC values.
- *Battery temperature breakpoints 1*: it is an array of M values of temperature, expressed in Kelvin, at which internal resistance values are computed.
- *Battery capacity breakpoints 2*: it is an array of L values of state of charge between 0 and 1 at which internal resistance values are evaluated.
- *Number of cells in series and parallel*: a battery pack consists of cells connected in series and parallel. The number of cells that are connected in series defines the system output voltage. Cells in series can be combined into a battery module. Battery modules connected in parallel increase the overall capacity of a battery pack at a defined system operating voltage [53], as it can be seen from Figure 3.5.

- *Initial battery capacity*: capacity of the battery when the simulation starts. It is expressed in Ah and in this way it is possible to simulate starting condition that differs from the case of battery fully charged.

All these parameters are set into Matlab through a proper script, as can be seen in Appendix A.2. Using this built-in block, it is possible to reproduce the behaviour of the battery using only data provided by its data-sheet. With respect to the model presented before, there is a loss in accuracy since in this case dynamic behaviours are not described. However this should not be a limit of validity of this model because in general the time scale of the electric domain and the one of aircraft are very different. This last model has been preferred and used for the simulation.

### 3.1.2 Bidirectional DC-DC

Since battery voltage drops with the decreasing of the state of charge, the battery can not be connected directly to the electric plant because the possible presence of other electric sources, such as solar arrays or fuel cells. So, supposing the presence of a DC plant, a DC-DC converter is needed to couple the battery to the electric bus. In the same fashion as the battery model, a built-in model present in the *Powertrain Blockset* has been used for modelling the DC-DC converter. The capability of this block is to be a bidirectional boost (step-up) or buck (step-down) converter. Unless the DC-to-DC conversion limits the power, the output voltage tracks the voltage command. Similar to battery, it is possible to specify electrical losses or measured efficiency [54]. This block allows the battery to discharge or charge depending on the situation: referring to Figure 3.4, when the required power to battery is grater than zero, and so the current has a 'positive' flow, from the battery to the electric plant, the DC-DC converter allows to match the battery voltage to the electric plant, making possible the battery to discharge, while when the required power is negative, and so a reverse current flow is present, from the electric plant to the battery, the battery is charging.

In the same way as the battery block, also this block doesn't represent a physical model of a true DC-DC converter since no electronics are modelled: the *Bidirectional DC-DC* block uses a time constant-based regulator to provide a fixed output voltage that is independent of load current. Using the output voltage and current, the block determines the losses of the DC-to-DC conversion. Then block uses the conversion losses to calculate the input current. The mask of this block is provided in Figure A.2 and the description of each variable is listed in the following. As for the battery, also in this case a script, has been developed in Matlab in order to provide numerical values to each variable, as shown in Appendix A.3.

- Input:
  - *VoltCmd*: commanded output voltage, in Volt. It is the voltage of the electric plant that has to be tracked by the system.
  - *SrcVolt*: input voltage, in Volt. It is the battery output voltage.
  - *LdCurr*: load current, in Ampere. It is the required current by PMCD and it is computed from the electric plant voltage and the required power.
- Output:
  - *Info*: signal bus that contains block calculations, such as converter output power.
  - *LdVolt*: load voltage, in Volt. It is the output voltage of the converter, that tries to keep it equal to VoltCmd.
  - *SrcCurr*: DC-to-DC converter input current, in Ampere. It is the output current of battery block.
- Parameters:
  - *Converter response time constant*, in seconds.
  - *Converter response initial voltage*: it is the starting voltage of the DC-DC converters, expressed in Volt. Generally it is set equal to zero.
  - *Converter power limit*: it is the maximum power of the DC-DC converter, expressed in Watts. If the power flow in the converter is higher, it will limit it to this value.
  - *Parametrize losses by*: it allows to select the loss option used to calculate electrical losses.

- *Single efficiency measurement*: electrical loss calculated using a constant value for conversion efficiency. So, the output power is the input one multiplied by this value.
  - *Overall DC to DC converter efficiency*: it is the efficiency constant value, in %.
- T*abulated efficiency data*: electrical loss is calculated using conversion efficiency that is a function of load current and voltage using a two dimensional look-up table.
  - *Vector of voltages for tabulated efficiency*: it is an array of N values of voltages, expressed in Volt, at which efficiency values are computed.
  - *Vector of currents for tabulated efficiency*: it is an array of M values of currents, expressed in Ampere, at which efficiency values are computed.
  - *Corresponding efficiency*: it is a M x N matrix that represents electrical efficiency map as a function of M load currents and N load voltages, in %.

## 3.2 Internal combustion engine (ICE)

Considering a hybrid-electric aircraft, the second source that is generally used in order to provide the power required for the flight is a combustion engine. In alternative, a fuel cell could be used as well, with a limitation about power the system can provide.

Referring to Chapter 2, the relative position of the engine with respect to battery defines the architecture used. In particular, in the case of a series configuration, ICE is connected to PMCD and so to battery through an electric generator: it converts mechanical power into electrical power. On the other hand, in the parallel configuration there is no link between ICE and battery. The coupling of power provided by the two systems is done in the gearbox just before the propeller: the mechanical power coming from electric motor, that is powered by battery, is mixed with the one provided by engine in order to provide enough power to move the propeller shaft. An intermediate solution is the series-parallel configuration: in this case the power coming from ICE can be both converted into electricity through a generator and/or can be provided directly to gearbox. This last configuration is not covered by this work because of the control logic complexity, however, the tool is developed in order to add features, such as an additional configuration, in an easy way in the future.

The ICE block includes many types of engines, considering spark ignition (SI), compression ignition (CI) and gas turbine engine as well. Systems can be modelled in Simulink to use them depending on the simulated powertrain, giving the possibility to the user to switch from one to another directly from configuration scripts in the same fashion as battery parameters. Of course when the simulation is running there is no possibility to change the engine type: changes can be done in the configuration phase. This allows, for example, to compare different configurations that use different power sources. The possibility to switch from one type of engine to another is provided by a *Variant Subsystem* [55]. In this way, when the simulation starts, Simulink disables/enables subsystems depending on a specific variable that is set by the user in Matlab during the configuration: this is an efficient solution that allows to have different subsystems in the simulator and to switch between them in each simulation. Variables that set the subsystems to be run during the simulation are defined in Appendix A.1. It is important to to note that in this work only spark and compression ignition engines are modelled because of time constraints.

Despite of the diffusion of this kind of engines, no models suitable for the purpose have been found in literature, except for gas turbine engine such as [56, 57, 58]. In particular a high number of models about specific issues are available but a quite poor documentation can be found about engine general performance: the few examples that are available are based

on empirical formulations which can not be verified, as in [59]. However in the *Powertrain Blockset* are available blocks about spark ignition [60] and compression ignition [61] engines. Both blocks implement a mapped engine model using power, air mass flow, fuel flow, exhaust temperature, efficiency, and emission performance lookup tables: in this way from data provided by manufacturers, it is possible to reproduce engine performance. These blocks are particularly indicated for vehicle-level fuel economy and performance simulations, that are the topics of the present work. Lookup tables are functions of two inputs: *commanded torque* $T$ and *engine speed* $N$ for what concerns spark ignition engine and *injected fuel mass* $F$ and *engine speed* $N$ for the other. So the considered engine characteristic $x$ can be expressed as $x = f(T, N)$ in the case of SI engine or $x = f(F, N)$ in the case of CI engine. It is important to note that in order to bound block output, blocks do not extrapolate the lookup table data. For each type of engine, a specific Matlab script has been built in order to store engine characteristics. In particular, in Appendix A.4 it is possible to have a look at the script related to spark ignition engine, while Appendix A.5 refers to combustion ignition engine. For what concern the former, in Figure A.3 it is possible to have a look at the mask block, while the block characteristics are listed in the following.

- Input:
  - *TrqCmd*: engine commanded torque from the controller, expressed in Nm.
  - *EngSpd*: engine speed that is defined by PMCD, in rpm.
- Output:
  - *Info*: bus signal that contains block calculations such as engine fuel flow, gas temperature and emissions.
  - *EngTrq*: engine brake torque, in Nm.
- Parameters:
  - *Breakpoints for commanded torque*: it is an array of N values, expressed in Nm, at which mapped quantities are computed.
  - *Breakpoints for engine speed input*: it is an array of M values, expressed in rpm, at which mapped quantities are computed.
  - *Number of cylinders*: is the number of cylinders that are present in the engine to be modelled.
  - *Crank revolutions per power stroke*.
  - *Total displaced volume*: volume displaced by engine, in m^3.
  - *Ideal gas constant air*: ideal gas constant of air and residual gas entering the engine intake port, in J/(kg K).
  - *Air standard pressure* in Pa.
  - *Air standard temperature* in K.
  - *Brake torque map*: it is a N x M matrix that represents engine torque, in Nm, lookup table as function of commanded engine torque and engine speed. An example can be seen in Figure 3.6, in which is presented the brake torque map with respect to commanded torque and engine speed of a generic spark ignition engine. The same applies to the characteristics that follows.

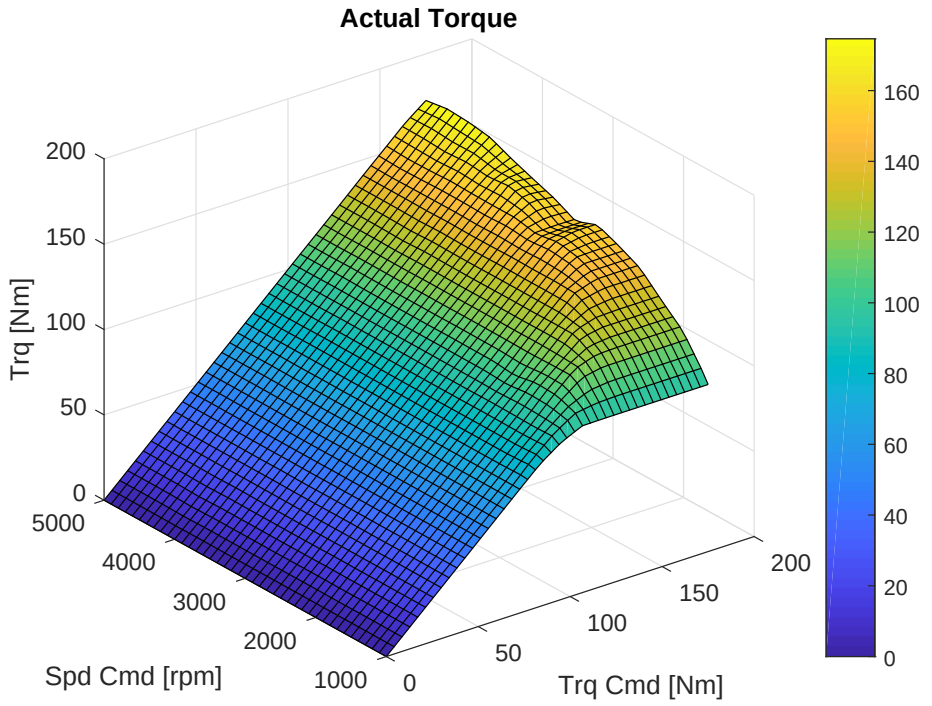


Figure 3.6: Brake torque map of a generic SI engine

- *Air mass flow map*: it is a N x M matrix that represents air mass flow, in kg/s, lookup table as a function of commanded engine torque and speed.
- *Fuel flow map*: it is a N x M matrix that represents fuel mass flow, in kg/s, lookup table as a function of commanded engine torque and speed.
- *Exhaust temperature map*: it is a N x M matrix that represents engine exhaust temperature, in K, lookup table as a function of commanded engine torque and speed.
- *BSFC map*: is a N x M matrix that represents brake-specific fuel consumption (BSFC) efficiency, in g/kWh, lookup table as a function of commanded engine torque and speed.
- *Emissions*: are a set of lookup tables, in the same fashion of the previous, that refers to gas emissions. In this work they are all set to zero because for the moment are out of interest. If in the future these values will be relevant it is possible to introduce them in the related Matlab script.

In the same manner, it is possible to have a view of compression ignition engine mask block in Figure A.4, in which it is possible to notice that the only difference with respect to CI engine block is in the first input port that refers to *commanded fuel mass per injection*, expressed in mg/inj, instead of *commanded torque*. Considering block parameters, the only difference is in having a *Breakpoints for commanded fuel mass input* that is an array of N elements, expressed in mg/inj, at which other quantities are computed.

Since there is a difference in one input signal between the two blocks, the source of the signal in the PMCD must be different in order to cover both cases: this will be discussed later. However, it is important to understand that both signals are present in the bus that links PMCD to ICE block and so, inside the latter, these signals can be distinguished thanks to a *Bus Selector*. In this way it is possible to switch from one type of engine to another without

directly modify the structure of the model, using specific variables defined in Matlab that allow the model to modify itself in an autonomous way.

In order to have an idea on how the entire engine model has been developed in Simulink, it is possible to have a look at Figure 3.7. There is one input, consisting in a signal bus, different subsystems that model the main aspects of a generic engine and five output, one signal bus and four signals that are related to generator and gearbox.

The possibility to have more than one combustion engine in the model is introduced in an easy way, based on the assumption that all the engines work at the same condition. From Figure 3.7 it is possible to note that there are two gains named *Num ICE*: the fuel flow required to run one engine is multiplied by the number of engines to provide the correct amount of fuel burnt. Also the power is multiplied by the number of engines to compute the total power available. In this way the power flow that interests different subsystems, such as ICE and generator or ICE and gearbox, is not affected by the number of engine used and so no edit to the scheme is needed to reproduce a multi-engine system. As in the Battery block, *Unit Delay* blocks are placed in the signals coming from PMCD in order to avoid Algebraic Loops.

Quantities needed to run the engine simulation are contained in the input bus. Up to now seven signals have been considered and presented in Table 3.2. As for the whole model, it is possible to add new output signals in an easy way using a *Bus Creator* [62]. For what it concerns output ports, in this case a signal bus, that is used to distribute all the information related to ICE to the blocks of interest, such as PMCD and FMS, and direct signals, that connect different items of the powertrain model depending on the configuration employed, are considered.

This system can be disabled, during the configuration phase, in order to simulate all-electric powertrain or other systems that are powered by alternative solutions such as fuel cells.

### 3.2.1 Engine

Mapped engine models discussed before are included in this block.

Referring to Figure 3.8, both engine models are included in the *Variant Subsystem* named *ICE Variant*. The two subsystems, *SI Engine* and *CI Engine*, that create the *Variant Subsystem,* have associated a variable defined in Matlab that is responsible of switching on and off the selected subsystem, as presented in Appendix A.1.

As already discussed, the two types of engine have different inputs and so, thanks to *Variant Subsystems* properties, it is possible to manage this difference automatically. On the other hand three common outputs have been considered. The first output is the fuel flow, expressed in kg/s, required by the engine. This signal is used to compute the residual fuel in the *Fuel Tank* block. The other two outputs are the torque, in Nm, and engine speed, in rpm, provided by the engine. These last two signals are used as input of the *Trq 2 Pwr* block, that has the task to compute the power provided by the engine given the torque and the speed. More in detail, after the engine speed has been converted from rpm to rad/s it is possible to calculate the power as the product between torque and speed. This is very useful because it allows to consider the power as the main variable used in the overall system. In this way the output of the *Engine* block are four, as detailed in Table 3.3.

### 3.2.2 Fuel tank

The *Fuel Tank* block, Figure 3.9, represents the fuel reservoir of the powertrain. Starting from the fuel flow coming from the engine model it is possible to compute, through integration, the fuel consumed during the simulation at each time step and so the residual fuel in the tank. The

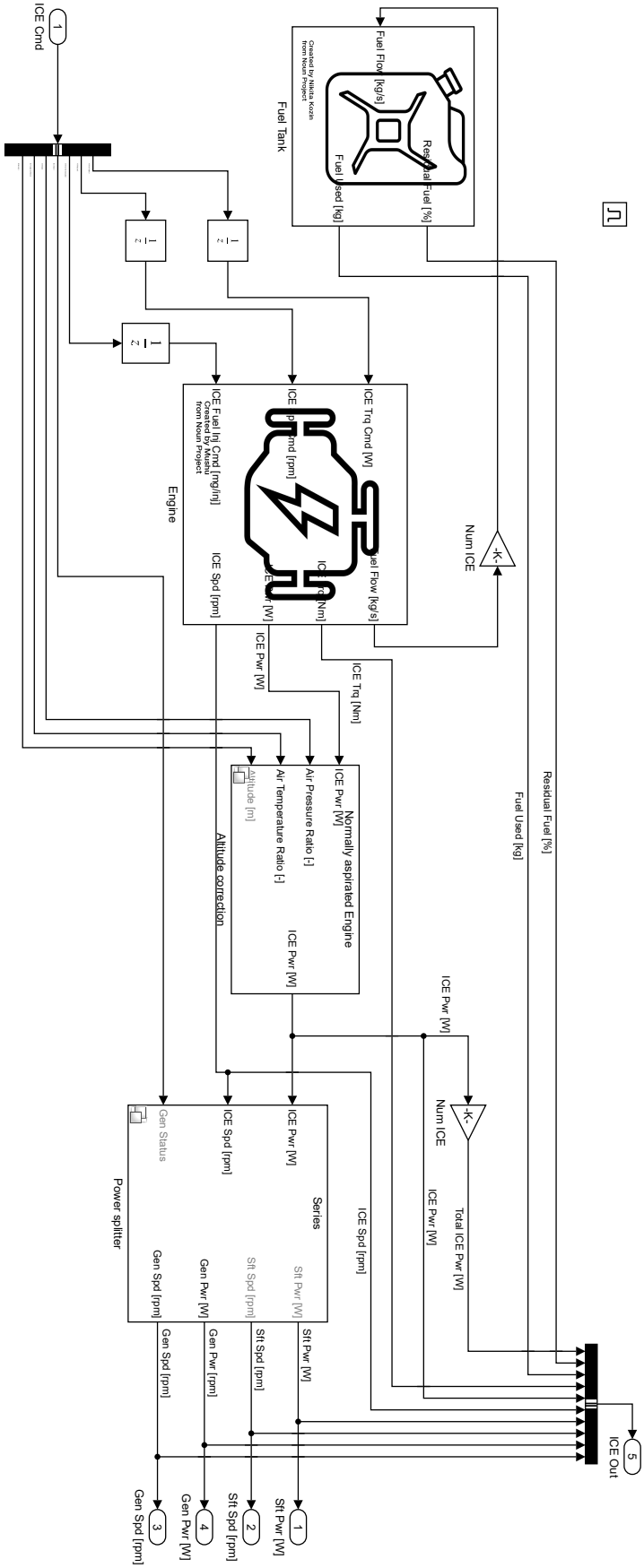


Figure 3.7: ICE model

| Input | Description | Source |
|---|---|---|
| ICE Cmd Trq [Nm] | Commanded torque in case of SI engine | PMCD |
| ICE Spd [rpm] | Commanded engine speed for both CI and SI engine | PMCD |
| ICE Cmd Fuel Inj [mg/inj] | Commanded fuel mass in case of CI engine | PMCD |
| Gen Status | Defines the status (ON/OFF) of the generator | PMCD |
| ICE Status | Defines the status (ON/OFF) of the engine | PMCD |
| Air Pressure Ratio [-] | Actual over standard pressure ratio | FMS |
| Air Density Ratio [-] | Actual over standard density ratio | FMS |
| Altitude [m] | Current altitude defined from flight profile | FMS |

| Output | Description | Destination |
|---|---|---|
| Total ICE Pwr [W] | Power provided by all the engines | PMCD |
| Residual fuel [%] | Residual fuel in the tank | PMCD |
| Fuel Used [kg] | Fuel burnt during simulation | FMS |
| ICE Trq [Nm] | Engine torque | PMCD |
| ICE Pwr [W] | Power provided by a single engine | PMCD |
| ICE Spd [rpm] | Engine speed | PMCD |
| Sft Pwr [W] | Shaft power delivered to gearbox | PMCD, GBX |
| Sft Spd [rpm] | Shaft speed related to gearbox | PMCD, GBX |
| Gen Pwr [W] | Power delivered to electric generator | PMCD, ED1 |
| Gen Spd [rpm] | Speed associated to electric generator | PMCD, ED1 |

Table 3.2: ICE input and output

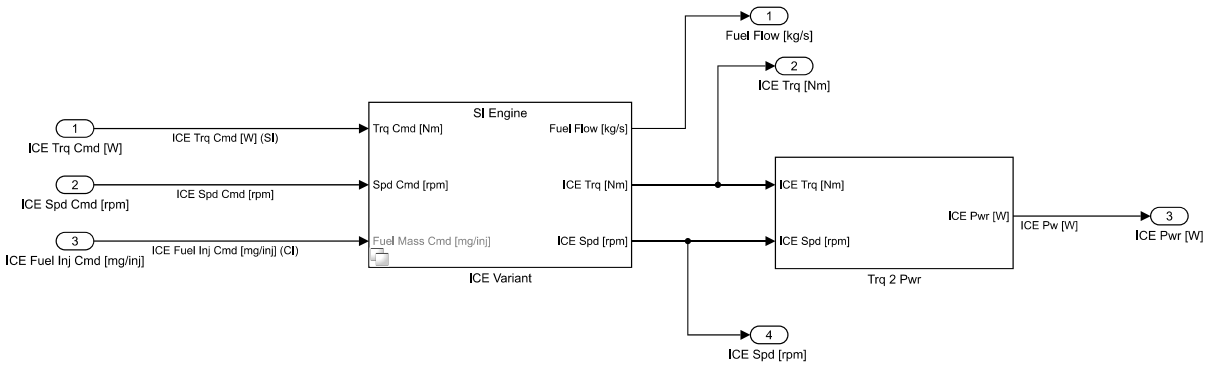


Figure 3.8: ICE/Engine model

| Input | Description | Source |
|---|---|---|
| ICE Cmd Trq [Nm] | Commanded torque in case of SI engine | PMCD |
| ICE Spd [rpm] | Commanded engine speed for both CI and SI engine | PMCD |
| ICE Cmd Fuel Inj [mg/inj] | Commanded fuel mass in case of CI engine | PMCD |

| Output | Description | Destination |
|---|---|---|
| Fuel Flow [kg/s] | Fuel flow used by the engine | ICE/Fuel Tank |
| ICE Trq [Nm] | Torque provided by engine | PMCD |
| ICE Pwr [W] | Power provided by engine | ICE/Altitude correction |
| ICE Spd [rpm] | Speed provided by engine | PMCD, ICE/Power splitter |

Table 3.3: ICE/Engine input and output

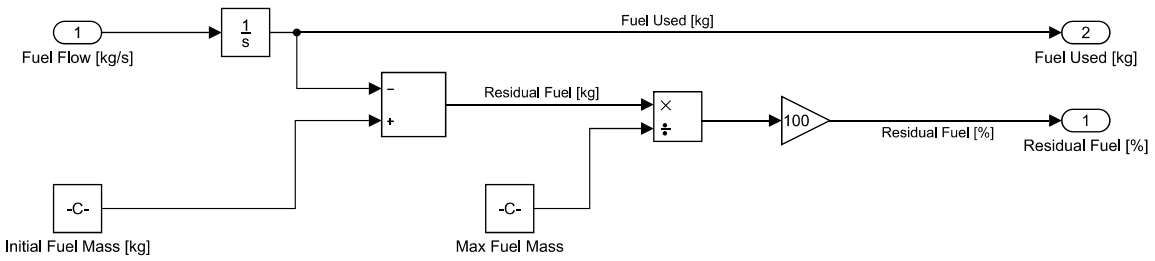


Figure 3.9: ICE/Fuel tank model

| Input | Description | Source |
|---|---|---|
| Fuel Flow [kg/s] | Fuel flow used by engines | ICE/Engine/ICE Variant |

| Output | Description | Destination |
|---|---|---|
| Fuel Used [kg] | Integration of fuel flow over time | FMS |
| Residual Fuel [%] | Residual fuel in the tank | PMCD |

Table 3.4: ICE/Fuel tank input and output

main parameters of this block are the starting fuel mass and the maximum fuel mass that can be stored in tanks. In this way it is possible to investigate situations that differs from full fuel tank at the take-off. The parameters are set, as usual, in Matlab, in a script that contains also other variables that refer to engine but are independent from which type of engine is involved in the simulation, as described in Appendix A.6. The input/output ports are detailed in Table 3.4.

### 3.2.3 Altitude correction

The purpose of this block is twofold: it introduces a correction to power provided by altitude and the possibility to consider a supercharged engine. For the former, a reduction in power due to a decrease of air density must be considered [63]:

$$\frac{P_z}{P_0} = \frac{p_z}{p_0}\sqrt{\frac{T_0}{T_z}}$$

The power at a generic altitude z, $P_z$, is lower than the one at sea level, $P_0$, by a factor that depends on the ratio between pressures $p$ and temperatures $T$ at the given altitude and sea level. The loss of power over altitude trend is depicted in Figure 3.10, in which it is also represented the trend related to a supercharged engine with critical altitude equal to 4000 m. In this last case the power remains constant, as first approximation, until the aircraft flies lower than the critical altitude, after which the power starts to decrease.

In this way, since the performance of the engine refers to mean sea level, it is possible to correct the power losses due to altitude. Of course there is the need to distinguish between the two cases: the normally aspirated and the supercharged engine. This can be achieved using *Variant Subsystems*. Variables related to this block are presented in Appendix A.1. It is important to note that in this work has been considered only single-stage supercharger in order to simplify the problem: the update to multi-stage supercharger is possible without effort. An input/output detailed list can be found in Table 3.5.

### 3.2.4 Power splitter

The aim of this block is to distribute the power and rotating speed to the correct item depending on the situation. In particular, in the case of series configuration, the power provided by the engine is delivered to the generator, while, in the case of parallel configuration, the signals have to reach the gearbox block. Furthermore, in the case of series-parallel configuration the power and rotating speed have to be delivered both to gearbox and electric generator. So, the *Power*

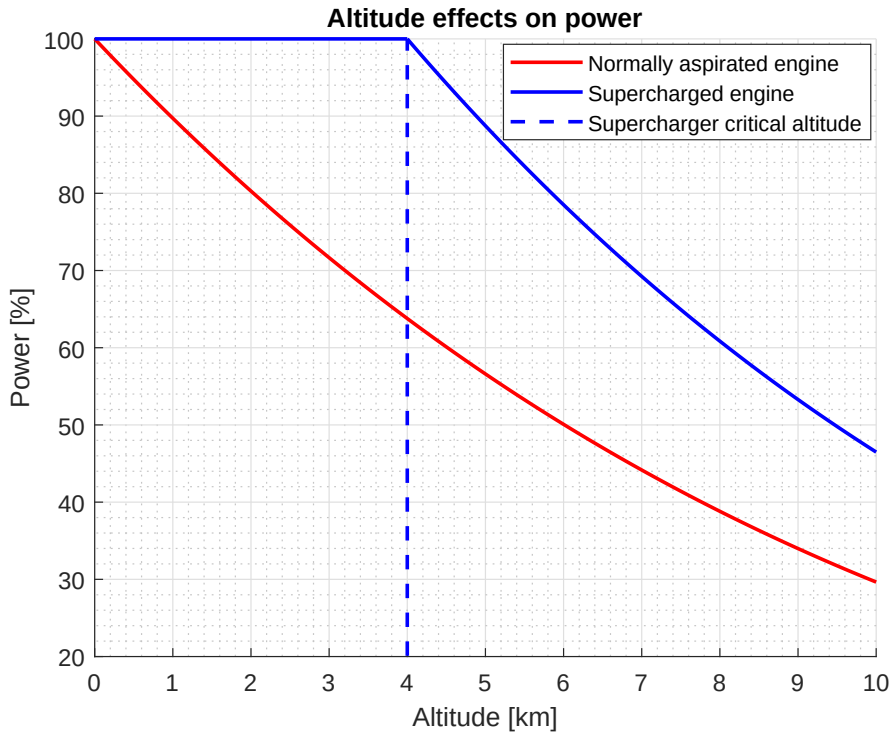


Figure 3.10: Altitude effects on power in case of normally aspirated and supercharged engines

| Input | Description | Source |
|---|---|---|
| ICE Pwr [W] | Power provided by ICE in standard condition | ICE/Engine |
| Air Pressure Ratio [-] | Actual over standard pressure ratio | FMS |
| Air Density Ratio [-] | Actual over standard density ratio | FMS |
| Altitude [m] | Current altitude defined from flight profile | FMS |

| Output | Description | Destination |
|---|---|---|
| ICE Pwr [W] | Corrected power provided by ICE | PMCD, ICE/Power Splitter |

Table 3.5: ICE/Altitude correction input and output

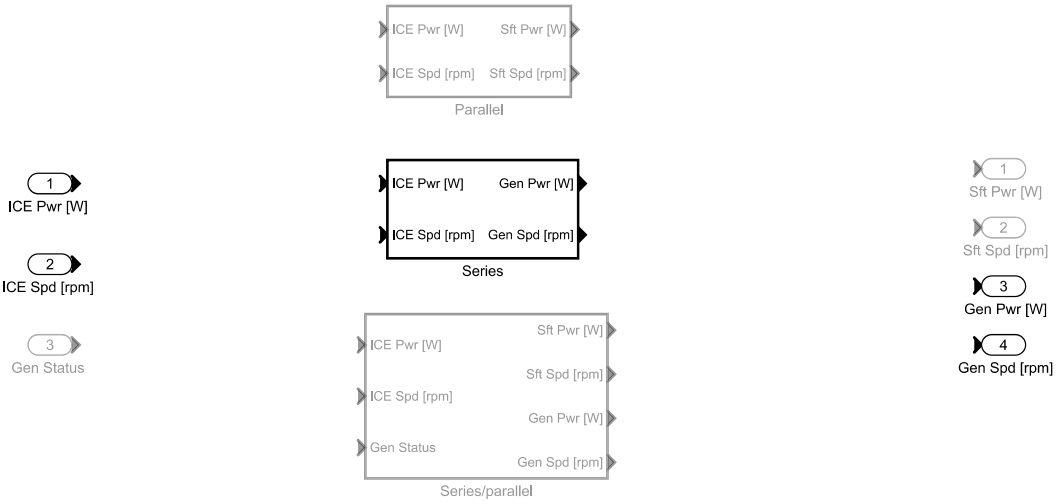


Figure 3.11: ICE/Power splitter model

*splitter* is a block that must be changed according to the configuration of the powertrain to be modelled: in order to achieve this result, also in this case a *Variant Subsystem* has been used. In particular, depending on the configuration that is set, a variable controls that the correct block is activated, allowing signals to flow in the considered model. In Figure 3.11 it is possible to see how this block has been built: in this case, the parallel configuration is enabled while the other two are disabled. Also, the output ports are automatically enabled/disabled depending on the situation. Input and output involved in this block are detailed in Table 3.6. Differently from the rest model, the series-parallel case is here introduced to prove that it is possible to develop additional configurations in an easy way, even if it is never used.

## 3.3 Electric generator (ED1)

As already explained in Section 2.1, in case of a series configuration the mechanical power provided by combustion engine must be converted into electricity in order to charge batteries or to power electric motors. The conversion from mechanical to electric domain is provided by an electric generator.

As for the battery and for the engine, also in this case there is not a physical model in the simulator. This is due, in the same fashion as electric motor presented in the following, to a generally lack of detailed information in data-sheets needed for the models proposed in literature, such as in [64]. Moreover, these models refer to specific architectures and can not be used to represent all the generator population. In order to solve this issue, only a global efficiency has been considered to model this component. In particular, given the input power and rotating speed, this block provides the electric power and current. Depending on the information available for the generator, two different solutions have been implemented: the first one is in considering only a single value of efficiency, while the second is related to an efficiency map that depends on the input power and speed. For the former, the input power is multiplied by the efficiency value: in this way the electric output power is computed. Knowing also the output voltage of the generator, it is possible to evaluate the output current. It is important to note that a converter is needed in order to switch from the voltage of the generator to the one of the electric system. This component is modelled in a similar way as for the converter related to battery, that can be found in Section 3.1.2, with the only difference

| Input | Description | Source |
|---|---|---|
| ICE Pwr [W] | Power provided by engine | ICE/Altitude correction |
| ICE Spd [rpm] | Engine speed | ICE/Engine |
| Gen Status | Status of the generator (ON/OFF) used in case of series-parallel configuration depending on the situation | PMCD |

| Output | Description | Destination |
|---|---|---|
| Sft Pwr [W] | Shaft power to be delivered to gearbox (parallel or series-parallel) | GBX |
| Sft Spd [rpm] | Shaft speed related to gearbox (parallel or series-parallel) | GBX |
| Gen Pwr [W] | Power to be delivered to electric generator (series or series-parallel) | ED1 |
| Gen Spd [W] | Speed related to generator (series or series-parallel) | ED1 |

Table 3.6: ICE/Power splitter input and output

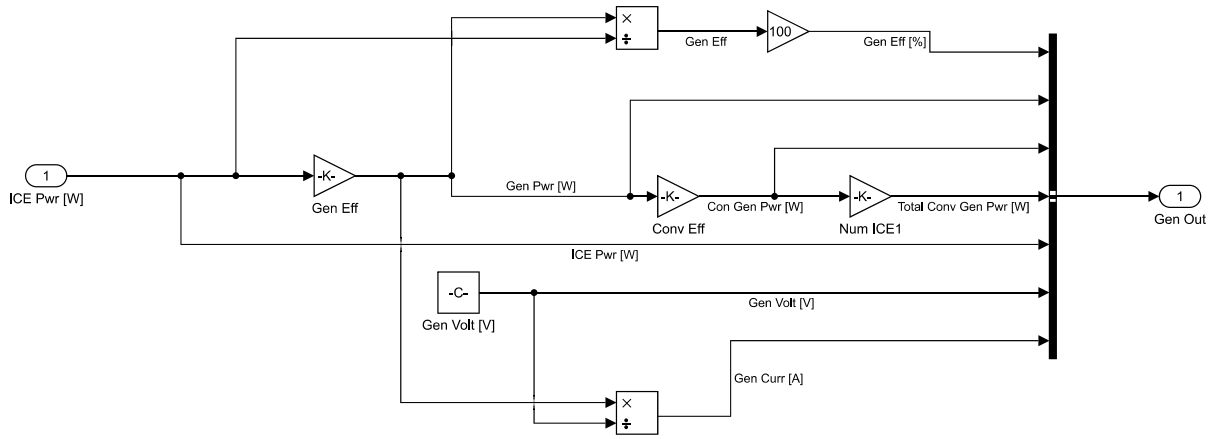


Figure 3.12: ED1/Single efficiency point model

that in this case only a single value of efficiency is considered to simplify the problem. Input power from engine is first converted and then conditioned by the presence of the generator and the converter. The second method used to model the generator consists in using lookup tables: given the input power and speed, it is possible to compute, through interpolation, the efficiency and other output quantities of the generator, in a similar way to the previous method. Also in this case the presence of a converter is modelled by a constant efficiency term.

Parameters, needed for the simulation, and the variables, that controls which model have to be run, are included in a dedicated script, discussed in Appendix A.8. As for other blocks the method exploited to switch from one model to another consists in using *Variant Subsystem*. The generator model, consisting in one single value of efficiency, is presented in Figure 3.12 to provide an idea about how this block has been implemented. The other method used to model the electric generator works in a quite similar way, except for the number of input used and for the mapped data. In addition to be a *Variant Subsystem*, this block is also an *Enabled Subsystem*, giving the possibility to switch on and off the generator during the simulation.

| Input | Description | Source |
|---|---|---|
| ICE Pwr [W] | Power provided by the engine | ICE |
| ICE Spd [rpm] | Engine speed used in case of mapped efficiency data | ICE |

| Output | Description | Destination |
|---|---|---|
| Gen Eff [%] | Generator efficiency | PMCD |
| Gen Pwr [W] | Output generator electric power | PMCD |
| DCDC Gen Pwr [W] | Output DC-DC converter electric power | PMCD |
| Total DCDC Gen Pwr [W] | Total power provided by ED1 block | PMCD |
| ICE Pwr [W] | Engine power | PMCD |
| Gen Volt [V] | Output voltage of the generator | PMCD |
| Gen Curr [A] | Output current of the generator | PMCD |

Table 3.7: ED1 input and output

The output of the entire block is a signal bus directed to PMCD. A detailed view of input and output related to this block is present in Table 3.7.

## 3.4 Electric motor (ED2)

This subsystem can be considered dual to electric generator: in this case, electric power from PMCD is converted in mechanical power thanks to an electric motor.

Even in this case, a wide variety of models are available in literature such as in [65, 66]. However, models depend on several electric characteristics, which values are not in general provided by manufacturers, and are very different depending on which type of motor is considered [67]. Since one type of motor differs a lot with respect to another and gotten the idea that modelling all the possible solutions is not feasible, a model similar to the one built for the electric generator is the only possible solution. In this way, different motors can be considered, independently that they are AC, DC, mono-phase and so on, giving the possibility to the model to simulate a large variety of possible alternatives.

As for the electric generator, two possibilities have been considered: modelling the component through a single value of efficiency or using tabulated data. In the fist case, global performance of the electric motor are related to its efficiency, kept constant in all operative conditions. This allows to simulate the presence of an electric motor, even in the case of lack of data about its characteristics. In the case of mapped motor, two lookup table have been considered: the first one relates input current and voltage to efficiency map, while the second links current and voltage to motor speed. In this way a more detailed behaviour of the motor is accounted for.

Since a generic electric drive can be considered in this block, a converter is needed: the presence of this item, whatever it is a DC-DC or a DC-AC converter, can be modelled through its efficiency, that in this case, for the sake of simplicity, it is set equal to a single constant value. Hence, the entire block models the series of a converter and an electric motor, as it is

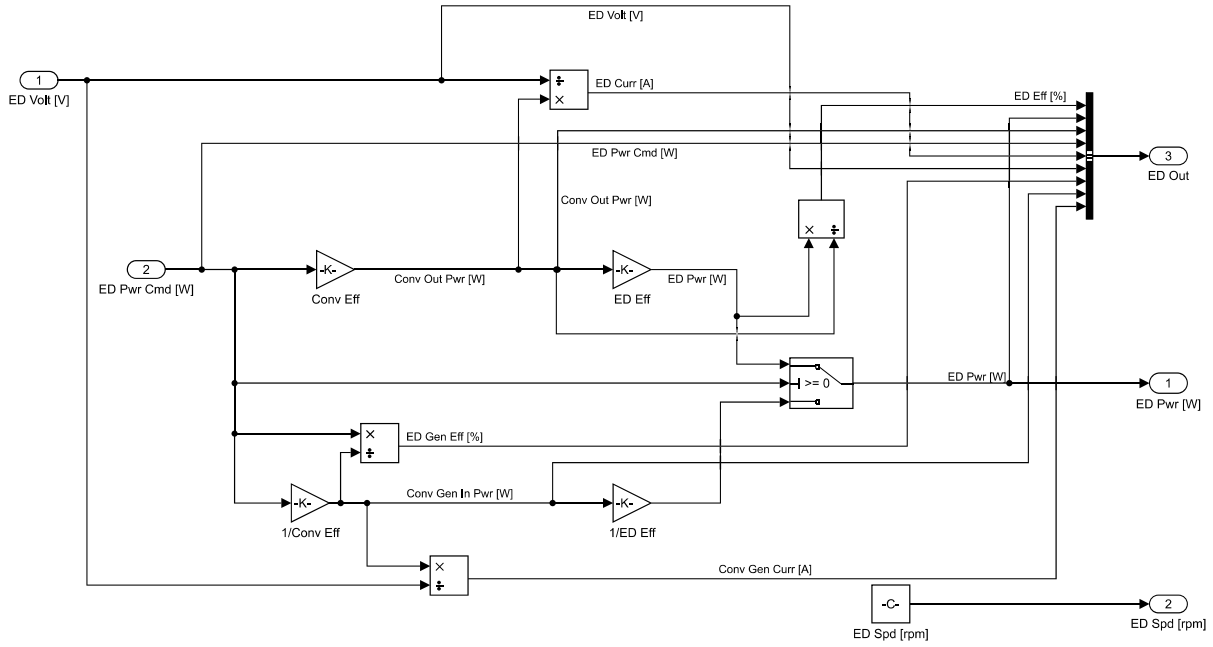


Figure 3.13: ED2/Single efficiency

possible to see in Figure 3.13, in which the case of single efficiency value is presented.

An important property of electric drive is the possibility to work both as generator and motor [67]: this is particularly of interest in simulating a generic aircraft powertrain. For example, considering a parallel configuration, the only possibility to charge batteries during flight is given by combustion engines that provide more power than the one required to flight. The extra power, through gearbox, is delivered to electric motors that in this circumstance act as generators, providing electric energy to batteries. In the case of series configuration, this peculiarity of electric drives can be considered important in the case one wants to exploit wind-milling operating condition to charge battery. The characteristic of having a bidirectional power flow is not easy to simulate in Simulink because several blocks are involved. In order to reproduce it, an artifice has been employed: when *ED Pwr Cmd*, the power commanded to electric motor from PMCD, is negative (and so ED2 has to work as generator), instead of multiply this value by efficiencies of the components, it is divided by such values, as presented in Figure 3.13. In this way, the negative power commanded to ED2 is lower, in modulus, to the one in gearbox block, modelling a power flow from gearbox to PMCD, conditioned by components efficiencies that are in this route: ED2, that it is acting as a generator, and the converter, that links the generator to the electric plant.

In order to switch from one model to another, a *Variant Subsystem* has been used . Also, to avoid Algebraic Loops a *Unit Delay* is placed outside this block. Variables related to this subsystem are set from Matlab script defined in Appendix A.7. In case one wants to simulate a system composed by more than one electric motor, for example one wants to investigate the capability of distributed propulsion [68], it is important to remark that this block simulates only one motor, in order to consider one power flow through electric motor and gearbox. The possibility of having more than one motor is managed in PMCD and TGM, depending on the situation. In other words, in the tool it is considered the possibility to several motors, even if *ED2* block refers only to a single motor.

This block has only one input, a signal bus coming from PMCD, and three output ports: one signal bus that contains all the characteristic values of this subsystem, as detailed in Table

| Input | Description | Source |
|---|---|---|
| ED Volt [V] | Electric system voltage | PMCD |
| ED Pwr Cmd [W] | Electric power provided to motor | PMCD |

| Output | Description | Destination |
|---|---|---|
| ED Pwr [W] | Mechanical power provided by electric motor | GBX |
| ED Spd [W] | Motor speed | GBX |
| ED Eff [%] | ED efficiency when acting as motoring device | PMCD |
| Conv Out Pwr [W] | Converter output power | PMCD |
| ED Pwr Cmd [W] | Electric power provided to motor | PMCD |
| ED Curr [A] | Current absorbed by electric motor | PMCD |
| ED Volt [V] | Electric system voltage | PMCD |
| ED Gen Eff [%] | ED efficiency when acting as generating device | PMCD |
| Conv Gen In Pwr [W] | Electric power provided, in generating mode, to converter | PMCD |
| Conv Gen Curr [A] | Current provided, in generating mode, to converter | PMCD |

Table 3.8: ED2 input and output

3.8, and two signal that are used as input of the downstream block, representing the power and speed delivered by the electric motor.

## 3.5 Gearbox (GBX)

Depending on the configuration exploited, the gearbox has different purposes. In the case of series configuration, the gearbox in general has to reduce the electric motor speed to the one feasible for the propeller: the aim of the gearbox is to provide the propeller the correct rotating speed. Speed reduction can be achieved in several ways, such as with a continuously variable transmission, that offers a continuum of gear ratios between desired limits. This allows the engine to operate more time in the optimum range given an appropriate control of the engine valve throttle opening and transmission ratio. In contrast, traditional and manual transmissions have several fixed transmission ratios forcing the engine to operate outside the optimum range [69]. Modelling this component in Simulink has been an hard task because of the large variety of possible configurations that can be exploited as explained in the following.

Given the input speed and the desired propeller speed, defined in CPT block, it is possible to compute the gear ratio and output torque. Differently from [70], in this work a global efficiency of this component is taken into account. As for other items, also in this case two approaches have been developed. The first one consists in a constant efficiency that models losses in the gearbox, as proposed in Figure 3.14 in the case of series configuration: this approach can be quite useful when no information about the component is available. The second option is a lookup table that maps the efficiency with respect to input torque and speed: a more detailed modelling of this component is achieved. In the same fashion as for the electric motor, also in

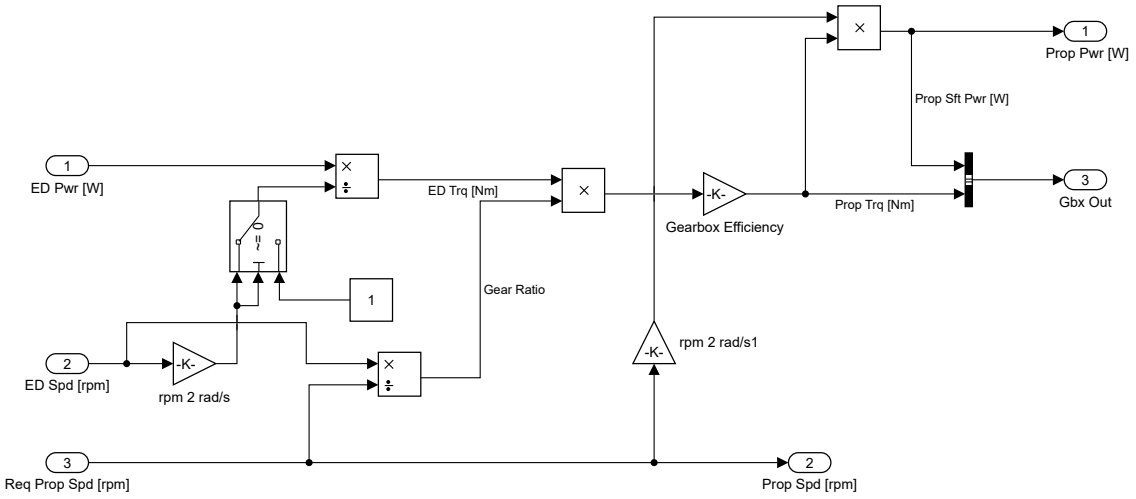


Figure 3.14: GBX model

this case the possibility of a power flow from propeller to ED2 is considered.

Since electric motors allow a larger variety of operating condition than combustion engine, it is possible to consider a direct drive between engine and propeller. This operating condition is feasible only in case of series configuration. If it is considered a parallel configuration, a direct link between electric motor and propeller is not possible because of the presence of engines: in this last case a gearbox is needed and it is modelled as described before.

In order to sum up how this block has been developed, depending on the situation, it is possible to refer to the following list. Three nested *Variant Subsystem* are needed to switch from one configuration to another. Variable related to this block can be found in Appendix A.9.

- Series:
  - Direct drive.
  - Gearbox:
    - Single efficiency value.
    - Mapped efficiency.
- Parallel:
  - Gearbox:
    - Single efficiency value.
    - Mapped efficiency.

The number of inputs of this block depends on the powertrain architecture: in the case of series configuration only signals coming from electric motor are needed, while, in the other case, signals coming from engine have to be taken into account. A more detailed list of input and output is presented in Table 3.9.

## 3.6 Propeller (TGM)

This is the last block of the power flow: the power, provided by batteries and engine, after has been transformed and conditioned by several components, it is converted in available power in

| Input | Description | Source |
|---|---|---|
| ICE Pwr [W] | Engine power | ICE |
| ICE Spd [rpm] | Engine speed | ICE |
| ED Pwr [W] | Electric motor power | ED2 |
| ED Spd [rpm] | Electric motor speed | ED2 |
| Req Prop Spd [rpm] | Desired propeller speed | PMCD, CPT |

| Output | Description | Destination |
|---|---|---|
| Prop Pwr [W] | Power provided to propeller | TGM |
| Prop Spd [W] | Propeller speed | TGM |
| Prop Sft Pwr [W] | Power provided to propeller | PMCD |
| Prop Trq [Nm] | Torque provided to propeller | PMCD |

Table 3.9: GBX input and output

order to sustain the flight. In this block propeller efficiency, depending on advance ratio and propeller pitch, is considered to compute available power and thrust, as pointed out in Figure 3.15. Once the advance ratio is computed, it is possible to find the actual propeller efficiency thanks to a lookup table that considers also the pitch of the propeller. If the propeller is a fixed-pitch type, only an array of efficiencies must be provided, while, in case of variable-pitch propeller, the variable related to propeller efficiency must be a matrix, as it is possible to note in Appendix A.10. Given the efficiency, it is possible to compute the available power and so the thrust knowing the airspeed.

This block allows to simulate more than one propeller: the number of propellers and other variables related to aircraft are defined in the script shown in Appendix A.11. It is important to note that, in general, one electric motor is associated to each propeller, independently on the powertrain configuration. If a parallel configuration is used, also the number of engines and the number of propellers must match. This is done in order not to have the need to modify the structure of the model every time a new configuration is simulated. The underlying hypothesis is that every propeller, engine or electric motor works at the same operative condition: no different operating points between the same components are allowed.

The list of input and output of this block is presented in Table 3.10.

## 3.7 Cockpit (CPT)

Signals necessary to the simulation about flight conditions and flight profile are produced by this block. So, this can be considered the starting block of the simulation: at each timestamp it provides power required to flight, airspeed, propeller pitch and speed, ICE and battery status and so on that will be detailed in the following. All available data are taken from Matlab *Workspace* in a proper *Struct*. Variables of interest can be found in Appendix A.12.

The block CPT presents itself as a *Variant Subsystem*: one variant block is named *Math*, while the other is called *Data*. The difference between these two blocks consists in the form of

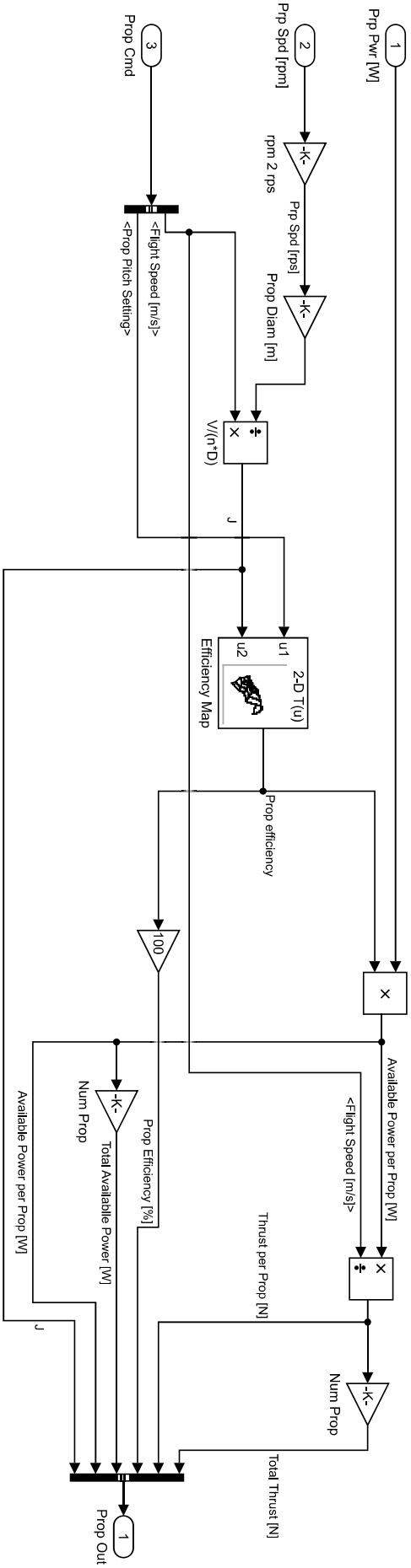


Figure 3.15: TGM model

| Input | Description | Source |
|---|---|---|
| Prop Pwr [W] | Propeller shaft power | GBX |
| Prop Spd [rpm] | Propeller speed | GBX, CPT |
| Flight speed [m/s] | Airspeed | PMCD, CPT |
| Prop pitch setting | Propeller pitch | PMCD, CPT |

| Output | Description | Destination |
|---|---|---|
| Total Thrust [N] | Thrust provided by all propellers | PMCD |
| Thrust per Prop [N] | Thrust provided by one propeller | PMCD |
| Prop Efficiency [%] | Propeller efficiency | PMCD |
| Total Available Power [W] | Available power | PMCD |
| Available Power per Prop [W] | Power provided by one propeller | PMCD |
| J | Advance ratio | PMCD |

Table 3.10: TGM input and output

the block output. In the first one, signals produced by CPT refer to fixed values during each flight phase. For example, during climb, the speed is considered constant and the same for other variables. It is important to note that, up to now, five flight phases have been considered: take-off, climb, cruise, descent and landing. The other block is distinguished by the fact that quantities are not subdivided in flight phases: the entire time history of each variable is given and imported in Simulink thanks to *From Workspace* blocks [71]. In this way, a more adherent to reality simulation can be run, allowing not only the simulation of the entire flight profile, but also manoeuvrers or a single flight phase can be considered. However, the drawback of the alternative solution is to retrieve data related to flight profile. Another flight mechanics simulator can be used to achieve this task while this tool can be used to assess the design of the power-plant. This second way can also be used to validate this tool using data coming from a real aircraft flight.

More in detail, the first option, the one related to flight phases, is depicted in Figure 3.16, in which physical quantities generated by this block can be seen. As already stated, each variable, except altitude, is kept constant during each flight phase: the result is a step-varying time history, as presented for example in Figure 3.17 in the case of power required flight profile. This can be considered a quite rough way to model reality, however this is the best way in terms of simplicity and of simulation results. In fact, a smoother way to reproduce data, thanks to Sigmoidal membership function [72], was introduced, and it is already present in the blocks but it is commented-out, since it introduces problems in other blocks because of data interpolation, providing not reliable results. Just to make an example, if a smooth variation of speed between two flight phases is considered, this should impact on propeller efficiency computation: if the blade pitch variation is provided in a small, finite number, changing airspeed means changing propeller advance ratio, causing the possibility to fall in a value that lies between two efficiency curves, leading to a very low efficiency that does not reflect reality. Even a smooth variation of propeller pitch does not resolve this problem and so a step-varying time history of all quantities, except from the altitude, is considered.

| Output | Description | Destination |
|---|---|---|
| Pwr Req Cpt [W] | Required power to flight | FMS, PMCD |
| Flight Speed [m/s] | True airspeed | PMCD, TGM |
| ICE Status | Status of engine. 1: On, 0: Off | PMCD, ICE |
| Batt Status | Status of battery. 1: On, 0: Off | PMCD |
| Prop Spd [rpm] | Propeller rotating speed | PMCD, GBX, TGM |
| Prop Pitch Setting | It identifies propeller pitch | PMCD, TGM |
| Lift over drag ratio | Lift over drag ratio, used to compute fuel weight loss | FMS |
| Altitude [m] | Defines aircraft altitude during simulation | FMS, ICE |

Table 3.11: CPT output

It is important to remark that powers defined in the script refers to mean sea level altitude, since a variation of power due to density reduction is provided in FMS block, as detailed in Section 3.8. For this reason power related to cruise, depicted in Figure 3.17, appears so high. Finally, airspeed refers to TAS because it is used to compute propeller performance.

In Figure 3.16 it is possible to note that two blocks, related to ICE and battery status, have the altitude as input: this has been done in order to provide multiple strategies to define the status of engine and batteries. In particular two different methods have been considered in this work, thanks to a *Variant Subsystem*. The first one is related to define the status of these subsystems based on flight phases, while the second one the status is based on altitude. More in detail, for what concerns the former, a step-varying time history between one (On) and zero (Off) can be provided based on flight phases, in the same fashion as other quantities. For example, in this way it is possible to turn on the battery during take-off and climb, while the engine is switched off, and so on, depending on the strategy exploited in using each power source. An alternative consists in turning on and off ICE and batteries depending on altitude: for example, when the aircraft is flying lower than a selected altitude, only electric source is used. Each subsystem, has its own switching altitude that can be defined in the already mentioned script. The status lower and higher the selected altitude can be arbitrary selected.

Since no inputs are present in the CPT block, only output signals are listed in Table 3.11.

## 3.8 Flight Management System (FMS)

In this block signals coming from CPT are conditioned and used to find new variables that are necessary to the simulation. Since the previous block is divided in two *Variant Subsystems*, also in this case a split is needed in order to take into account the output differences between the cases described in Section 3.8. In case the cockpit outputs are provided in the form of mathematical, step-variant signals, the FMS block is responsible for correcting this data in terms of altitude and fuel weight reduction, as shown in Figure 3.18. More in detail, the required power is multiplied by air density ratio in order to consider its variation over altitude. For this reason, powers that are previously defined in CPT block have to be computed considering standard air density at zero altitude. Moreover, also temperature and pressure ratio are computed in this block: these quantities are exploited in ICE block in order to find engine power losses due to altitude, as detailed in Section 3.2.3. Quantities that are related to

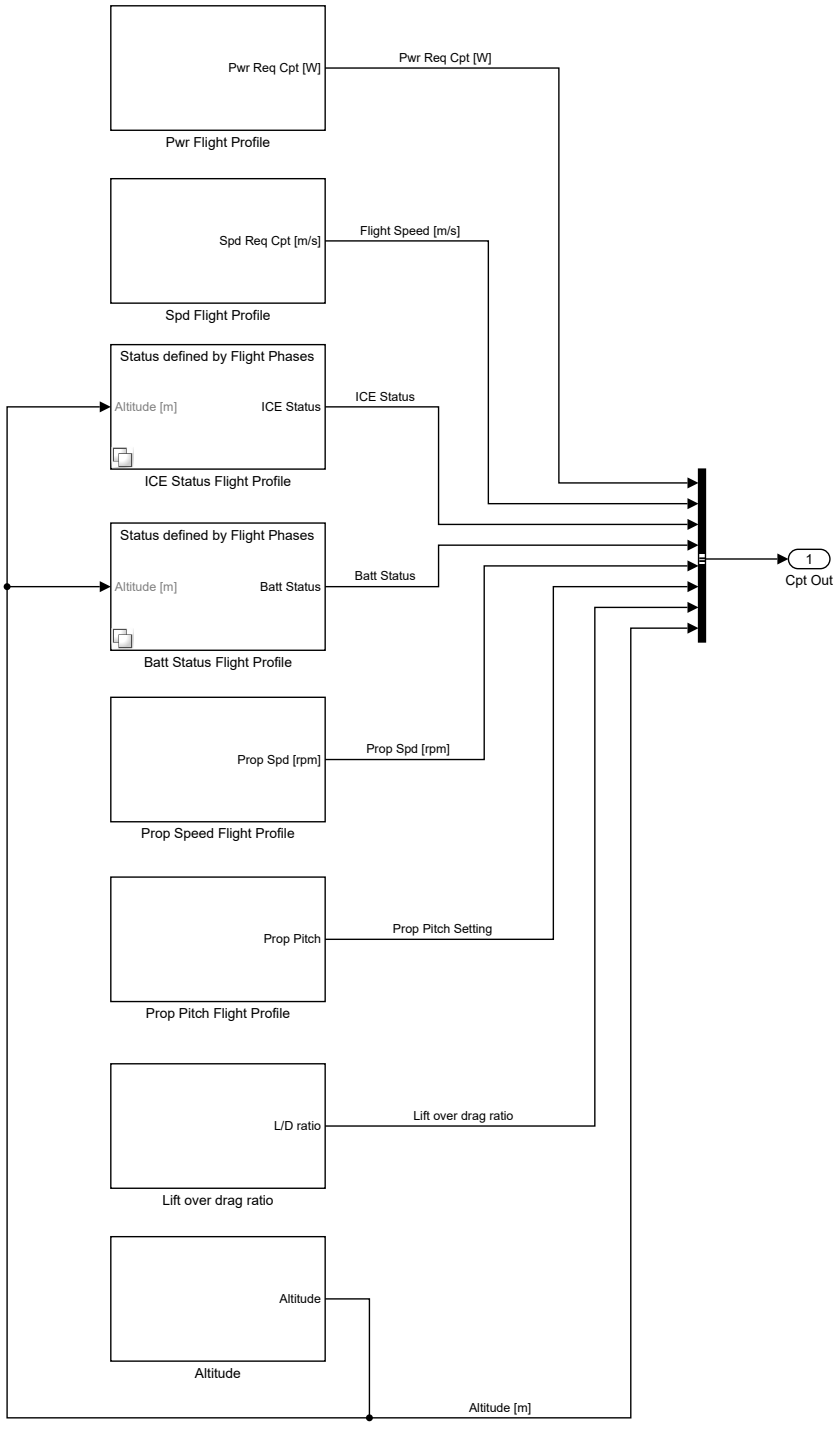


Figure 3.16: CPT/Math model

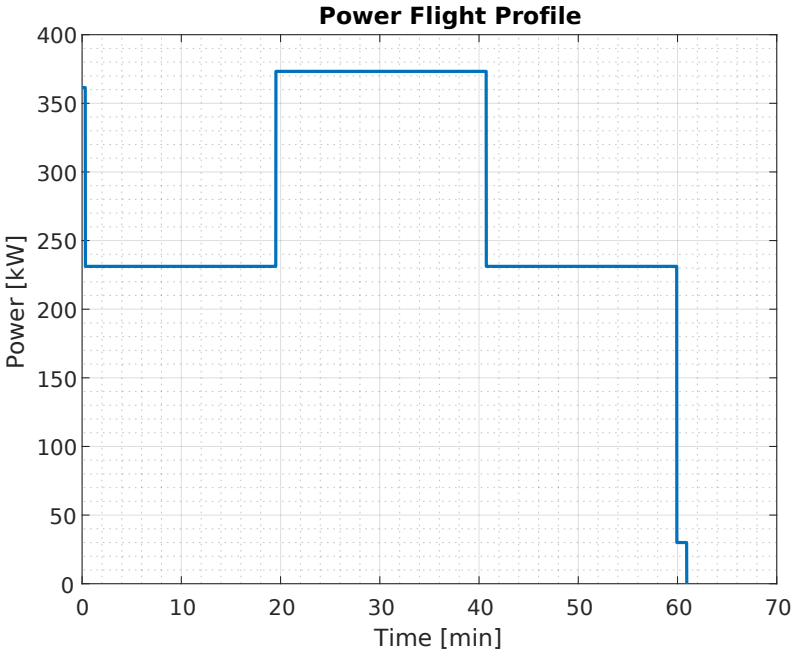


Figure 3.17: Example of power flight profile

atmosphere are computed thanks to Simulink built-in *ISA Atmosphere Model* [73], included in *Aerospace Blockset*. Finally, also a reduction in required power over time due to fuel consumption has to be taken into account. In order to achieve this result, the fuel used by engine is introduced in this block to compute the aircraft weight variation. This, through lift over drag ratio, can be related to drag variation and so to power reduction:

$$P_{req} = P_{FP} - \frac{m_{fuel}\, g}{E} V,$$

where $P_{req}$ is the actual required power, $P_{FP}$ is the constant (during each flight phase) power coming from CPT block, $m_{fuel}$ is the fuel mass consumed by combustion engine, $g$ is gravity acceleration, $E$ is lift over drag ratio of the considered flight phase and $V$ is the related airspeed. These computations are done at each time-step to provide the corrected required power that is used to compute commanded powers to each subsystems.

In case flight profile signals in CPT are provided in the form of time histories thanks to *From Workspace* block, it is assumed that power variation over altitude and weight reduction are already accounted for and so it is not necessary to modify the required power signal. However, atmospheric data has to be computed to be used in ICE block.

Independently of which method is used to provide the simulation flight profile data, the number of input and output of this block are the same as detailed in Table 3.12.

## 3.9 Power Management, Control and Delivery (PMCD)

The Power Management, Control and Delivery can be considered the core of the simulator: in this block signals provided by other subsystems are collected in order to check their status. Then, a request of demanded or output power is given to all the other systems. Both connections related to power flow and data transmissions are here included in order to follow a selected control strategy.

A first classification between power management systems can be introduced: these can be passive or active. A passive system is the simplest form of power controller. It only protects

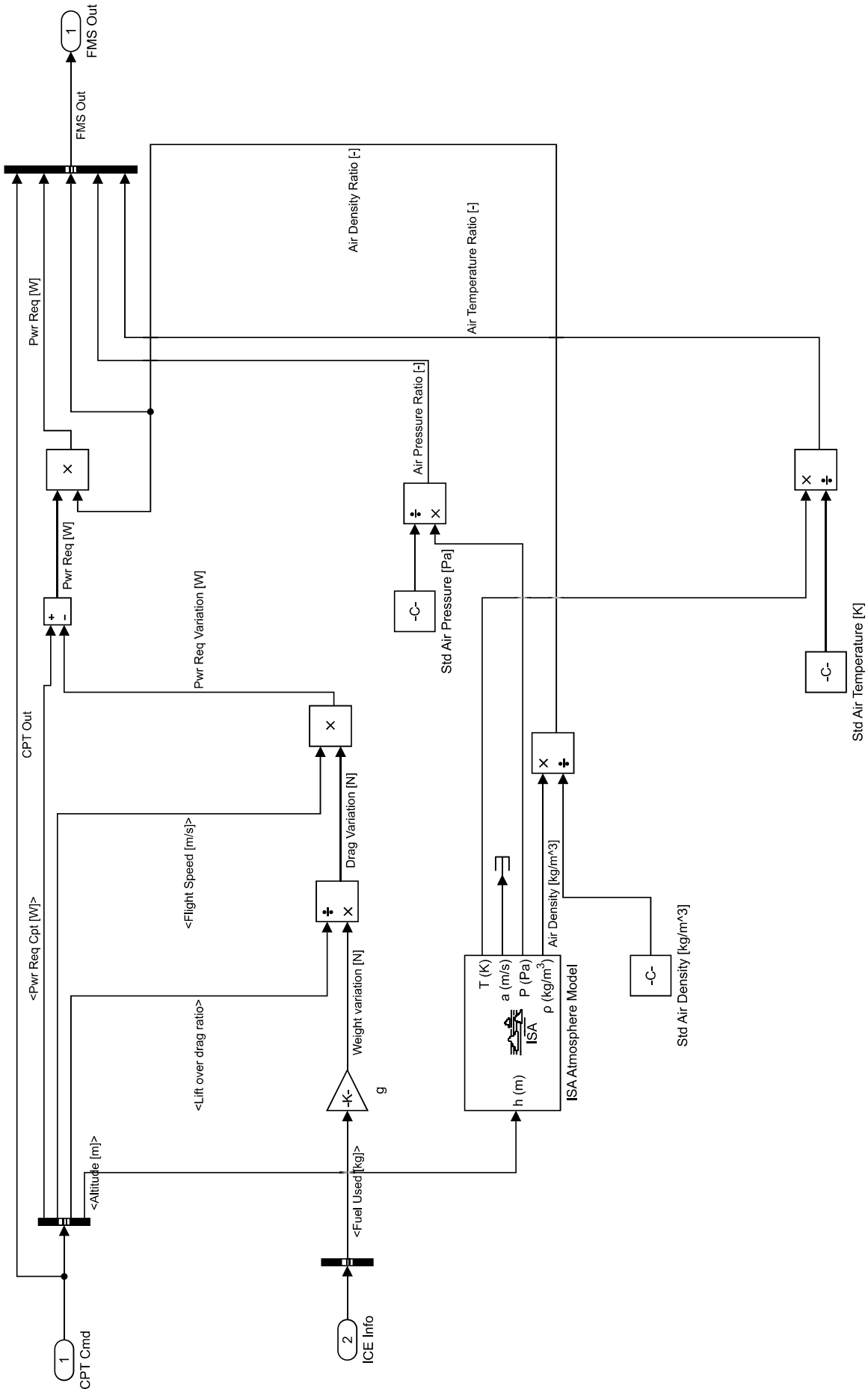


Figure 3.18: FMS/Math model

| Input | Description | Source |
|---|---|---|
| CPT Out | Output signal bus of CPT block | CPT |
| Pwr Req Cpt [W] | Required power | CPT |
| Flight Speed [m/s] | TAS related to the considered flight phase | CPT |
| Lift over drag ratio | Lift over drag ratio related to the flight phase | CPT |
| Altitude [m] | Aircraft current altitude | CPT |
| Fuel Used [kg] | Fuel used over time | ICE |

| Output | Description | Destination |
|---|---|---|
| CPT Out | Output signal bus of CPT block | PMCD, GBX, TGM, ICE |
| Pwr Req [W] | Required power corrected with density and weight variations | PMCD |
| Air Density Ratio [-] | Ratio between actual and standard air density | Not Used |
| Air Pressure Ratio [-] | Ratio between actual and standard air pressure | ICE |
| Air Temperature Ratio [-] | Ratio between actual and standard air temperature | ICE |

Table 3.12: FMS input and output

the power sources: the output power is manually controlled according to the behaviour of the system. In this kind of management system, each power source is directly connected to the power bus without a converter or controller in between, resulting in a benefit of weight reduction. Therefore, the output terminal voltage of every power source is the same as the bus voltage, meaning that the operational voltages of the solar cells, fuel cells and batteries should match to the bus voltage [3]. On the other hand an active power management system takes control of the individual power source, introducing more weight but with a beneficial effect on safety and power distribution efficiency over the system.

In active control systems, about which a good introduction to power management systems can be found in [74], three main categories of existing energy management and strategies can be found in literature. The first type employs simple and heuristic control techniques, such as the concept of battery load-levelling control strategy, that it is used as an example in this work. The logic attempts to operate the internal combustion engine in an efficient area while the battery acts as a load-levelling device: it is used to provide the remaining power demand [4] or to absorb extra-power provided by ICE, depending on the situation. Alternative approaches are based on optimisation methods that at each time-step determine the most efficient way to split required power between available energy sources by minimising a cost function: an example of performance index that can be used is the fuel mass consumed over a mission of a given duration, in addiction to other constraints such as emissions. The simplest methods are related to static optimisation, in which the controller structure is such that the considered output power is a function of the power demanded [75]. More sophisticated controllers are based on numerical optimisation methods, in which a cost function and constraints are considered in order to find the best operating condition for each subsystem. Direct numerical optimization

methods require substantial amounts of computational time. One approach that often permits a reduction of the computational effort is based on the minimum principle, that introduces an Hamiltonian function to be minimised. Several examples about implementation of these methods can be found in literature. Just for the sake of an example, in [4] static optimization algorithm aims at minimising the total equivalent fuel consumption, considered as the sum of the fuel consumption and battery energy consumption rates at each step, is applied to an hybrid-electric truck.

## 3.10 Battery load-levelling

One of the final aims of the proposed tool is considering different control strategies in order to provide a comparison between them. This, due to the large amount of work done in previous stages, has not been achieved and it would be author's pleasure to see this completed in the future. However, differences in powertrain configuration and involved subsystems modify the considered control strategy in terms of system to be controlled and input/output relations. The controller must be designed for each situation. For this reason a first discernment between series and parallel architecture is done in the proposed model through a *Variant Subsystem*: in each case, different control logics can be considered and can be managed in the form of *Variant Subsystem* too. In the applications, presented in 4, only a rule-based control logic has been implemented, with additional improvements in order to be exploited in different circumstances.

Considering the system presented in the previous sections, composed by a battery and a combustion engine, this strategy in general consists in ICE operating at minimum brake specific fuel consumption (BSFC) condition while battery levels gaps between required and provided by ICE power. In particular, when this difference is positive, so the required power is greater than the one provided by engine, batteries levels this difference discharging. When the difference is is negative, and so the power provided by engine is greater than the one required, the battery absorbs the extra-power charging itself: this can be considered the overall functioning strategy.

More in detail, considering a series configuration (the same applies also to parallel with few differences that are specified in the following), signals coming from subsystems are collected in PMCD block. Here, the difference between the required power coming from FMS and available power provided by TGM is computed. This difference can be considered as a 'power error' between the system output, namely the total available power, and a power reference value, also known as the required power. This quantity is the input of a PI controller, implemented with the corresponding Simulink built-in block [76], which constant are set by trial and error in order to satisfy robustness and performance of the simulation. PI controller provides a controlled required power. Then, a difference between this signal and the power provided by electric generator is computed, as presented in Figure 3.19, to evaluate the effective extra-power that is required by the system. In case of parallel configuration this difference is computed between controlled required power and power provided by engine. This surplus power, also named differential power in the model, can be both positive or negative, as already explained, and it is one of the input of three different operative situations that are considered in the tool, as presented in Figure 3.20. All these situations, detailed in the following, are controlled by an *If condition* [77], that, depending on the operative status (On and Off) of battery and ICE during the simulation, activates the desired strategy. Commanded input to engine and batteries are defined through this control logic. Also, other variables used in different blocks are defined in PMCD: for example, in the case of series configuration, the commanded electric motor power is computed from the sum of the powers coming from generator and battery. Considering a parallel system, the electric motor input power is only due to battery.

Changes to the control strategy can be easily done, also thanks to standardised relations

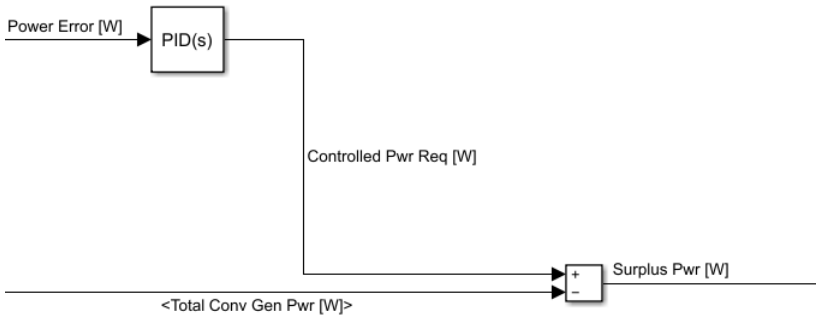


Figure 3.19: Computation of required power in battery load-levelling control logic

between blocks. Moreover, the possibility of introducing new components such as solar arrays or fuel cells can be reached with minimal changes.

### 3.10.1 ICE On, Battery On

This can be considered the nominal operating condition of a battery load-levelling control logic: in this situation both combustion engine and battery are cooperating to provide the correct amount of power required to fly. Since the input of ICE block depends on the type of engine modelled in the simulator, as discussed in Section 3.2, also in the control logic this distinction has to be taken into account: it is achieved thanks to a *Variant Subsystem*. Referring to spark ignition engine as example, the control logic is depicted in Figure 3.21.

Three inputs are considered: the surplus or differential power, the battery state of charge and the residual fuel. If the battery SOC is higher than a threshold fixed by user and the fuel level is higher to the one admissible, the ICE works at minimum BSFC condition while the battery provides extra power, until the selected minimum level of SOC is reached. Minimum BSFC condition is found from engine tabulated data through a proper Matlab function. Given the map of engine efficiencies and the corresponding inputs, that are different for the two types of considered engine, the function aims at finding the minimum value of BSFC in a given area of the map. The result of this optimisation function can be seen in Figure 3.22.

In case the battery level is lower than the minimum allowed, the engine is forced to work at maximum power operating condition, in attempt to provide enough power to fly and to charge batteries. Also in this situation, a Matlab function has been written in order to find the engine maximum output power condition from its tabulated data. In this situation, if the surplus power is negative, the battery is charging up to a prescribed SOC value. Once the maximum state of charge is reached, the system returns to nominal condition. In case the battery state of charge is higher than the maximum value, the battery can not absorb negative extra-power and so a reduction to engine output power is consider to match the required power. In order to do this, since ICE output torque, and so power, are defined through a two-dimensional map and the considered variable in this case is the extra-power provided by engine, the engine map must be inverted: given power as input it should provides commanded torque and speed (or commanded fuel injection and speed). This has been achieved thanks to another Matlab function that, considered the power range of the engine, divides this range in smaller, arbitrary defined, intervals. For each interval, the function finds the couple of torque and speed that provide the considered power and minimise BSFC. The result of this mapped data inversion can be found in Figure 3.23. In this way, a two-input (commanded torque and speed or commanded fuel injection and speed), one-output (power) correlation has been inverted in

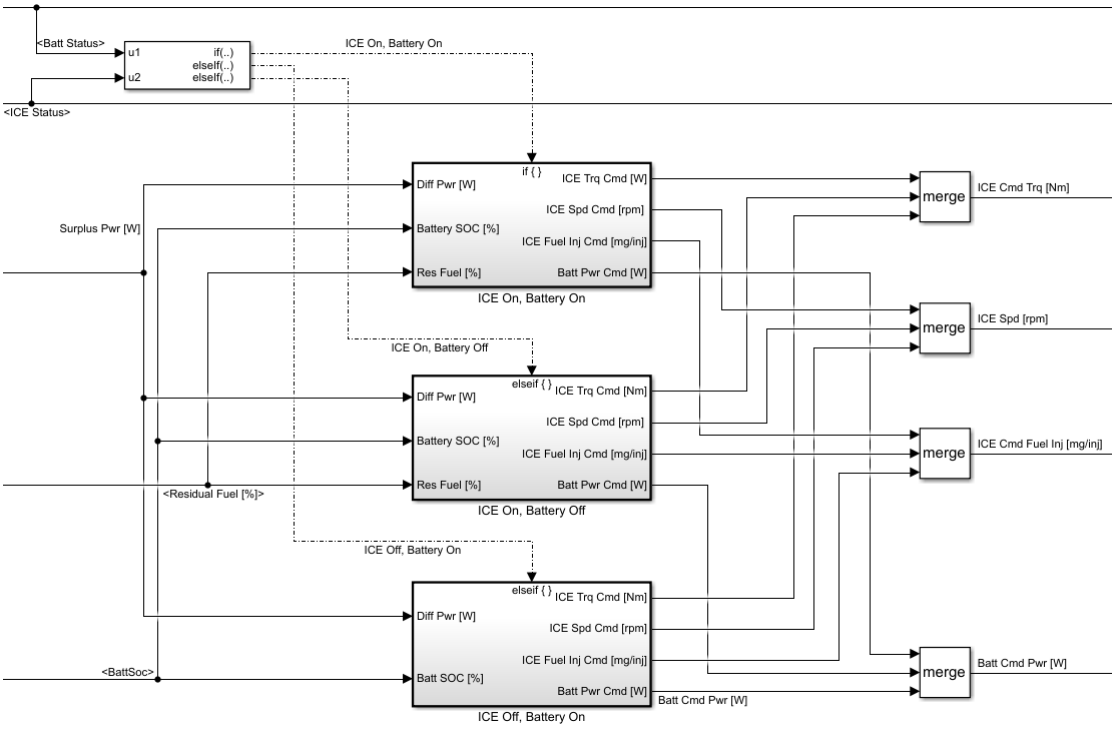


Figure 3.20: Operative cases in the control logic

one-input (power), two-output relation that it is managed through two one-dimensional lookup tables in the model.

A final case must be considered: when the residual fuel is lower than the one admissible. In this situation, ICE goes at minimum fuel consumption operative condition, providing a small amount of power, while the battery satisfies the request of power until it is completely discharged. Also in this case a proper Matlab function has been built to find ICE operative condition of interest.

It is important to note that even if three main engine operative conditions, minimum BSFC, maximum output power and minimum fuel flow, have been considered, one can exploit alternative conditions depending on the situation. For example, if the user does not want to use minimum engine efficiency condition but instead he wants to define a desired output power as nominal situation, it is possible just overwrite variables that define minimum BSFC condition with the new ones. Threshold values related to engines and batteries are set in configuration scripts detailed in Appendix A.

### 3.10.2 ICE Off, Battery On

This represents a pure electric operative condition of the powertrain: all the request of power is provided by battery, until a residual charge is present, while engine is switched off, as presented in Figure 3.24. This strategy can be very useful on ground and when flying at low altitude, for example during take-off and landing, in order to reduce noise and local emissions as presented in Chapter 1. Exploiting this condition, it is possible to simulate all-electric aircraft as presented in Section 4.

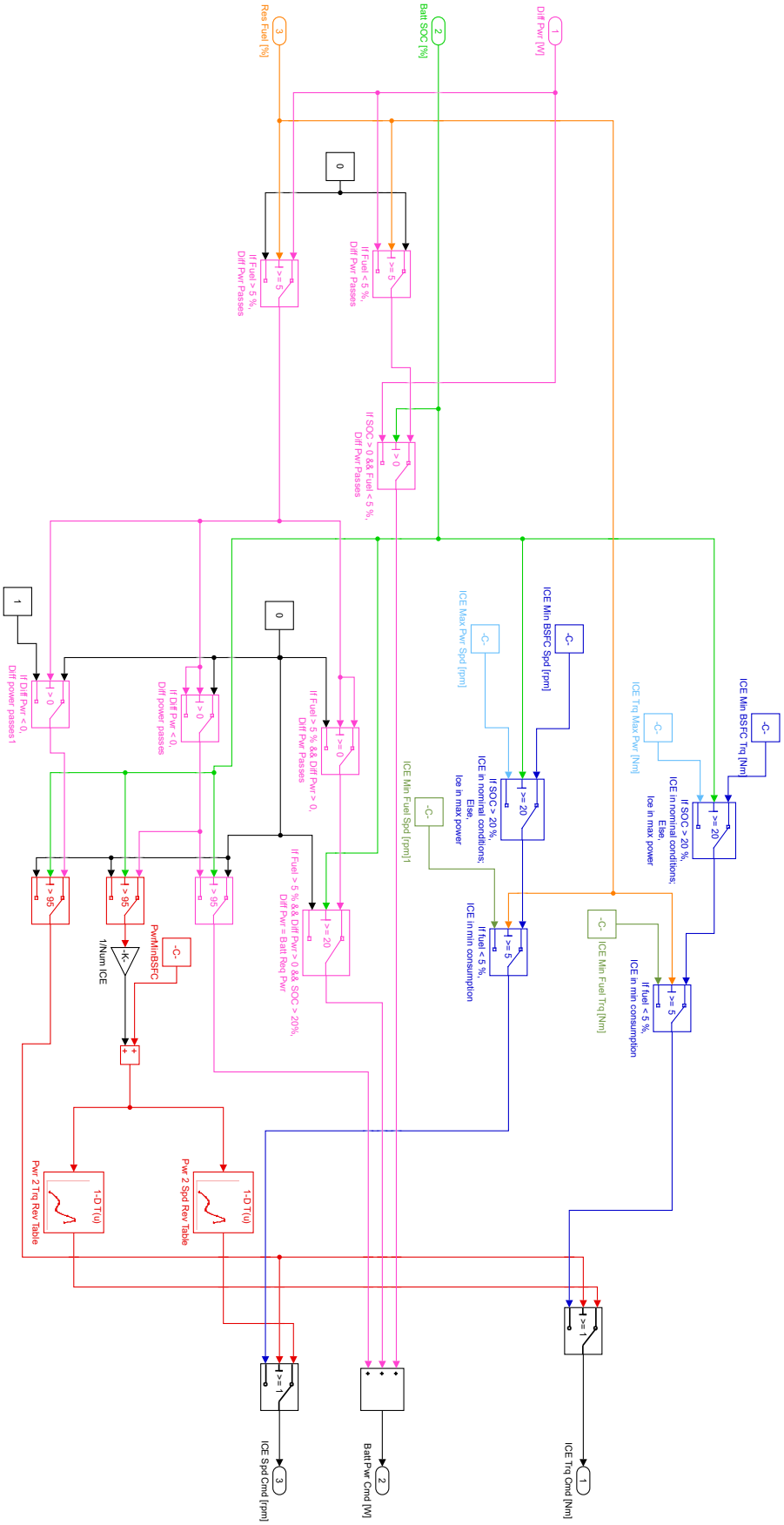


Figure 3.21: ICE On, Battery On control logic

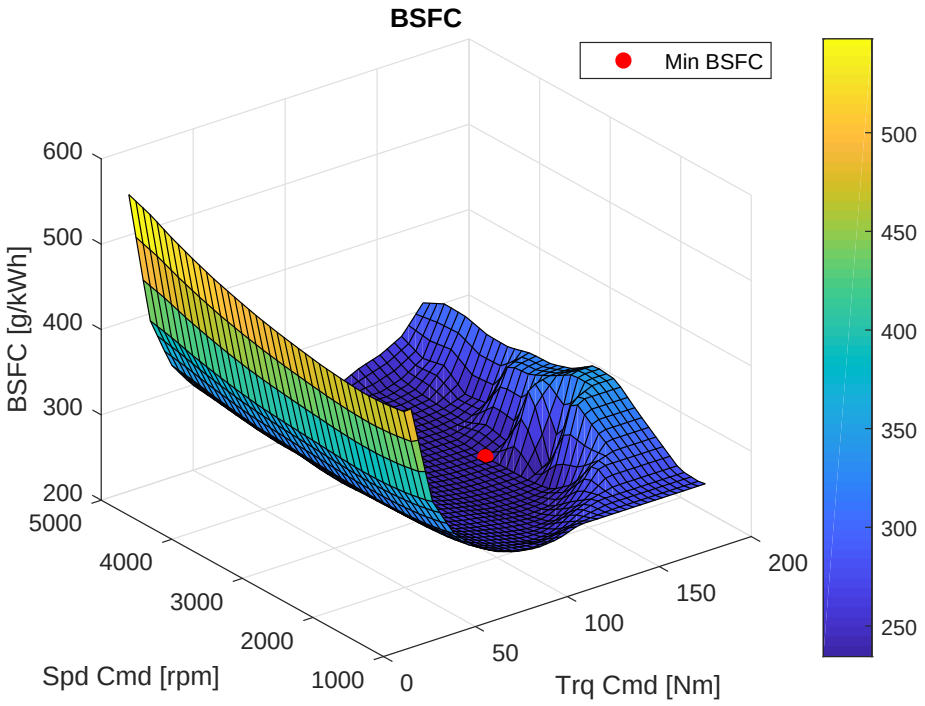


Figure 3.22: Minimum BSFC

### 3.10.3 ICE On, Battery Off

In this situation the battery does not provide power to fly and so, if the battery SOC is enough high, the engine output power matches the one required. However, in the case the battery level is lower than the one admissible, more power is required to engine in order to provide enough power to fly and to charge battery. Negative extra-power is absorbed from battery during charhe until a maximum SOC value is reached. In case the residual fuel is lower than a prescribed value, the battery is activated in order to produce electrical power while the ICE is set to minimum fuel consumption operative condition, as it is possible to see in Figure 3.25. This control strategy could be exploited after the one presented in Section 3.10.2 is used, in order to charge batteries during cruise.

A *Variant Subsystem* is used to take into account different types of engine.

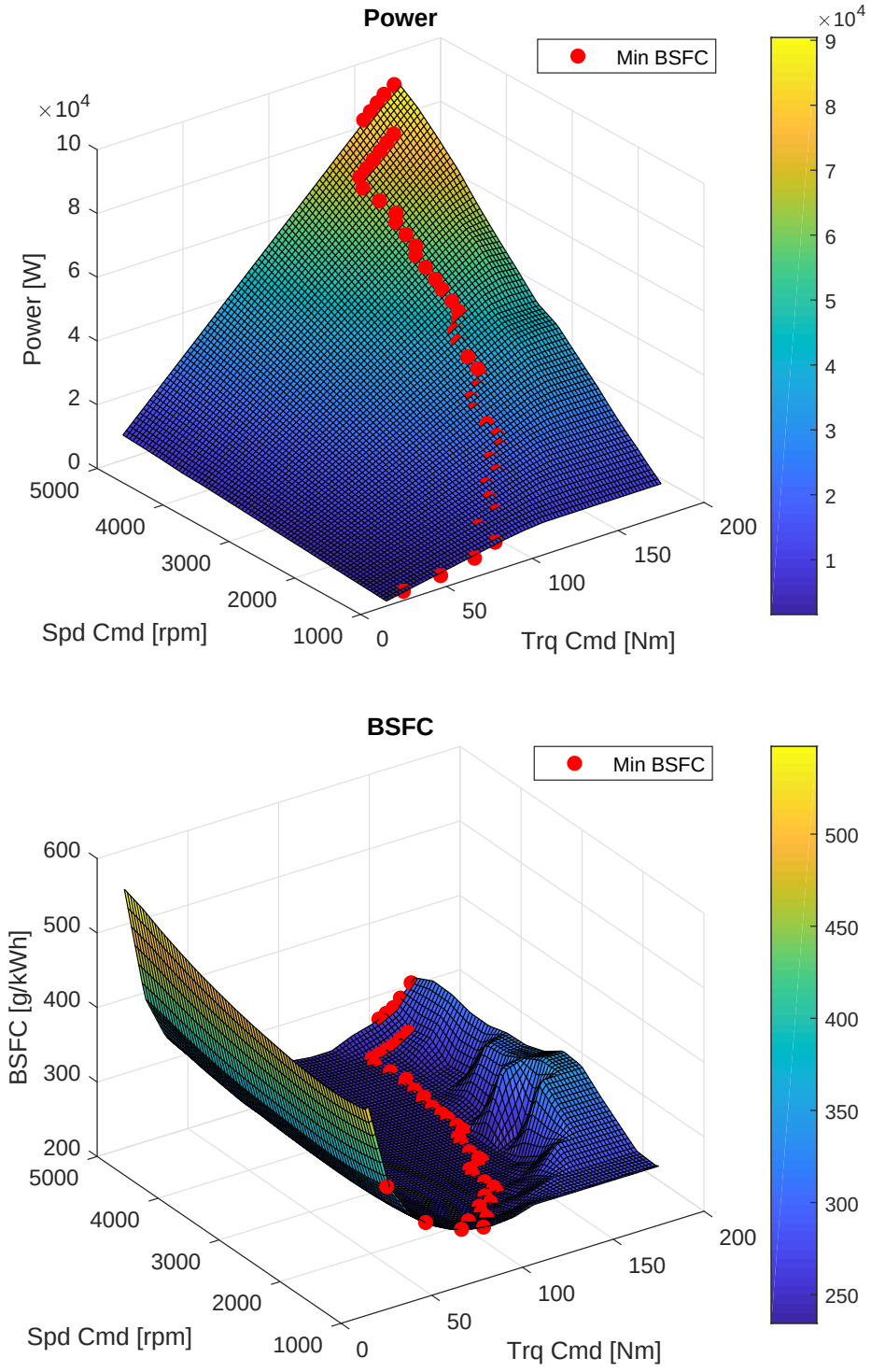


Figure 3.23: Inversion of engine mapped data to find operative conditions given a value of power

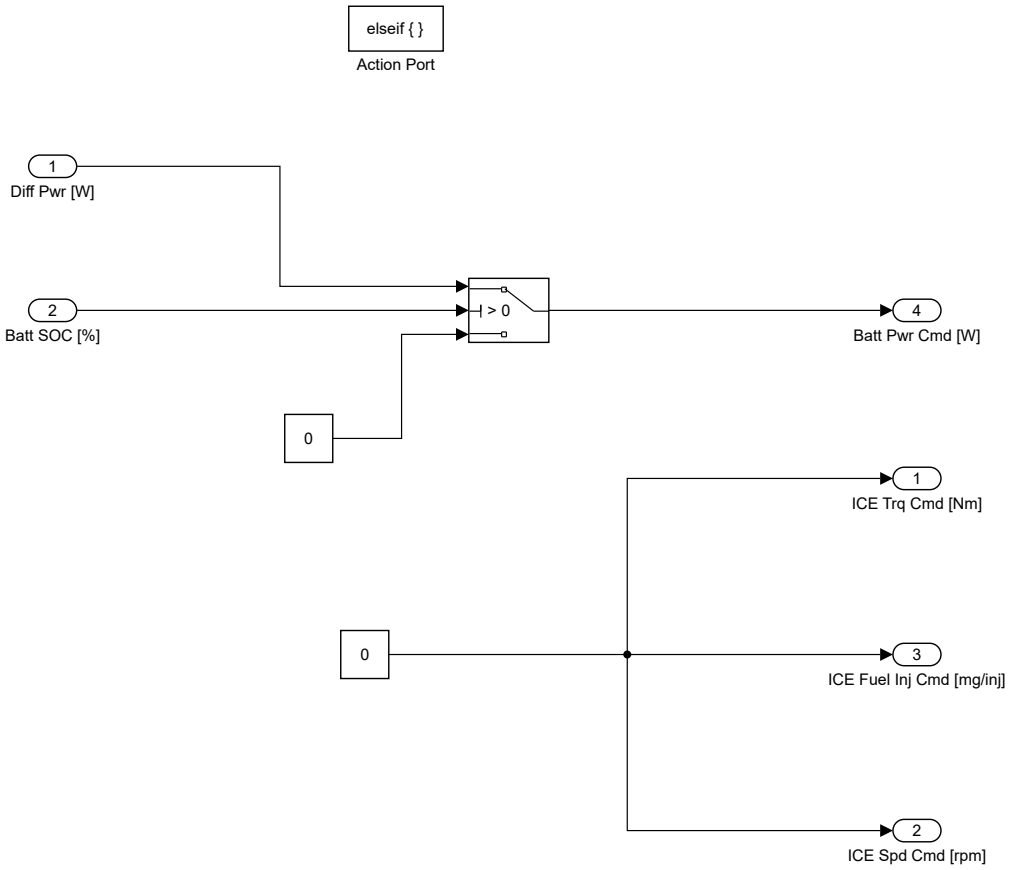


Figure 3.24: ICE Off, Battery On control logic

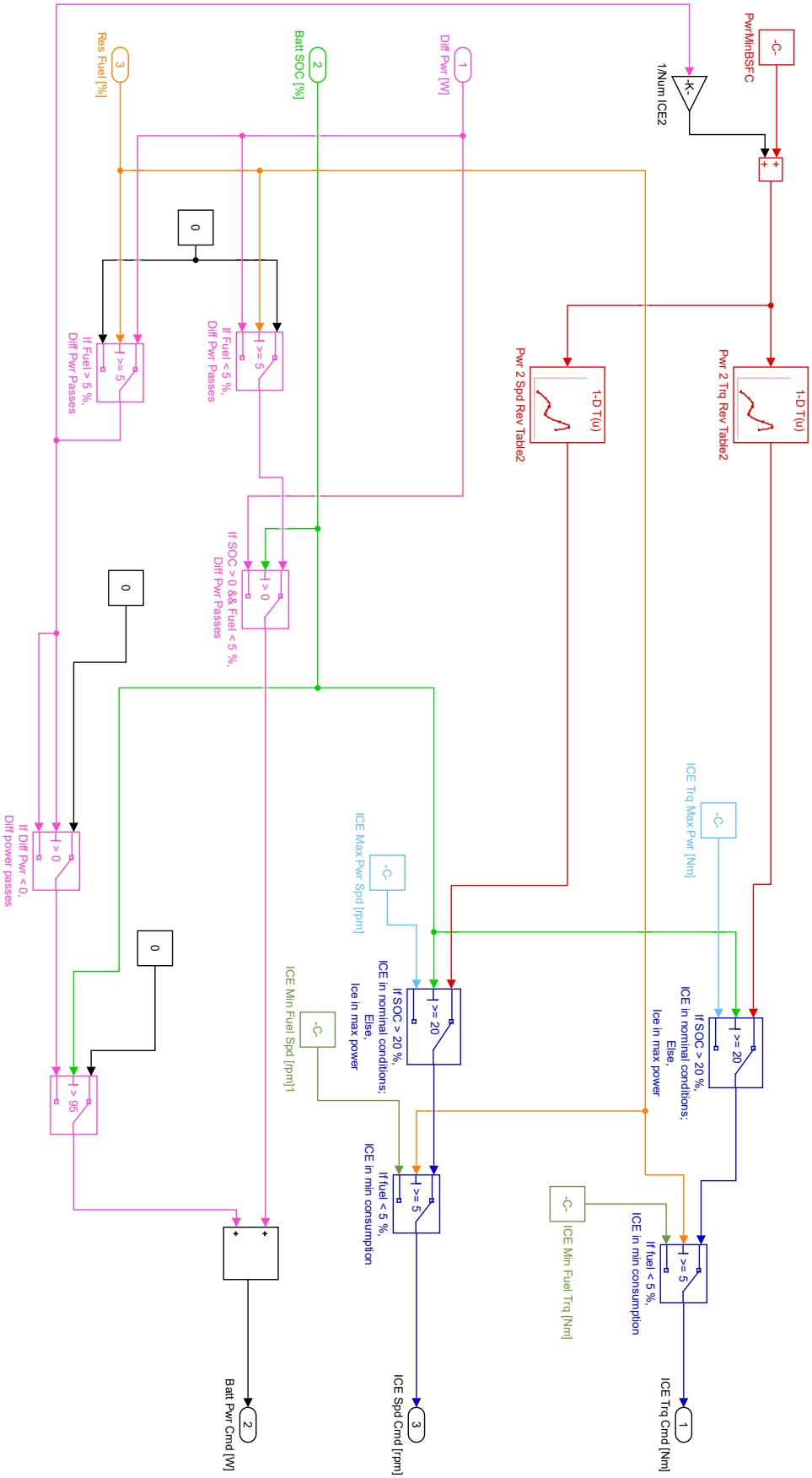


Figure 3.25: ICE On, Battery Off control logic

# Chapter 4

# Applications

Once the model presented in Chapter 3 has been developed, three different aircraft powertrains have been considered in order to show characteristics and usability of the simulator. In particular, one all-electric aircraft and two hybrid systems, one series and one parallel, have been taken into account. These, as already discussed in Introduction, are preliminary design concepts coming from students who attained Aircraft Design Course held of Politecnico di Milano by Professor Trainelli. This has allowed to easily retrieve data used to set up simulations.

It was also possible to investigate how systems vary with respect to different parameters or models used in the simulation. This feature could be very useful when developing a new aircraft because, if the model is sufficiently accurate, it can show design failures or critical components shortcomings.

The considered vehicles are briefly described and simulation results are presented in the following sections, also considering some examples of possible parametric studies.

Data is taken from corresponding project reports. If parameters or tabulated maps were not available, the default built-in blocks values were exploited, eventually scaled in order to match the correct trend and magnitude.

Since the whole mission of each aircraft was simulated, a variable step solver based on Matlab *ode23tb* has been exploited to improve simulation time efficiency. If other situations are under investigation, such as single high-g manoeuvrers, a different solver may be selected to provide higher accuracy.

## 4.1 All electric: Project A

Project A is an all-electric aircraft that was designed starting from the following application:

> "Study the possibility to exploit the existing small local airport European network to provide a micro-feeder service to larger hubs through a small passenger hybrid or all-electric airplane, starting in 2025-2030. The service should seek to enable the ACARE policy towards a 4-hour door-to-door total journey time reduction. Design such an airplane and provide a complete operational model for its usage".

The team, composed by seven students, after more than one year of work presented the result depicted in Figures 4.1 and 4.2. It is an eight-passengers, twin-engine, all-electric aircraft with a maximum take-off weight higher than 3000 kg. Thanks to 480 Ah batteries, the airplane is expected to cruise at 8000 ft with a speed of 220 knots up to 270 km [78].

| | Valore | Unità di misura |
|---|---|---|
| **Equipaggio** | 1 | [-] |
| **Numero di passeggeri** | 8 | [-] |
| **MTOW** | 3062 | [$kg$] |
| **Propulsione** | Elettrica | [-] |
| **Numero di motori** | 2 | [-] |
| **Potenza motori** | 540 | [$kW$] |
| **Capacità delle batterie** | 480 | [$Ah$] |
| **Superficie alare** | 20.2 | [$m^2$] |
| **$C_l$ al decollo** | 2.0 | [-] |
| **$C_l$ all'atterraggio** | 2.6 | [-] |
| **Velocità di crociera** | 220 | [$kn$] |
| **Quota di crociera** | 8000 | [$ft$] |
| **Range** | 268 | [$km$] |
| **Endurance** | 56 | [$min$] |

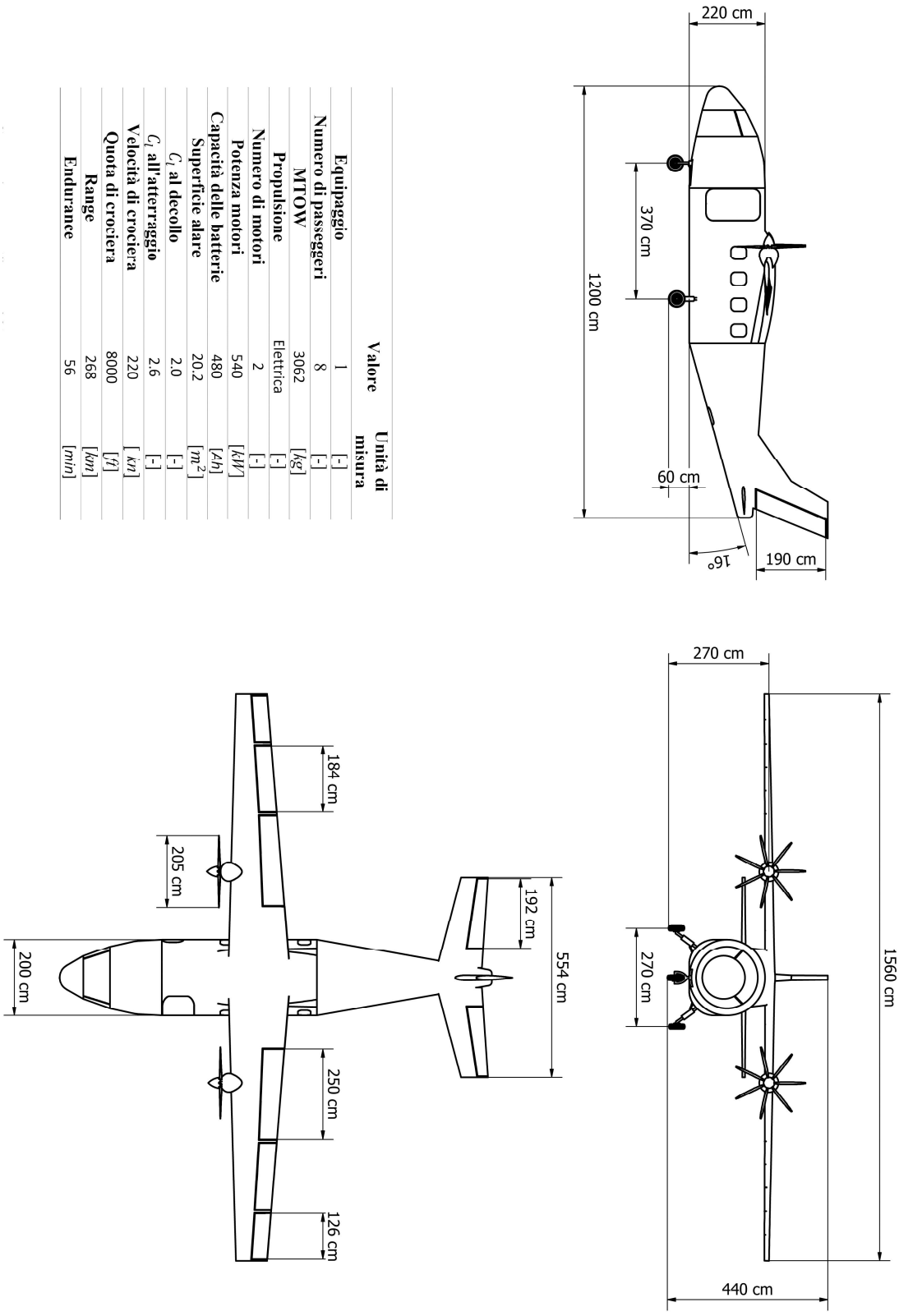


Figure 4.1: Project A - three views, [78]

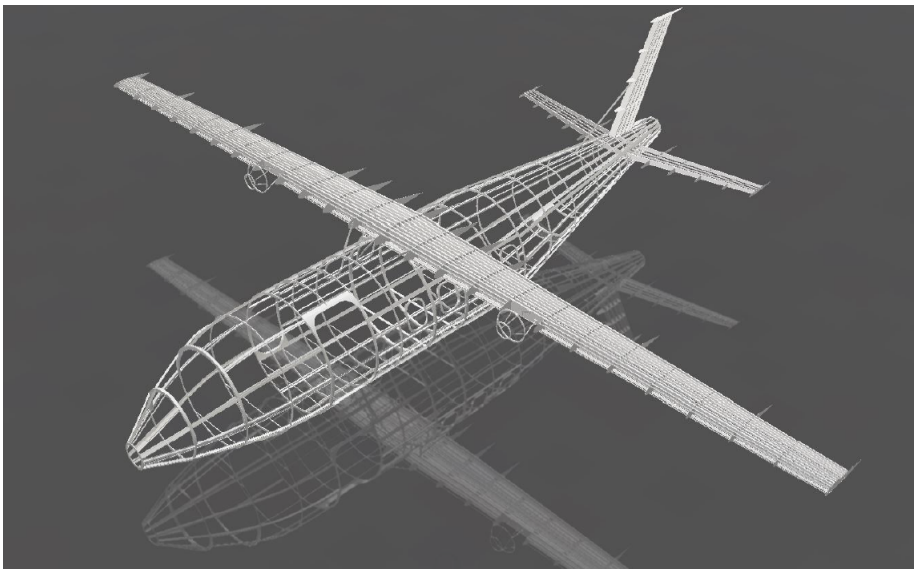

Figure 4.2: Project A - structure, [78]

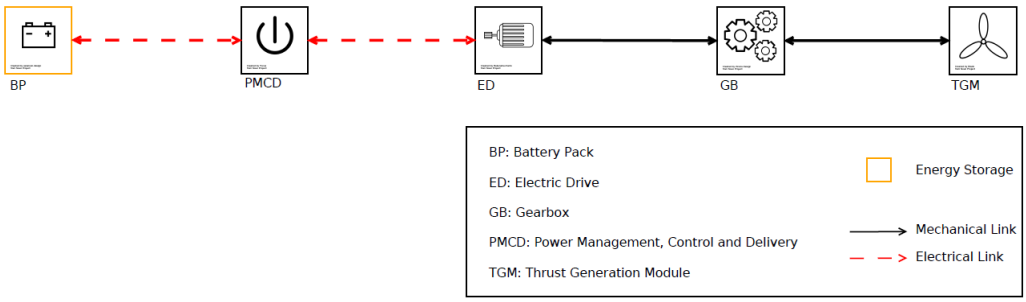


Figure 4.3: Project A - powertrain

It is important to note that even if the tool is not developed specifically to simulate all-electric aircraft, it allows to provide an analysis of this kind of powertrain as well. The scheme of the powertrain is shown in Figure 4.3.

For this particular aircraft, a series configuration is set in the tool, considering the engine switched off since it has not to be considered. DC-DC converter efficiency is modelled using both strategies presented in Section 3.1.2, in order to show differences between the two simulations, if any. The flight profile is defined through the step-varying method discussed in 3.7. Electric motor and related converter efficiencies are considered as constants, while propeller efficiency is provided in the form of map, as discussed in Section 3.6, for three different blade pitch angles.

After parameters and aircraft characteristics are set in scripts, as presented in Chapter 3 and in Appendix A, it is possible to run the simulation. Some of possible results are presented in Figures 4.4, 4.5 and 4.6.

In Figure 4.4 an overview of the mission is depicted: in the top plot the power time history is presented referring to powertrain main systems. Required, in solid blue, and available power, in dashed red, are superimposed during the whole flight, proving that the aircraft was correctly designed. Propeller efficiency makes propeller shaft power, depicted in yellow, higher than reference value. Power provided by battery, shown in purple, is higher than the others because several efficiencies are considered in the power flow.

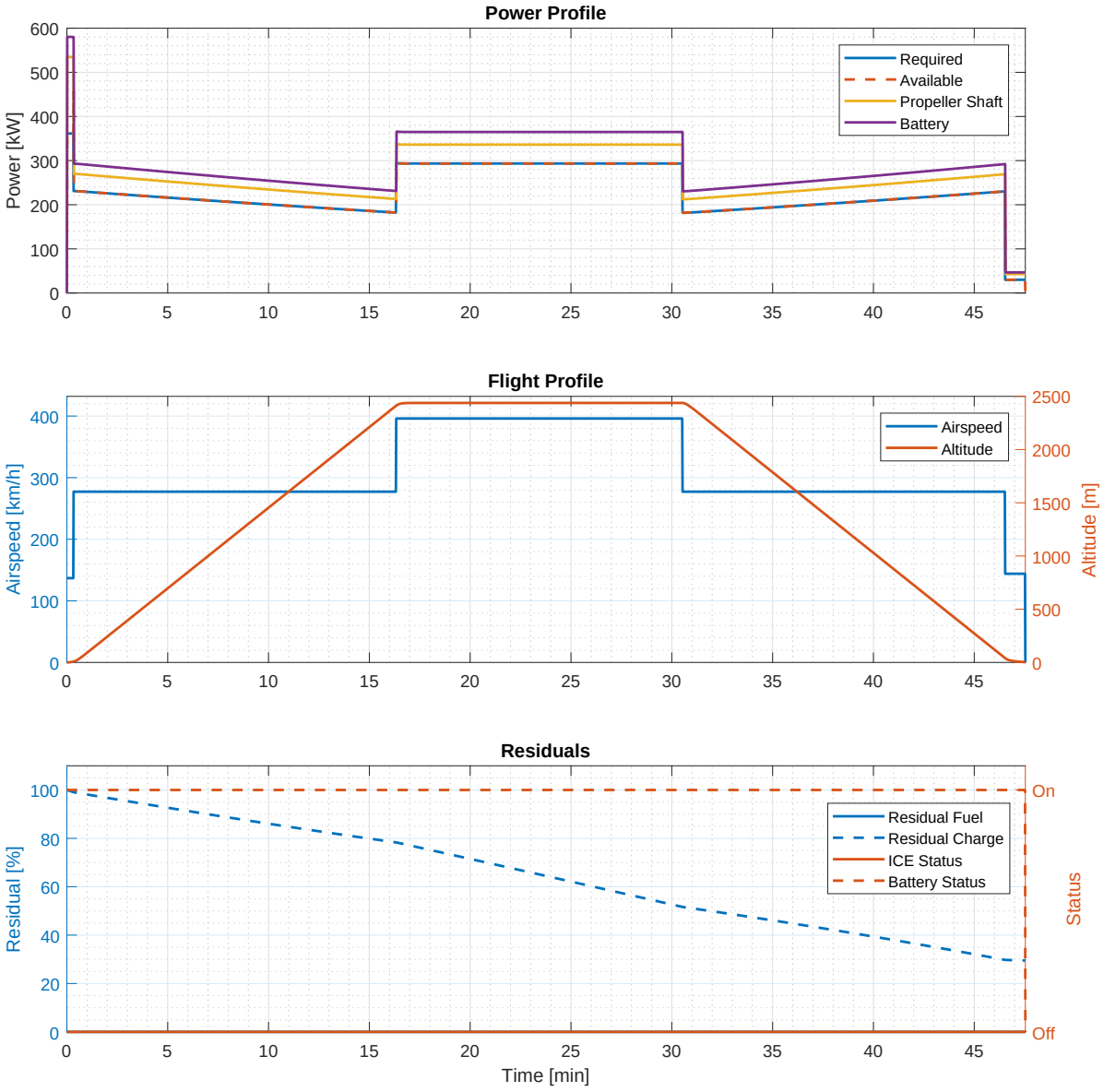


Figure 4.4: Project A - mission profile simulation

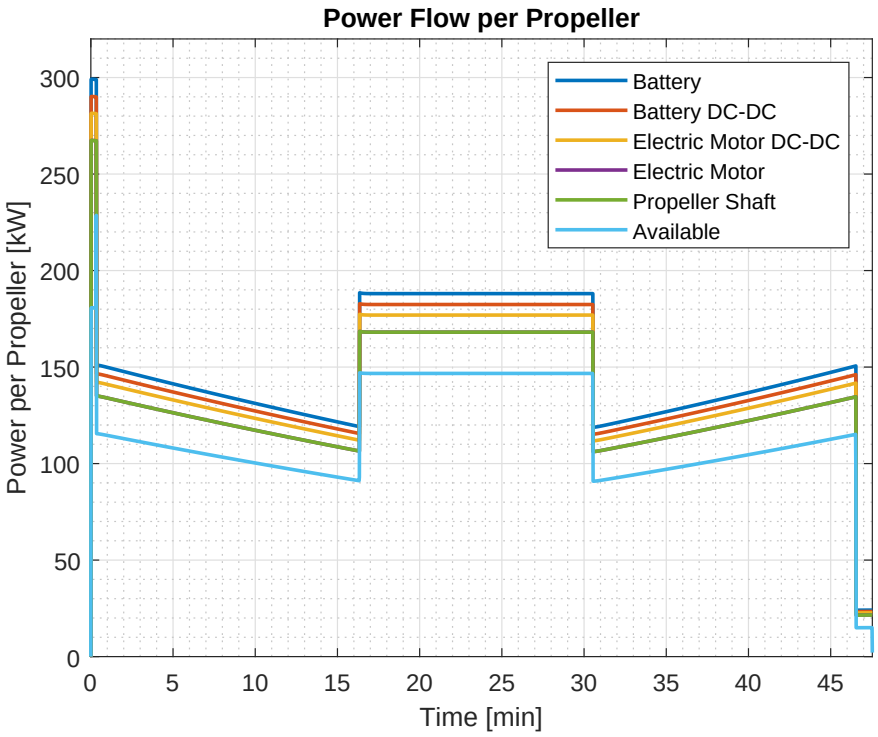


Figure 4.5: Project A - power flow simulation

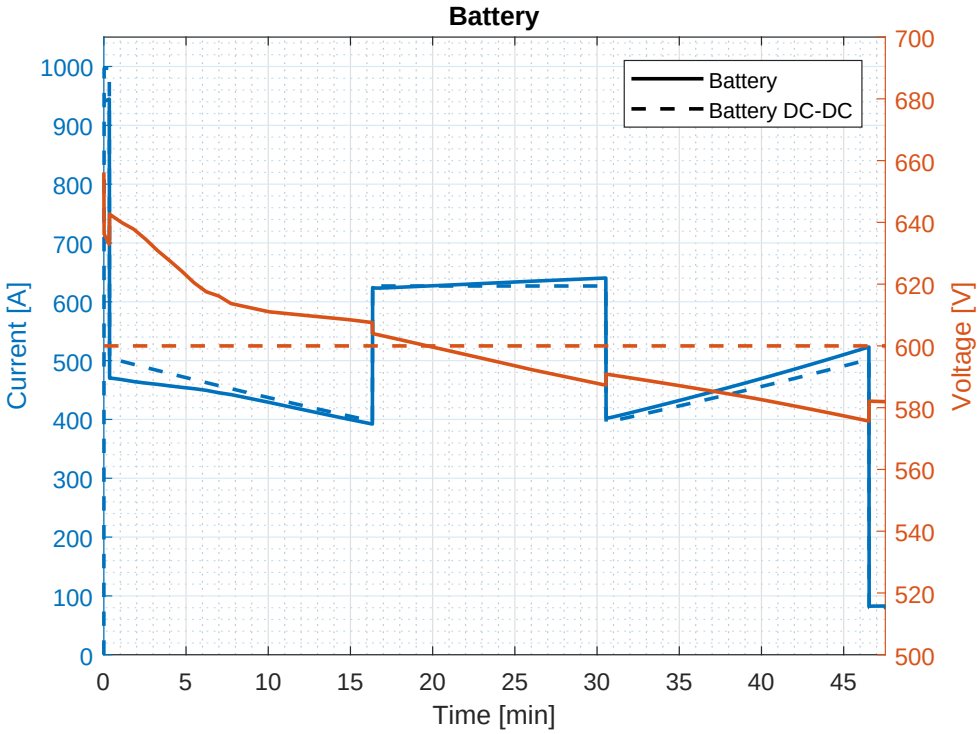


Figure 4.6: Project A - battery pack simulation

At the end of the mission the residual charge is equal to 30%, similarly to team estimates, even if, during designing phase, efficiencies related to converters and motors have not been taken into account. It is clear that, because of high efficiency values of these components, this miss does not lead in a design failure. It is important to point out that the simulated state of charge is overestimated because the loiter phase is not considered, as it is possible to see from the graph in the middle: this could not be a problem since a sufficient amount of charge to cover loiter is present at the end of the simulation. Also, this phase is characterised by low required power to batteries.

In the same figure the status of each power system is presented: the battery status, shown by a dashed line, is always on, while ICE is switched off during the entire mission. In this way the tool, developed to simulate hybrid-electric powertrain, can model all-electric aircraft. In dashed blue is presented the battery state of charge: it is possible to note that climb, cruise and descent are characterised by different rate of discharge since required powers during each phase are distinct.

In Figure 4.5 it is possible to have a look at power time histories of relevant subsystems considered in the model: a first power loss is due to converter between battery and electrical bus, as it is possible to note from the power gap between power provided by battery, in blue, and output power of converter, presented in red. Then, another conversion is needed to provide electricity to motors, and so a difference between red line and yellow one, related to output power of the motor converter, is visible. Since a direct drive between motor and propeller is considered in this aircraft, electric motor output power, drawn in purple but not visible, is equal to the one delivered to propeller shaft, shown in green. Finally, propeller efficiency is used to compute the overall available power for flight, that it is presented in light blue.

The tool has been developed with the possibility to investigate any variable of each block of interest during simulation and analysis. An example of this can be found in Figure 4.6, in which battery states are shown. This system can be considered the core of this kind of airplane, since it is the only energy source of the system. Hence, a detailed depiction of its variables could be very useful in this phase. In the mentioned picture, both currents, in blue, and voltages, in red, of battery and DC to DC converter are presented. Battery voltage, shown in solid line, decreases during time, in agreement with Figure 3.2, while converter voltage, presented by dashed line, is constant and equal to the target value. Small discontinuities in battery voltage are due to sudden changes in required power, since it is defined through steps. This does not affect the simulation: battery SOC time history does not show discontinuities. A possible solution to this issue has been developed, however this led to simulation problems, as presented in Section 3.7. Currents of the two subsystems are depicted with blue lines in the considered graph. Converter output current is higher than battery during first phases of flight because battery voltage is higher than the one required by electric system: in this condition the converter is acting as a step-down device. When the battery output voltage is lower than the target one, the converter is acting in the dual mode.

Different results can be obtained considering a tabulated efficiency map of DC-DC converter instead of a single constant value, as presented in Section 3.1.2. In this case, a modification in the Simulink model is needed, since the type of efficiency model used during simulation is set through a block mask. Results, related to mapped efficiency, are shown in Figure 4.7, in which conditions different from converter design point, selected to guarantee best performance during cruise, are more penalised with a lower efficiency. Considering more than one efficiency measurement allows to provide an higher fidelity model, reducing the gap between simulation and real system. In particular, higher current values during take-off, climb and descent can be noted in the second case than in the previous one. This lead to a faster battery discharge, as it is possible to note in Figure 4.8, in which the comparison between states of charge is displayed.

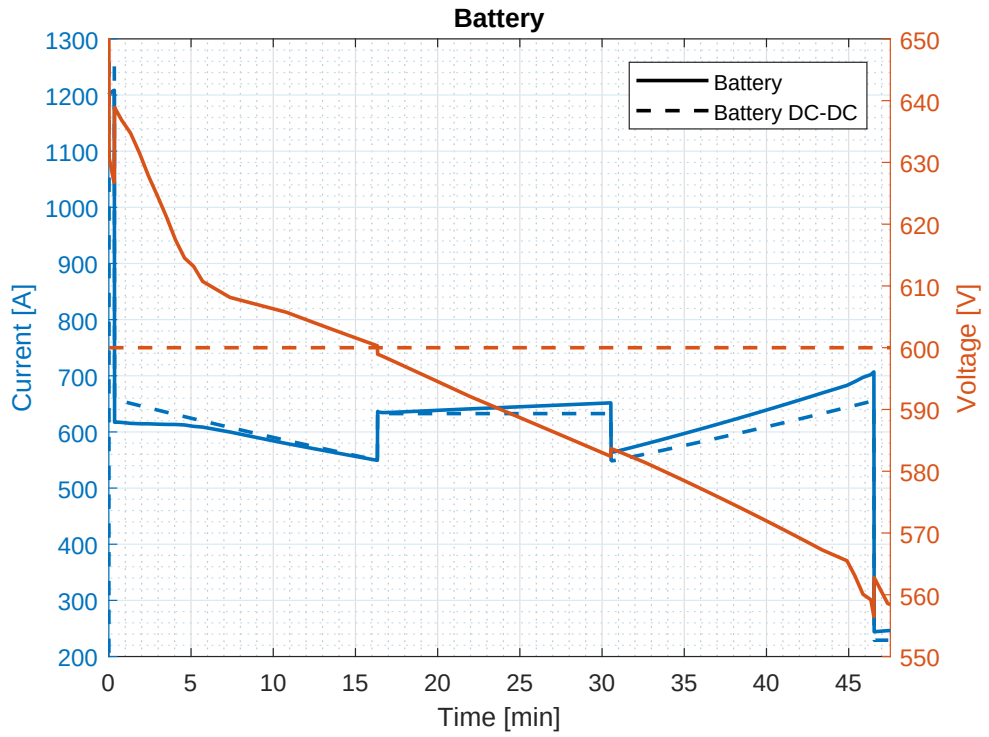


Figure 4.7: Project A - battery pack simulation using efficiency map

The second simulation is characterised by an higher power provided by battery because of lower efficiency values in flight phases different from cruise, leading to a faster discharge of the battery: at the end of the considered mission a difference of 18% in the final state of charge can be noted. A possible design solution that comes from this analysis could be in considering another converter that have a lower efficiency during cruise but higher values in other phases.

## 4.2 Serial hybrid: Hybris

Hybris team was founded in October 2015 to participate to the design competition "'E' conditions Fixed-Wing Aircraft Design Challenge 2016" launched by RAeS. The result is a four-seat, series hybrid aircraft, designed for tourism and training, with a maximum take-off weight of 1300 kg, a cruise altitude of 8000 ft and a range of 825 km [79]. The reference touring mission is considered in this analysis. In particular, a different power management is exploited depending on altitude: below 3000 ft (925 m) the propulsion is purely electric, while at higher altitude an hybrid propulsion is used, as presented in Figure 4.9. In this way, a strong reduction of noise and emissions on ground is achieved. The powertrain scheme is presented in Figure 4.10.

Another new technology is introduced in this aircraft and it is related to structural batteries, that are carbon fibre composites capable of storing electric energy and can also been exploited for structural tasks, as depicted in Figure 4.11. Since this type of battery, up to now, has limited performance, another kind of battery has been added in order to achieve the desired energy capacity. To simulate this feature, only standard batteries have been considered, taking into account a number of cells that allow to reach the total amount of charge required by the mission.

The selected engine for the aircraft is a diesel engine. Due to lack of data, default maps of compression ignition engine block have been used, scaled in order to reproduce the considered

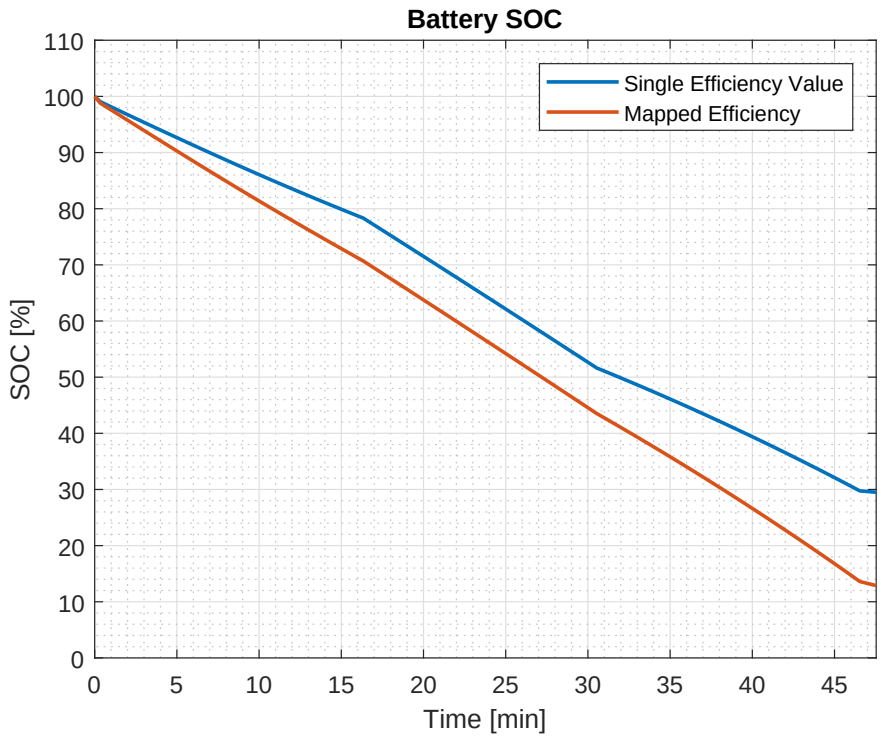


Figure 4.8: Project A - battery SOC comparison

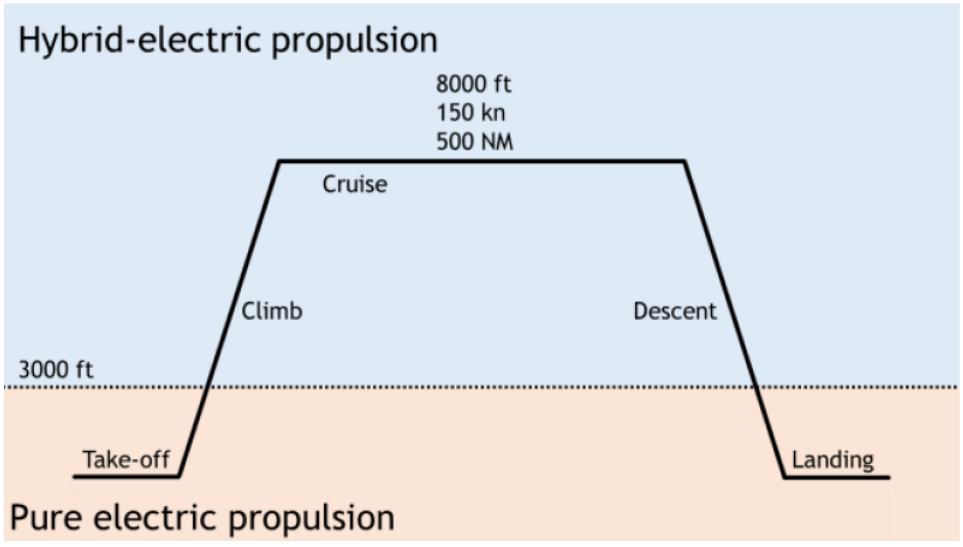


Figure 4.9: Hybris - propulsion strategy, [79]

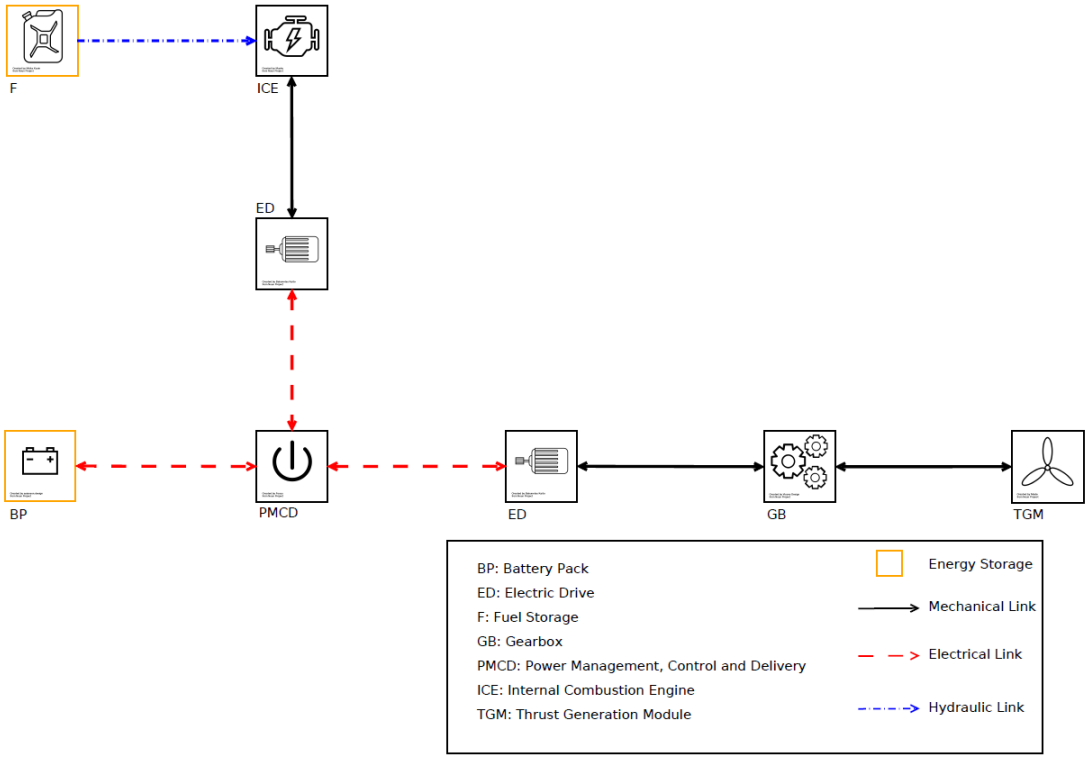


Figure 4.10: Hybris - powertrain

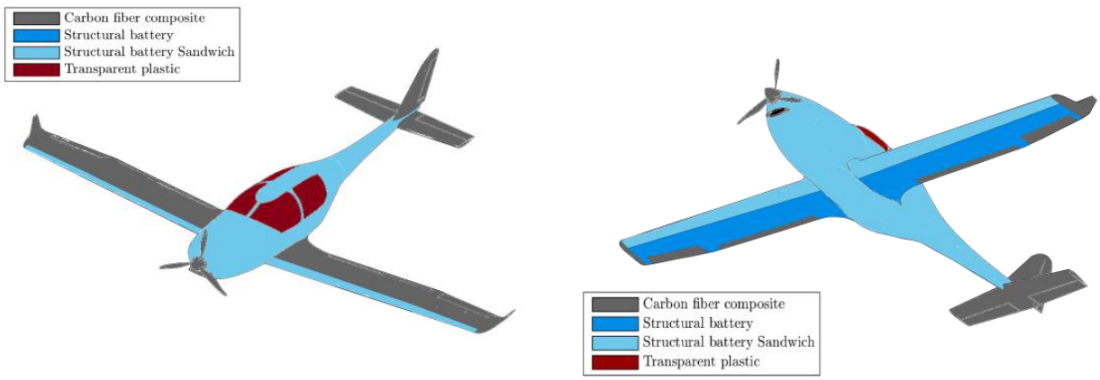


Figure 4.11: Hybris - structural materials, [79]

engine. Power for each flight phase has been estimated from maximum power provided by engine because these values were not provided in the report [80]. For what concerns propeller, only one pitch setting, representing the whole efficiency envelope, has been considered to model this component.

In Figure 4.12, it is depicted an overview of the simulation. During the electric propulsion phase, the battery rate of discharge is very high: after seven minutes the SOC is equal to 55%, as it is possible to note from the graph on the bottom, in which battery state of charge is presented by a dashed blue line. It is evident that, when aircraft reaches the selected altitude, ICE is turned on, as it is possible to note both in the graph on the top, where the green line shows the generator output power, and in the plot on the bottom, where in solid red line it is depicted the status of the diesel engine. After the ICE is turned on, the power provided by the battery, shown in purple, is reduced. During cruise, engine provides most of the required power while battery is delivering a small amount of it. When the aircraft is in the descent phase, batteries are charging because the power delivered by engine is greater than the one required to fly. In this way, available power, shown in dashed red line, matches the required power, in solid blue, since the amount of power required to fly and power absorbed by battery is equal to the one provided by engine, considering generator losses. It is possible to note that, differently from the previous case, required power decreases during flight: this is due to fuel weight reduction.

In this case the graph related to power flow in the system is more complicated than the one in the case of all-electric aircraft, as shown in Figure 4.13, because of the differences in powertrain schemes. Differently from the previous case, the power flow related to ICE is present. In particular, the mechanical power provided by engine, presented in yellow, is transformed into electrical power thanks to a generator. The power transformation loss is evident in the figure, since a gap between the yellow line and the purple one, representing the generator electrical output power, is present. Then, a converter modifies voltage and current to admissible values of electrical bus, taking into account the efficiency of the converter, as depicted by green line. The efficiency of DC-DC converter is noticeable since power provided by battery, shown in solid blue, and output converter power, presented in solid red, are slightly different. In PMCD both electric powers are merged and delivered to electric motor, shown in dark red. Also in this case, propeller shaft power, displayed in dashed blue, is superimposed to the one related to motor because direct drive is considered. Power related to battery, except for the phases in which engine is turned off, is low since it has only to level differences between ICE and required powers.

Current and voltage time histories, for both battery, in solid lines, and related converter, in dashed lines, are presented in Figure 4.14. Current, depicted in blue, is negative when battery is charging, following conventions defined in Section 3.1.2, while voltage, shown by red line, is increasing. In the same fashion as Project A powertrain simulation, discontinuities are due to sudden variations of flight profile quantities.

ICE states of interest are presented in Figure 4.15, in which it is quite clear that engine is turned on some minutes after take-off and operates at the designed condition for the rest of the mission until it is switched off, following the prescribed propulsive strategy.

Considering a change in the selected altitude at which engine is turned on, it is possible to point out some considerations. Results are presented in Figure 4.16. In particular, a value of 800 m instead of 925 m has been considered in this case. Differently from the nominal situation, residual charge at the end of the mission is equal to 20% while in the previous simulation it was 10%, as it is possible to note from Figure 4.17. This is due to a shorter time in which only battery is exploited to power electric motor since the reference altitude is reduced. Instead, no noticeable differences in fuel consumption appear. It is possible to conclude that in the second

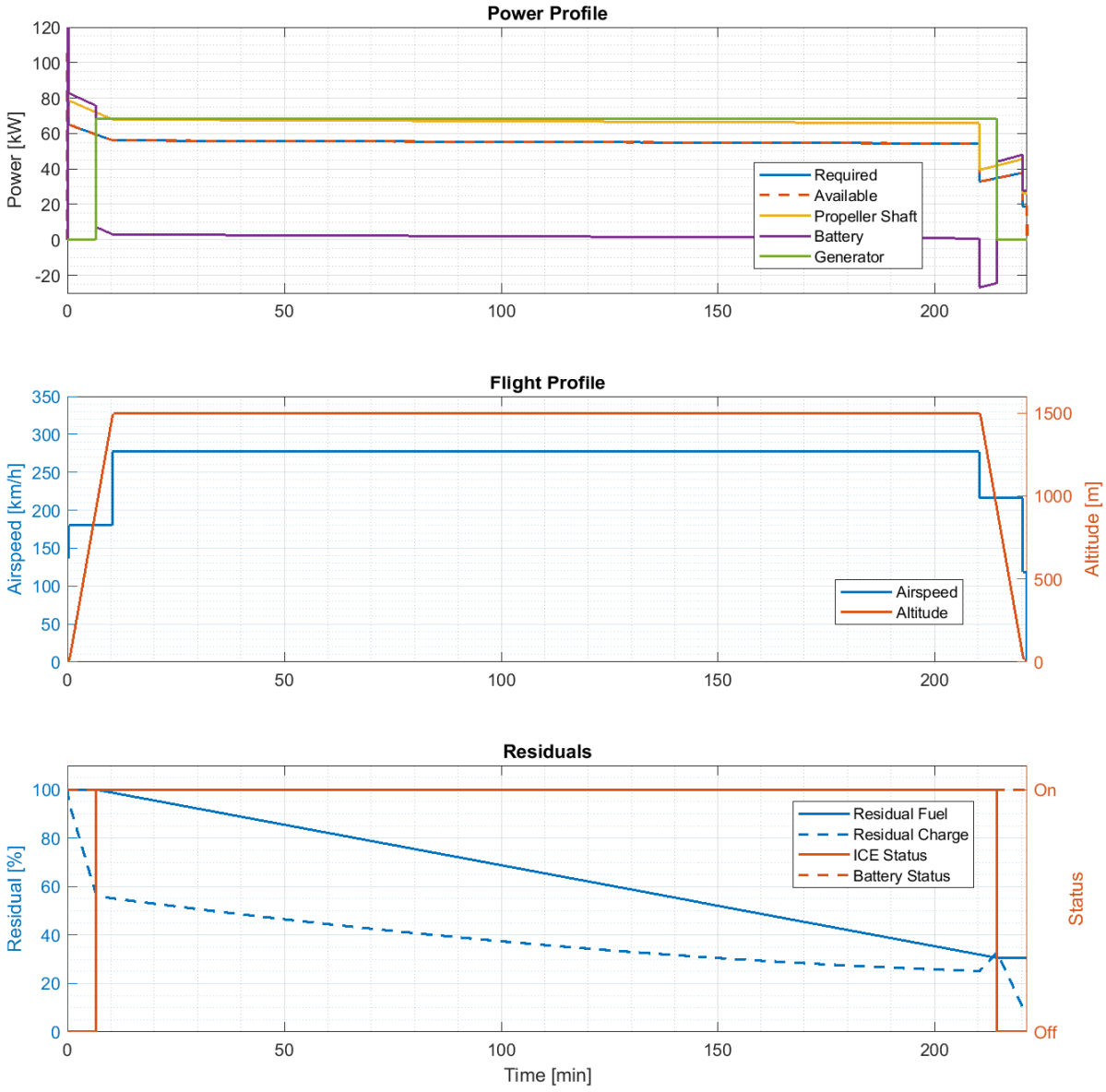


Figure 4.12: Hybris - mission profile simulation

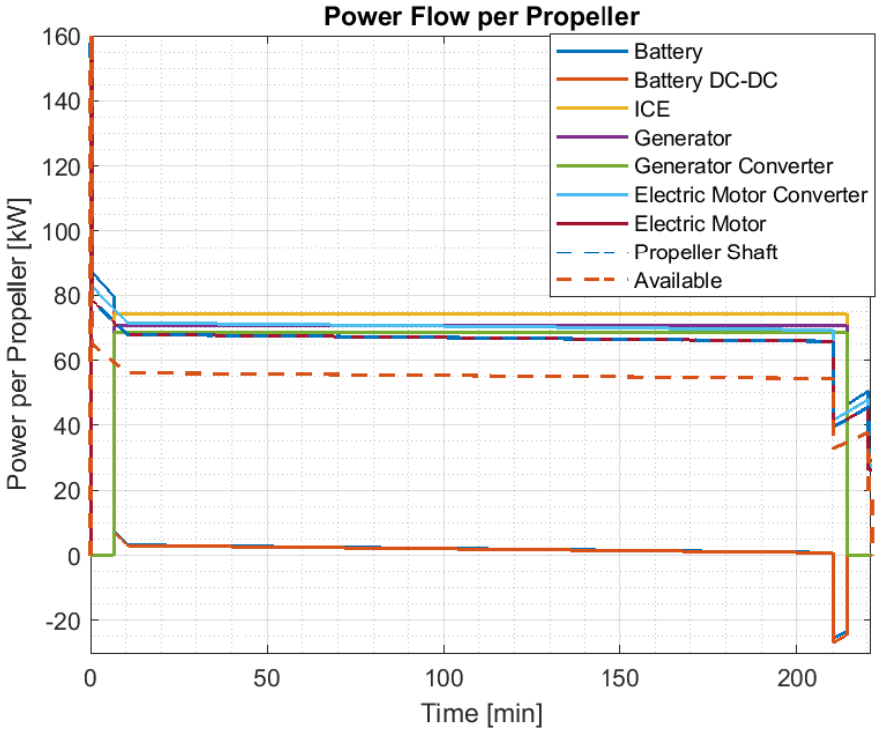


Figure 4.13: Hybris - power flow simulation

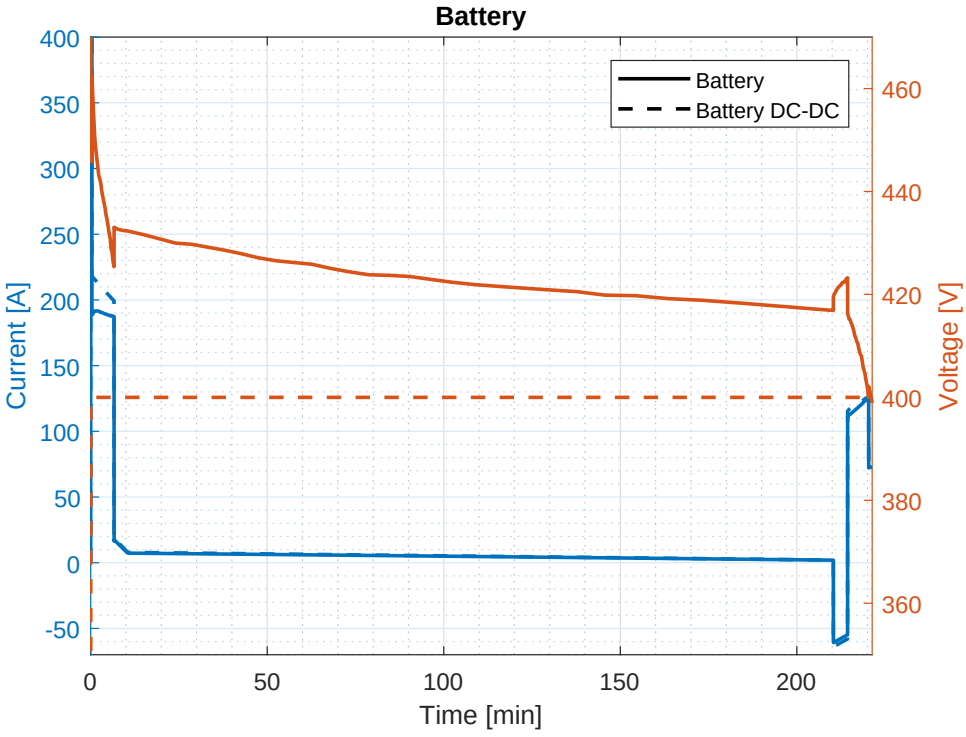


Figure 4.14: Hybris - battery pack simulation

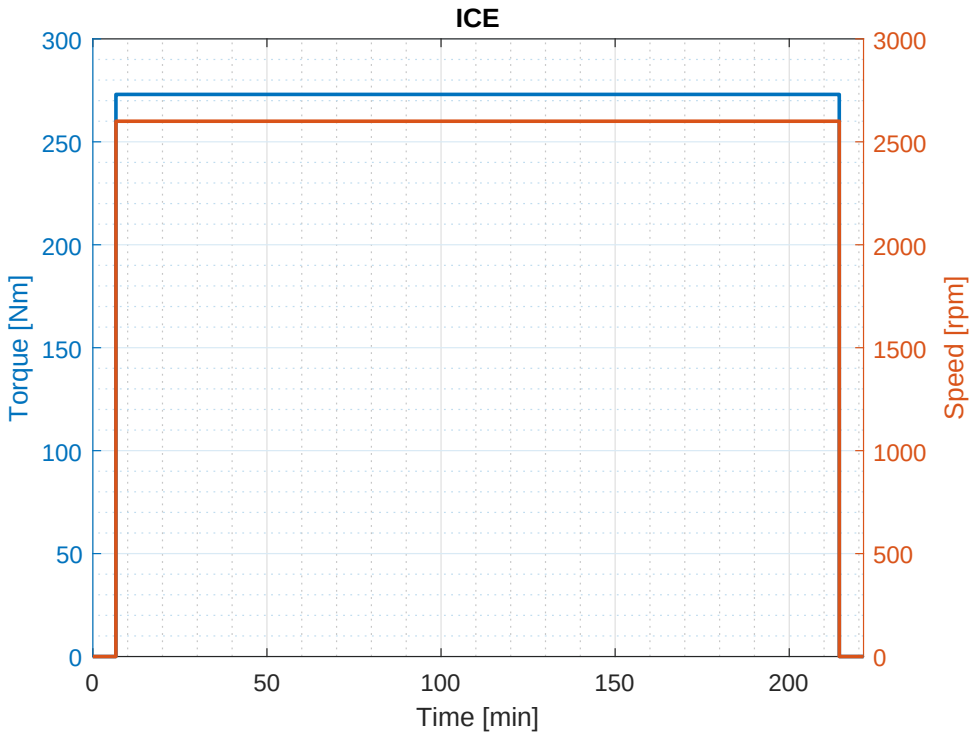


Figure 4.15: Hybris - engine simulation

case battery capacity is overestimated. More in detail, considering same conditions, 10% of battery weight, equal to 9 kilograms, can be spared. This result appears negligible, however it must be considered that weight reduction refers to standard batteries, while structural batteries, with a lower energy density, are also employed in the aircraft, leading in a possible not negligible difference in weight. Moreover, it could be of interest in case one wants to scale this result in order to consider a larger aircraft: the 10% of battery weight could not be so negligible. On the other hand, a lower altitude means more environment pollution near airfield, that is in contrast to one of hybrid-electric aircraft targets presented in Chapter 1, justifying the team choice in considering more weight to reach an higher reference altitude.

## 4.3 Parallel hybrid: Flybrid

Flybrid is a project developed to participate in "2030 regional airliner considering hybrid electric propulsion, 2011-2012 AIAA undergraduate individual aircraft design competition". The aircraft is shown in Figure 4.18. The configuration exploited by this aircraft is parallel hybrid with twin-gas turbine engines in order to have 340 knots in cruise at 25000 feet [81]. To reproduce this type of engine, since gas turbine has not been modelled, substantial changes were applied to ICE block in order to simulate it: a spark ignition engine has been used instead of gas turbine, while ICE parameters have been modified in order to provide similar results to the engine to be modelled. The scheme of the considered powertrain during simulation is presented in Figure 4.19.

Another special feature is the control logic considered in Flybrid: it is based on degree of hybridisation, discussed in Chapter 1. In particular, the project team pointed out the idea of splitting the required power from each component in a mathematical way: for example, electric motors have to provide 25% of total power. This logic requires the development of a new controller to be placed in PMCD. However, to take this difference in the system, it has

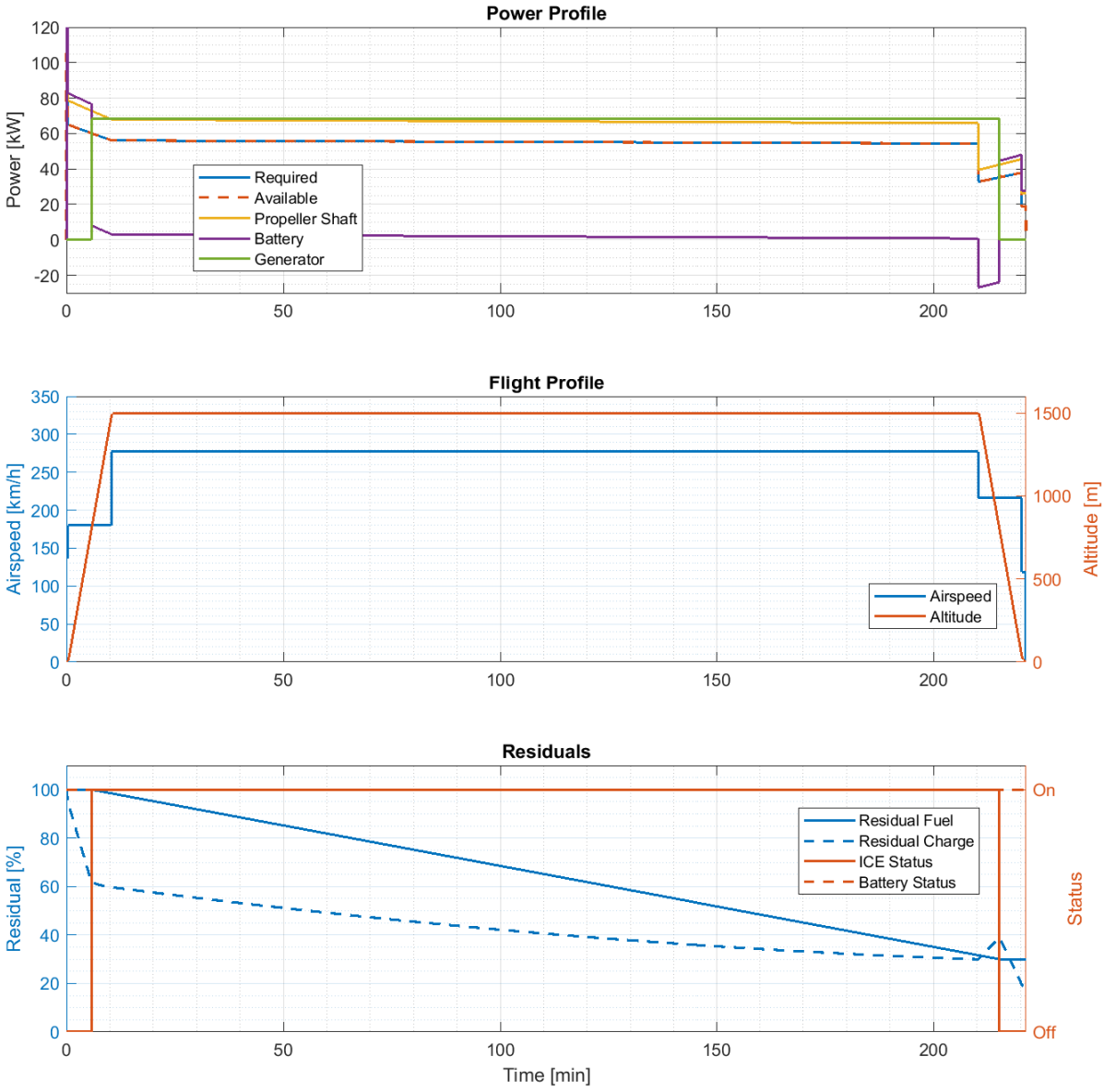


Figure 4.16: Hybris - mission profile simulation considering reference altitude set to 800 m

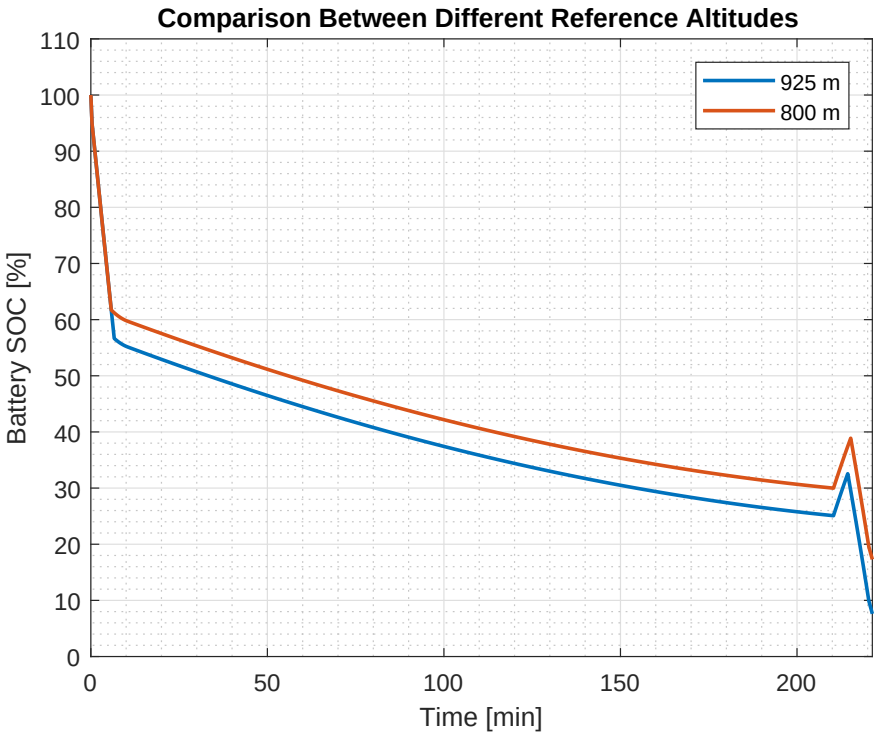


Figure 4.17: Hybris - battery SOC comparison

been slightly modified in order to cope with the already existing logic. This allows to show characteristics of battery load-levelling controller that were not evident in previous applications.

In Figure 4.20 it is presented a general view of the simulation over the aircraft mission. In this case, the status of battery and engines is defined over flight phases instead of altitude, even if the two subsystems are always operative during the simulation. Battery, shown by a purple line in the plot on the top, provides extra power, especially in the first part of the flight, until the descent starts. During descent, battery is charging because engines provide more power than the one required to fly. In this case, a difference between propeller shaft power and the sum of the powers delivered by engines and motors is present, this is due to considering gearbox efficiency. The simulation ends with 10% of residual fuel and 30% of residual charge: there is enough energy to cover loiter, that it is not considered in the simulation. Engines do not change their operative condition: this is due by the fact that battery charge during all the simulation is at an higher value than the one prescribed for changing engine functioning point, as it is possible to note in the graph on the bottom, in which battery state of charge is presented through a dashed blue line.

In parallel configuration the power flow is different from series hybrid, as shown in Figure 4.21. In this case the electric motor is fed only by batteries, while motor and engine outputs are merged in gearbox. Power losses due to transmission both in ICE and motor are simulated: power loss in gearbox related to engines is presented by the difference between solid blue line and solid red one. The same can be seen referring to motor power. More in detail, it is possible to note that when the battery is charging, the power flow comes from gearbox to battery: the power in gearbox related to electric motor, shown in dark red, is higher in modulus than the one in the electric drive, depicted in light blue. In this situation, the electric drive is acting as generator. The negative value of the power refers to absorbed power by the subsystem while the battery is charging.

In this application it is clearly visible the meaning of the term battery load-levelling: the


Figure 4.18: Flybrid, [81]

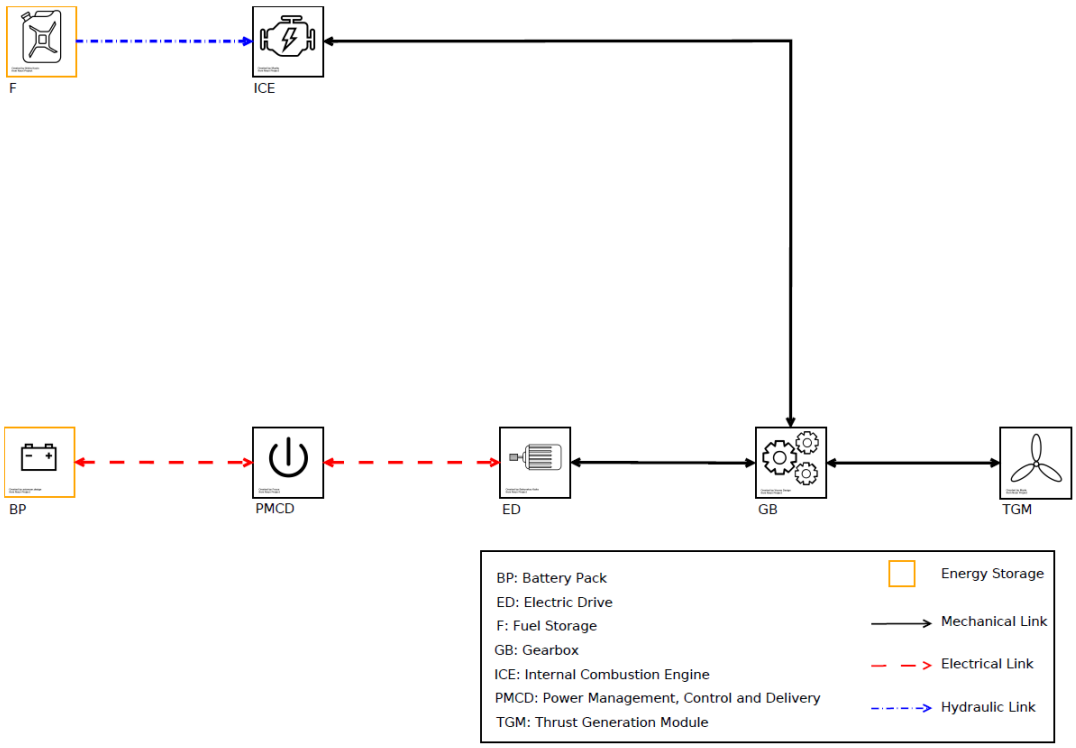


Figure 4.19: Flybrid - powertrain

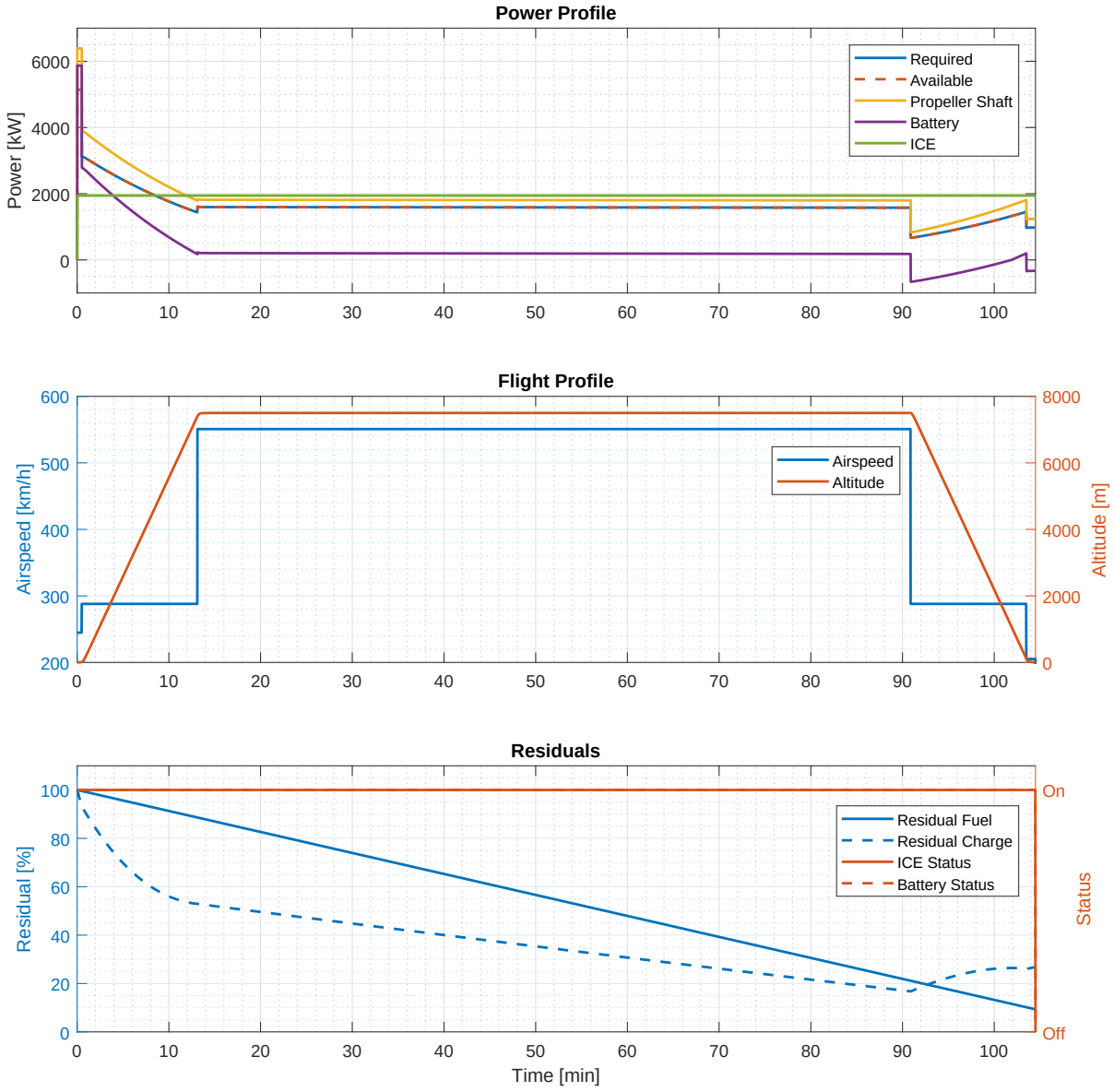


Figure 4.20: Flybrid - mission profile simulation

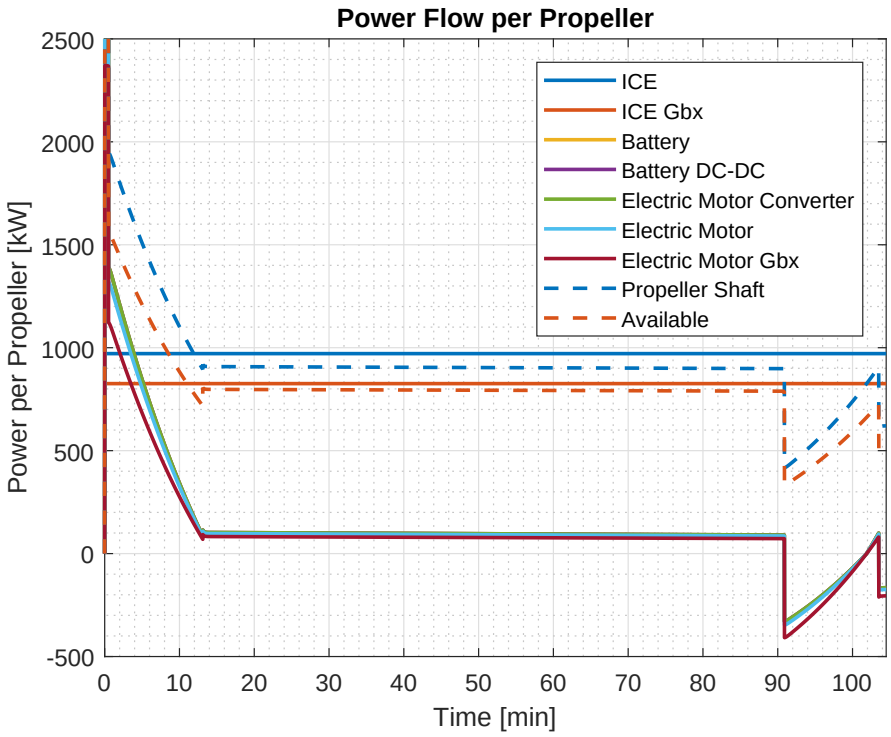


Figure 4.21: Flybrid - power flow simulation

engine is operating in a fixed condition while battery provides or absorbs extra power, depending on the configuration.

A possible demonstration of how this tool can discover design shortcomings is in considering less fuel. Results are presented in Figures 4.22, 4.23 and 4.24, in which only the final part of the flight is shown. In particular, it is possible to note that, when residual fuel is less than 5%, the value selected as fuel threshold during the configuration phase, a modification in engine operating condition is visible, as presented in Figure 4.24. More in detail, during the last part of the flight, engine works in minimum fuel flow condition, providing a very low amount of power, as depicted by blue line in Figure 4.23. Battery has to provide the remaining part of power needed to fly. However, the battery state of charge is very low and the large amount of required power drains it to zero: in the very last phases the aircraft has not enough power to sustain the flight, as shown in Figure 4.22, in which a difference between required and available power is depicted. The result is that higher capacity batteries or more fuel are needed to complete the mission.

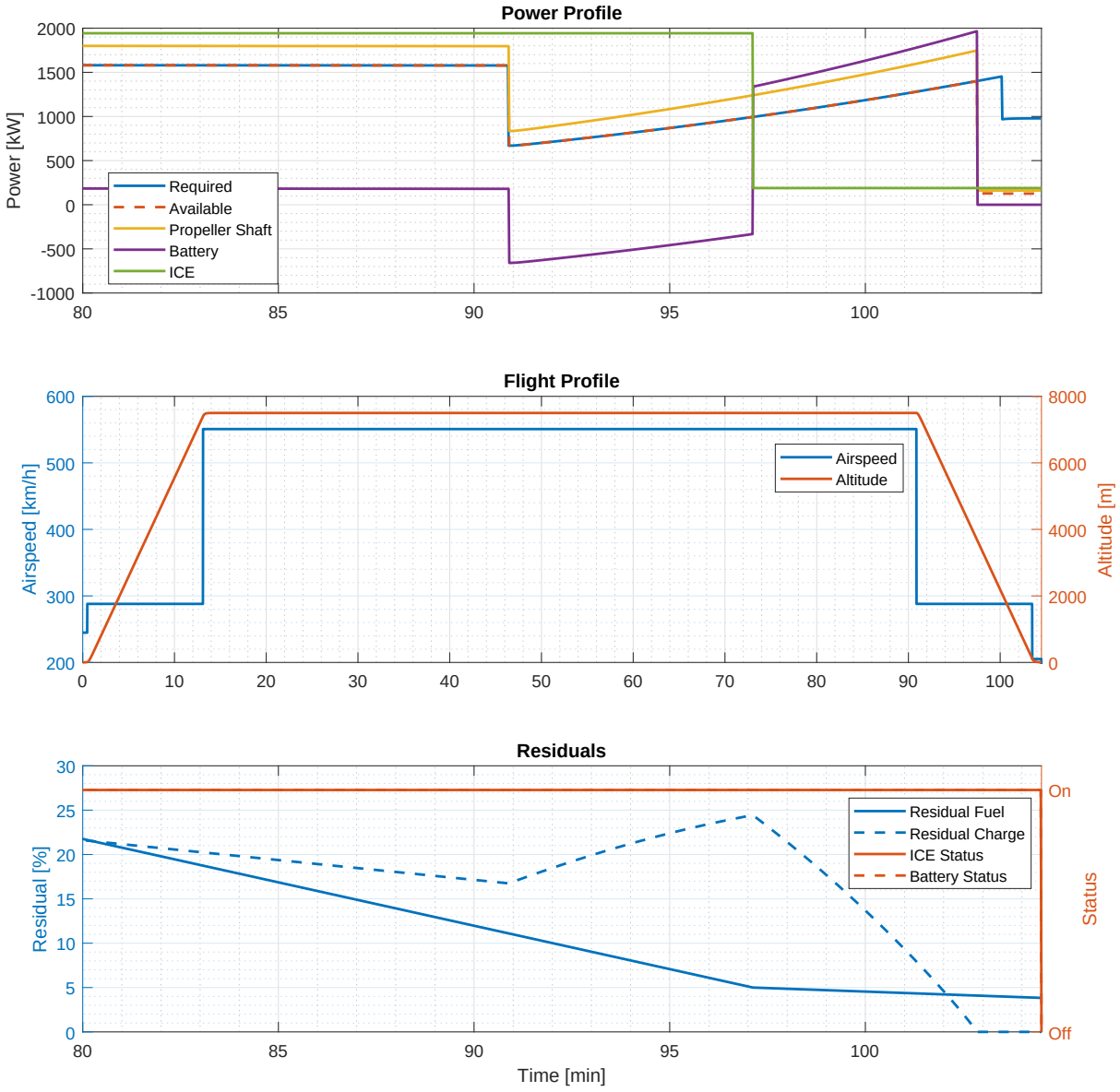


Figure 4.22: Flybrid - mission profile in case of less fuel

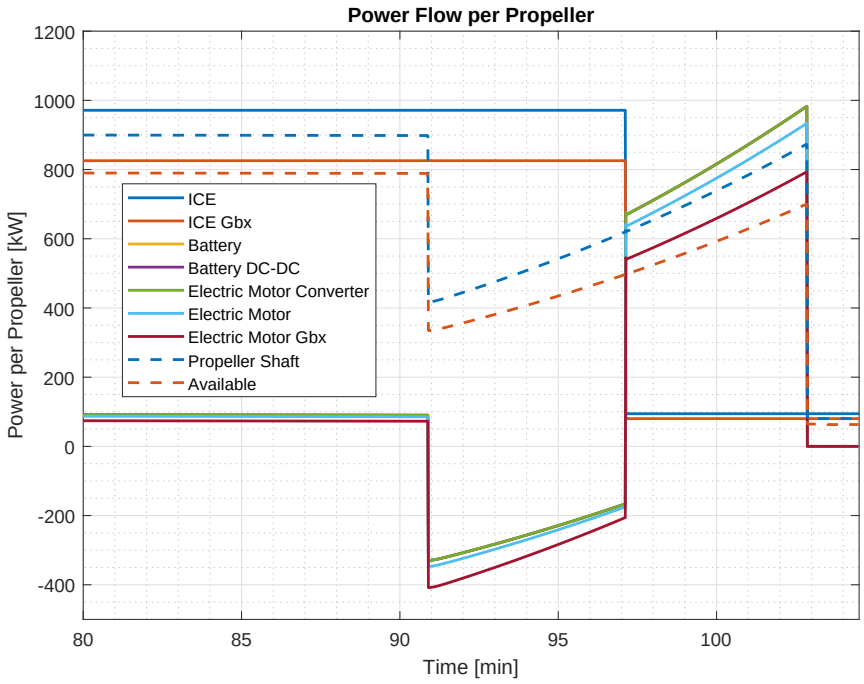


Figure 4.23: Flybrid - powerflow in case of less fuel

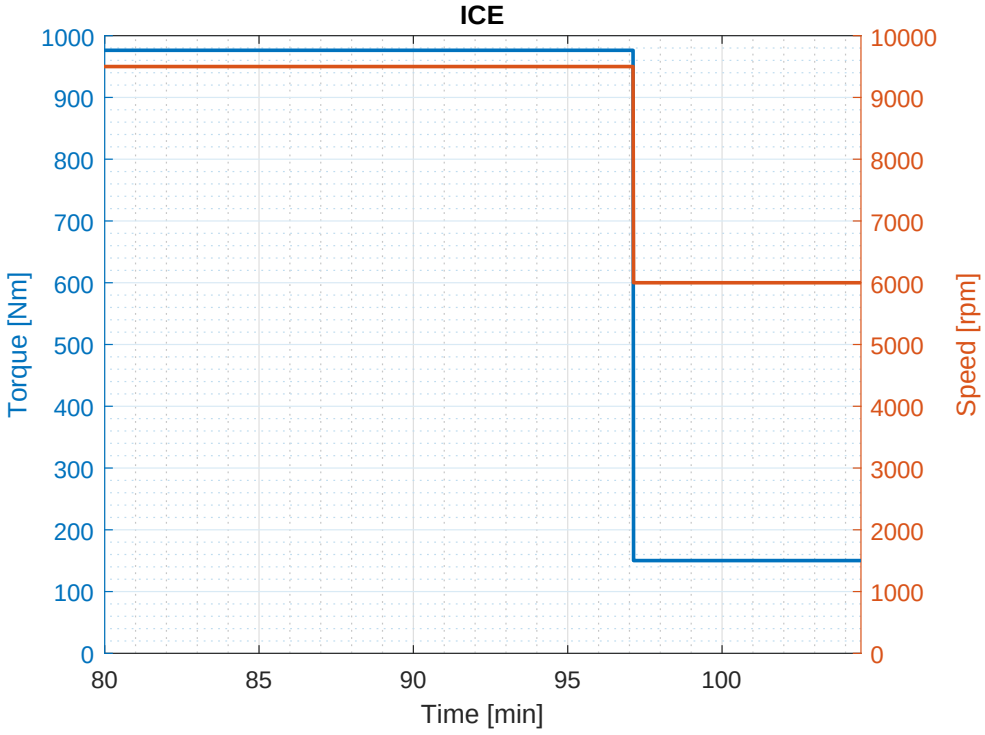


Figure 4.24: Flybrid - engine simulation in case of less fuel

# Chapter 5

# Conclusions

The aim of this work is the development of a simulator of hybrid-electric powertrains to support the design phase of aircraft types. The tool has been developed to consider different hybrid-electric powertrain configurations applicable in aeronautics: series, parallel and their variations. The possibility to deal with several powertrains allows to investigate about advantages and disadvantages of a given architecture applied to a specific aircraft and mission. The capability to take into account all architectures in one single modelling framework, without the need for the user to manually modify it every time, has been achieved thanks to a modular approach. In this way, the opportunity to modify or add new subsystems and features is provided.

Several components of the power-plant have been taken into account to simulate a complex system fed by combustion engines and batteries. Each subsystem can be modelled in different ways: some alternatives have been presented through this text and in the simulator developed in Simulink. A complete hybrid-electric aircraft powertrain can be simulated by this tool. Particular attention has been placed in simulator efficiency and flexibility, allowing to run simulations on any standard personal computer.

The possibility to exploit a parametric model for powertrain components is obtained: thanks to this feature it is possible to evaluate a generic aircraft propulsion system, independently of its configuration or size. This is of relevant importance in conceptual and preliminary aircraft design applications. For instance, the opportunity to interface the model with preliminary sizing and simulation tools related to overall aircraft parametric analyses is provided.

Considering the current historical period, in which hybrid-electric systems are experiencing a phenomenal growth, the possibility to use a tool capable of comparing different powertrain configurations of the same aircraft and different strategies to employ available sources is essential. This allows to choose the best configuration and logic controller depending on the specific application. Moreover, the opportunity to compare different parameters and see how these changes affect powertrain performance can be very important in the initial phases of aircraft design, as well as during aircraft life-cycle to select a possible upgrade.

Two different methods have been considered to retrieve reference quantities related to the flight profile in the simulation. However, only one has been used in the applications described in Chapter 4, while the other, related to the time-histories of each quantity of interest, was not exploited. This last alternative could be helpful in simulating specific test cases related, for example, to manoeuvrers or single flight phases, while the first method can be useful in considering global performance of the whole mission, as in the presented applications.

The control logic named *battery load-levelling* has been implemented in the simulator. This controller is based on the idea that combustion engines work in a specific condition, while batteries have to cover the residual required power. In this way it is possible to achieve a high engine efficiency: in optimum condition this can reach up to 30%, while, if a conventional engine

driving cycle is considered, the overall efficiency could be very low. Other ICE conditions have been considered to exploit one single controller in different situations. In particular minimum BSFC, maximum output power and minimum fuel flow have been used in some applications, while it is even possible to use arbitrary selected operating conditions. These conditions, used models and the implemented logic are strictly correlated: if one changes, in general, also the others have to be changed.

The last task of this work, related to applications, has been exploited to prove the suitability of the tool. Several model parameters have found to be very simple to modify in order to reproduce the correct behaviour of aircraft systems. An example of this can be found in the battery block, where parameters have been easily modified to obtain a correct representation of the considered battery pack. On the other hand, the modification of engine block parameters to achieve a good relationship with the system to model was a difficult task. The engine block implemented in the simulator takes into account both spark ignition and compression ignition engines. These systems are modelled through tables that correlate input quantities to outputs. Two factors occur in this situation: on one hand there is a lack of data in reports and in data-sheets that can be found in internet. This increases the difficulty in reconstructing engine maps. On the other hand, it could be possible that used models are too detailed with respect to retrieved information. However, even if a very attained to reality simulation of the considered engines has not been achieved in applications, correct trends and magnitudes have been reproduced. Another important aspect of exploited engine models is the opportunity to compute emissions. This feature can be considered fundamental since one of the purposes of hybrid-electric vehicles is in reducing environmental pollution and control strategies can be implemented basing on minimising emissions.

The developed tool, named *HEAPSim*, which stands for *Hybrid-Electric Aircraft Powertrain Simulator*, has the capability to simulate an aircraft powertrain composed by several combustion engines and batteries, regardless of which specific configuration is considered. With minimal changes, it is possible to consider different energy and power sources, such as turbine engines and fuel cells. As the architecture of the tool is clearly defined, several possibilities are left for the future continuation of this project.

## 5.1 Future developments

In the course of this work, several tasks have been completed, starting from initial studies related to hybrid-electric aircraft to the development of the simulator. This work ends with the prospect that it will be continued in the future. In these last few lines the author intends to give some suggestions about future developments, in addition to those presented in Section 2.1.

Different configurations have been taken into account during implementation. The possibility of introducing the series-parallel architecture is given, as discussed in Section 3.2.4, but was not already implemented. As already stated in Chapter 1, complex hybrid was not considered, since it is quite difficult to employ this configuration for an airplane.

It is important to note that in the proposed models no dynamic effects are considered. This choice is due to several reasons. Firstly, for a detailed description of a number of components further multi-disciplinary knowledge is needed. A great effort has been made in order to understand new subjects such as the electrical behaviour of a battery or of a solar array. For this reason, simple models have been preferred to not lose contact with the goal of the entire work, that consists in providing a tool capable of computing global performance of an aircraft powertrain. A second reason can be found in retrieving data: very detailed models are often used in specific contexts and researches, where retrieving data is not a problem thanks

to databases or experimentation. However, in the considered case, data has to be found in commercial data-sheets that are not so detailed to allow a high-fidelity simulation. Moreover, more precise models are often related to complex mathematical depictions of reality, that leads to other considerations: more complex models need higher computational time and may impact considerably on the implementation and computational methods. For what concerns the former, since simulations have to be run by normal personal computers in a reasonable amount of time, simpler models have been preferred.

Different subsystems described in Chapter 2 were not implemented in this tool. Some research has been done in order to develop a model for fuel cells and solar arrays and results were obtained. Considering solar arrays, several models can be found in literature: the suggestion is in starting from [38, 39], while for fuel cells it is possible to have a look at [3, 32]. Also, depending on the situation, it is possible to use different models than the ones proposed through this work. For instance, if it is of interest investigating about delay of each subsystem to reach a commanded output value, it is possible to refer to dynamic models. For what concerns engine block, it is possible to note the absence of the turbine engine: this is only due to time constraints. A simple turbine model can be used as well. The longer task could be in introducing the model in the control logic in order to consider three different types of engine.

Other controllers can be developed and considered in the model. In particular, the study on how different logics can control or modify the behaviour of a given system could be an interesting topic. Moreover, it is possible to compare different control logics to find the best controller for the powertrain under development or for a particular flight condition: this can be achieved also using optimisation. The opportunity to have a controller that aims at minimising emissions during each flight phase can be very interesting. Parametric controllers can also be considered, as described in Section 3.9. For instance a controller based on the degree of hybridisation, as the one employed in Flybrid [81], can be optimised to find the best amount of power coming from batteries or other systems in a particular situation or mission.

There is the possibility of introducing a flight mechanics model in the tool. In this way, it will be possible to simulate climbs at given vertical speed or turns with a defined radius. Moreover, this allows the opportunity to have trade studies depending on aircraft configuration, such as wing surface, weight, lift coefficient during cruise and so on. This could expand the area of interest of the tool: not only the propulsive system can be reproduced but also a tool capable of simulating the entire aircraft could be obtained. The opportunity to have a parametric tool capable of exploring aircraft performance could be of interest during its design phase.

A real-time simulation environment consisting of several linked software packages, based for instance on X-planes and Simulink, as presented in Introduction, could be the final goal of the tool: a complete flight simulation model could be interfaced to the powertrain simulator to provide a simulation that takes into account pilot inputs.

Finally, once some developments will be carry on, the possibility of changing the computational environment must be considered: Simulink is a very powerful tool, allowing to explore several alternatives just by drawing a line, however this impacts on computer performance. More efficient programming languages than Simulink and Matlab, such as C++, must be taken into account when looking at increasing the tool capabilities.

# Acknowledgements

I'd like to thank the Professors staff that has followed me in these last months: Prof. Carlo Riboldi, Prof. Alberto Rolando and Prof. Lorenzo Trainelli. Your support and knowledge during this project have been very precious. Also, I'll thank you for your teaching role, that I have experienced during my years in Politecnico di Milano. My gratitude goes to Eng. Francesco Salucci, that during these months has spent a lot of time alongside me, advising me in design choices and development issues.

My heartfelt thanks to my family, that allows me to experience these fantastic years. To my pets, Gastone, Oliver and Piper, that brought me good times during my studies. To Elena, who supported and borne me in these last years.

A special thanks to all my friends, particularly to Mauro: our endless discussions about aerospace and electronics were a source of inspiration for this work. Also, I'd like to thank all the fantastic people that I've met during my years in university, at work and in SOS Novate.

# Appendix A

# Script overview

The model has been developed in Simulink. Parameters needed to simulation are provided in *Workspace* thanks to several scripts that are run before simulation starts. Each script is related to a specific block or component modelled in the tool. Every script has an output *Struct* that contains variables related to the considered model. A brief description of scripts, developed in Matlab, can be found in the following.

## A.1 Settings_Configuration.m

In this script, all the variables related to aircraft configuration and subsystems considered during simulation are defined. Variables are clustered into a *Struct* named `Settings`. In particular, the variable `Settings.Arch`, that it is set to zero if a parallel powertrain have to be considered or it is equal to one if a serial hybrid is modelled, controls all *Variant Subsystems* that depends on power-plant architecture. Other variables are used to switch on or off, depending if they are equal to one or zero, components in the powertrain. More in detail, `Engine` selects which type of ICE is used during simulation.

Other general quantities are defined within this script such as the voltage of electric system or standard air properties.

## A.2 Settings_Battery.m

Here, quantities related to battery block are defined. More precisely, variables used by *Datasheet Battery* discussed in Section 3.1 and in [52] , presented in Figure A.1, are set depending on the battery used in the aircraft. Parameters related to logic controller that define battery thresholds during charge and discharge, such as `Battery.SOC_H` and `Battery.SOC_L`, are here defined. The output of the script is a *Struct* named `Battery` that contains all the variables of interest.

## A.3 Settings_DCDC.m

Variables related to DC-DC converter placed between battery and electric system are declared in this script. Referring to Figure A.2, all the parameter of interest are defined to model this component. In particular, converter efficiency is set both considering an overall single value and a two dimensional map depending on input voltage and current. Differently from the rest of the tool, the selection of the used model is set directly in the mask.The *Struct* generated by this script is named `DCDC`.

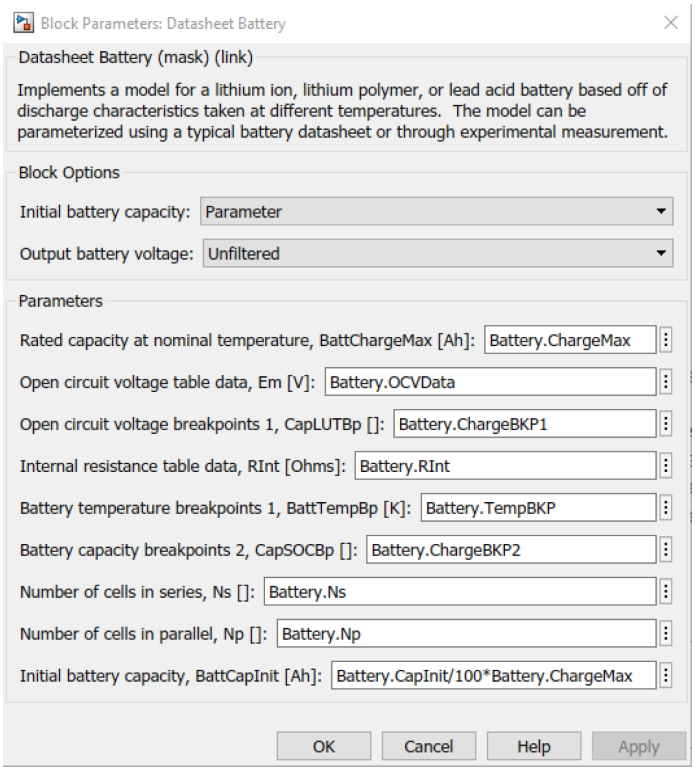


Figure A.1: Datasheet Battery mask

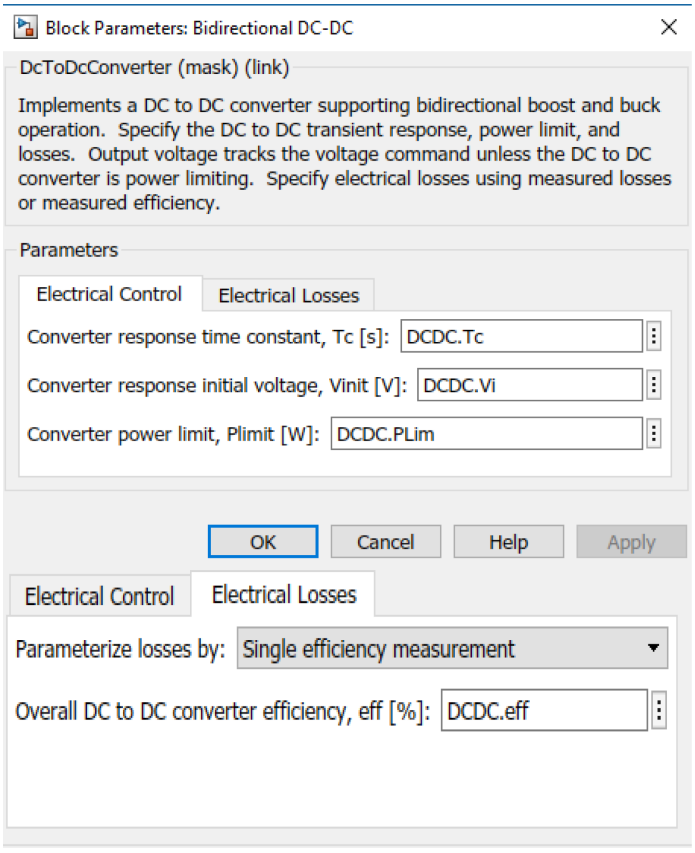


Figure A.2: DC-DC converter mask

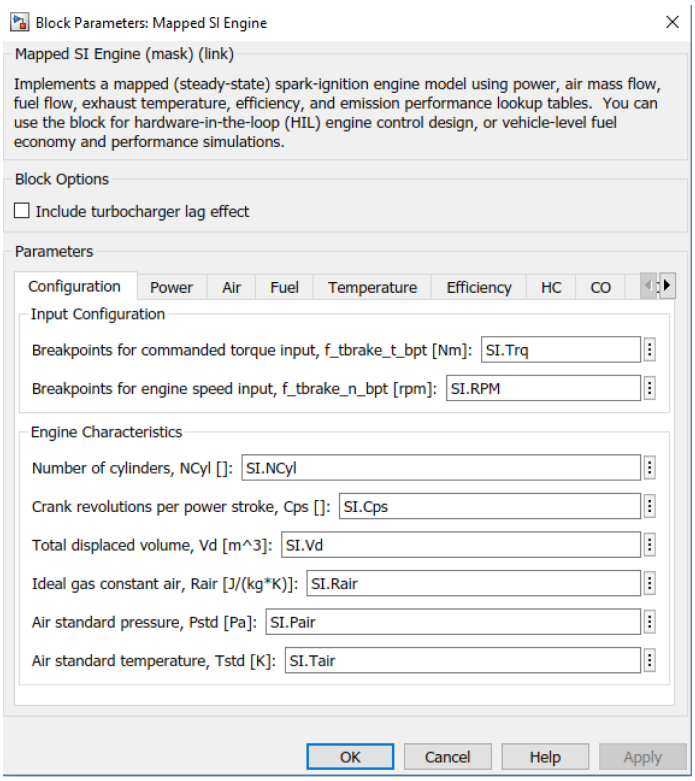


Figure A.3: Mapped SI engine mask

## A.4 Settings_SIEngine.m

Parameters related to spark ignition engine are defined in this script. All of them are collected in `SI` *Struct*. In particular, engine parameters, like those presented in Figure A.3, and two dimensional maps related to engine performance are set depending on the engine to model. Spark ignition block, based on [60], has as input commanded torque and speed, and so maps are defined on these variables.

Of particular interest are maps related to fuel flow, BSFC and emissions: a control logic that aims at minimising these values can be developed, such as the one described in Section 3.9 and exploited in Section 4. Engine operative conditions of interest can be found in engine maps thanks to Matlab functions that aims to minimise or maximise a specific value. Functions are developed inside this script.

## A.5 Settings_CIEngine.m

In the same fashion as SI engine script, variables related to compression ignition engine are defined in this script. The main difference, as it is possible to note in Figure A.4, is that CI engine inputs are commanded speed and fuel mass per injection [61]. Variables are defined in `CI` *Struct*.

## A.6 Settings_ICE.m

All the variables related to engine but that are independent by the type of ICE used in the simulation are set in this script. For instance, the fuel tank capacity is defined by `ICE.FuelTankCapacity`, while the starting fuel mass is set trough a percentage stored in

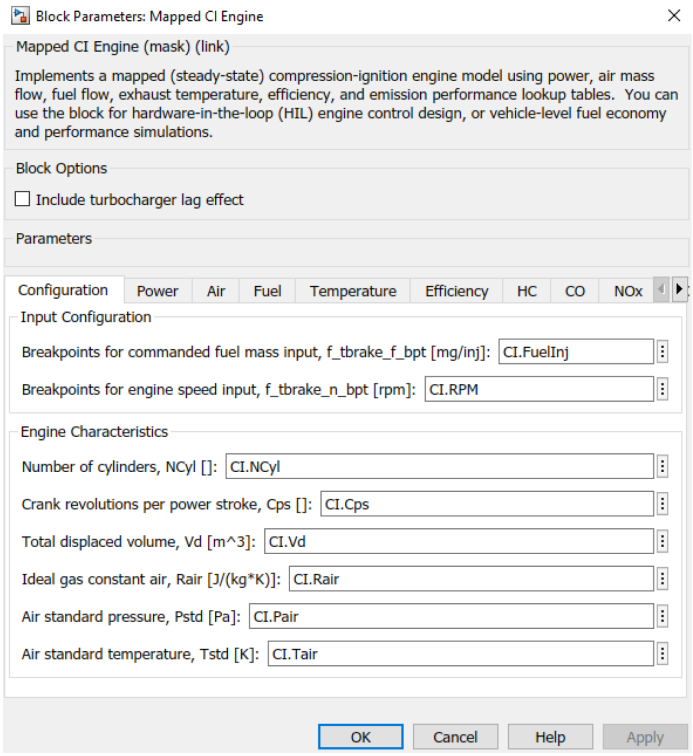


Figure A.4: Mapped CI engine mask

`ICE.FuelStart`. In this way, different fuel starting values can be explored during simulations. Moreover, `ICE.FuelLow` defines the lower fuel threshold considered in Section 3.10.2.

In this script are also defined variables related to *Variant Subsystem* altitude correction block, presented in Section 3.2.3.

## A.7 Settings_ElectricDriveM.m

Motoring electric drive has been defined as a *Variant Subsystem* that is controlled by a variable set in `Settings_ElectricDriveM.m`. In particular if the variable is equal to zero, ED parameters are defined as constant values, while if it is equal to one efficiency and output speed are defined through lookup tables that depends on input current. The generic converter efficiency is defined in this script. Variables are stored in a *Struct* named `EDM`.

## A.8 Settings_ElectricDriveG.m

The variables definition of this script is similar to the one related to electric motor. The only difference consists in the definition of the map related to efficiency: it is a two dimensional map that given in input power and speed coming from engine it provides the efficiency of the component. This allows to compute the generator output electric power. Variables are defined thanks to a *Struct* named `EDG`.

## A.9 Settings_Gearbox.m

Gearbox block is composed by three nested *Variant Subsystems*. The first one is related to powertrain configuration, the second refers to direct drive in case of serial hybrid, while the

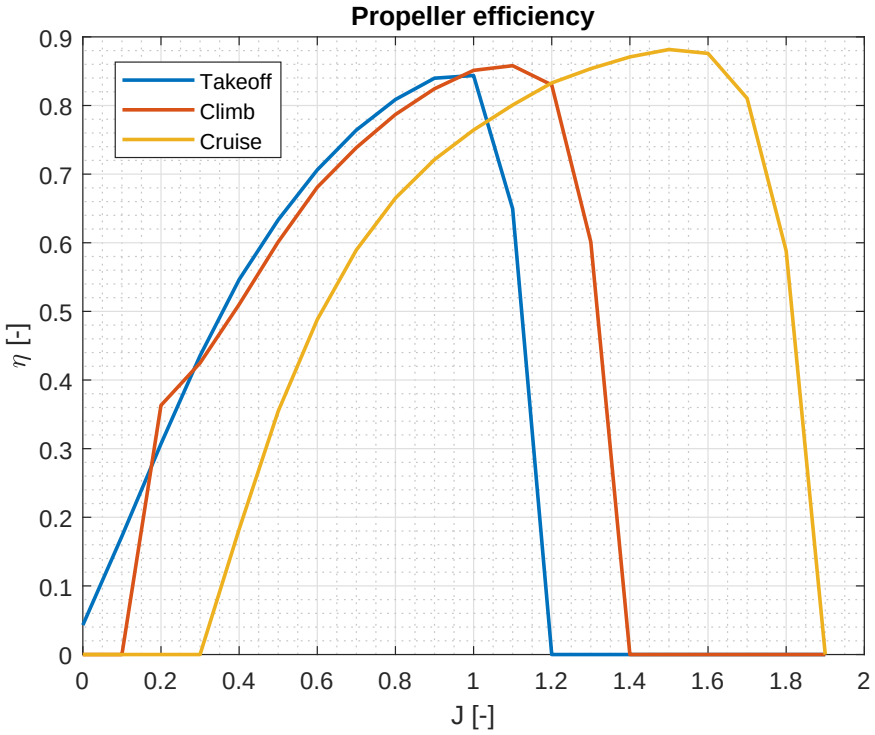


Figure A.5: Propeller efficiency map

latter specifies which model is used to describe power losses: both single value and mapped efficiency, depending on input torque and speed, are considered in the simulator. All the parameters of interest are defined in this script and values are contained in `Gbx` *Struct*.

## A.10 Settings_Propeller.m

All variables related to propeller are defined in this script. In particular, both propeller diameter and the map that correlates efficiency to propeller advance ratio and blade pitch, as shown in Figure A.5, are contained in the *Struct* named `Prop`. The broken line trend of efficiency does not lead to a loss of accuracy since an interpolation is provided by *Lookup Table* block in the Simulink model.

## A.11 Settings_Aircraft.m

Parameters that are related to aircraft such as number of propellers and number of engines are defined in `Settings_Aircraft.m` script through `AC` *Struct*. It is important to remark that in case of parallel configuration the number of ICE must be equal to the number of propeller. In a serial hybrid, the possibility of using more than one engine is allowed.

## A.12 Settings_FlightProfile.m

Variables related to *Variant Subsystems* contained in CPT block are defined in the considered script. So, it is possible to select which type of flight profile quantities input method is used in the simulation and which strategy is considered in defining the status of the components during flight.

```
%% Flight Profile Specs & Settings
%

FlightProfile=1; % 1: Math Profile, 0: Data Profile
FlightProfile_Math=Simulink.Variant('FlightProfile==1'); % Mathematical data used
FlightProfile_Data=Simulink.Variant('FlightProfile==0'); % Simulated data used

AltitudeStatus=0;
FlightProfile_Altitude=Simulink.Variant('AltitudeStatus==1'); % ICE and Batt status based on altitude
FlightProfile_FlightPhase=Simulink.Variant('AltitudeStatus==0'); % ICE and Batt status based on flight phase

%% Math Profile
if FlightProfile==1
    FP.TakeoffPwr=361500; % Power during takeoff [W] (at sea level)
    FP.ClimbPwr=231200; % Power during climb [W]
    FP.CruisePwr=373270; % Power during cruise [W]
    FP.DescentPwr=231200; % Power during descent [W]
    FP.LandPwr=30000; % Power during landing [W]
    FP.MaxPwr=FP.TakeoffPwr; % Max power during flight [W]

    FP.TakeoffSpd=38; % Speed during takeoff [m/s] (TAS)
    FP.ClimbSpd=77; % Speed during climb [m/s]
    FP.CruiseSpd=110; % Speed during cruise [m/s]
    FP.DescentSpd=77; % Speed during descent [m/s]
    FP.LandSpd=40; % Speed during landing [m/s]

    FP.TakeoffH=0; % Takeoff starting height [m]
    FP.ClimbHStart=15; % Climb starting height [m]
    FP.ClimbHFin=2438; % Climb final height [m]

    FP.TakeoffPropSpd=2000; % Propeller speed during takeoff [rpm]
    FP.ClimbPropSpd=2000; % Propeller speed during climb [rpm]
    FP.CruisePropSpd=2000; % Propeller speed during cruise [rpm]
    FP.DescentPropSpd=2000; % Propeller speed during descent [rpm]
    FP.LandPropSpd=2000; % Propeller speed during landing [rpm]

    FP.TakeoffPropPitch=1; % Propeller pitch during takeoff [-]
    FP.ClimbPropPitch=2; % Propeller pitch during climb [-]
    FP.CruisePropPitch=3; % Propeller pitch during cruise [-]
    FP.DescentPropPitch=2; % Propeller pitch during descent [-]
    FP.LandPropPitch=1; % Propeller pitch during landing [-]
```

Figure A.6: Example of `Settings_FlightProfile.m`

Depending on the method used, required power, flight speed, cruise altitude, components status and so on are defined in the script and collected in the variable `FP`. Matlab script appears in the form of the one presented in Figure A.6.

# Bibliography


[1] Friedrich, C., & Robertson, P. A. (2014). Design of hybrid-electric propulsion systems for light aircraft. In 14th AIAA aviation technology, integration, and operations conference (p. 3008).

[2] Cipolla, V., & Oliviero, F. (2016). *HyPSim: A Simulation Tool for Hybrid Aircraft Performance Analysis*. In Variational Analysis and Aerospace Engineering (pp. 95-116). Springer, Cham.

[3] Lee, B., Park, P., Kim, C., Yang, S., & Ahn, S. (2012). Power managements of a hybrid electric propulsion system for UAVs. Journal of mechanical science and technology, 26(8), 2291-2299.

[4] Zou, Y., Shi-jie, H., Dong-ge, L., Wei, G., & Hu, X. S. (2013). Optimal energy control strategy design for a hybrid electric vehicle. Discrete Dynamics in Nature and Society, 2013.

[5] Grammatico, S., Balluchi, A., & Cosoli, E. (2010, September). A series-parallel hybrid electric powertrain for industrial vehicles. In Vehicle Power and Propulsion Conference (VPPC), 2010 IEEE (pp. 1-6). IEEE.

[6] Mathworks. Explore the Hybrid Electric Vehicle Multimode Reference Application, `https://it.mathworks.com/help/releases/R2017b/autoblks/ug/explore-the-hybrid-electric-vehicle-multimode-reference-application.html`, March 2018

[7] Riboldi, C. E., Gualdoni, F., & Trainelli, L. (2018). Preliminary weight sizing of light pure-electric and hybrid-electric aircraft. Transportation Research Procedia, 29, 376-389.

[8] Annual energy outlook 2018, with projections to 2050. US Energy Information Administration, Washington, DC.

[9] Friedrich, C., & Robertson, P. A. (2014). Hybrid-electric propulsion for aircraft. Journal of Aircraft, 52(1), 176-189.

[10] Chau, K. T., & Wong, Y. S. (2002). *Overview of power management in hybrid electric vehicles.* Energy conversion and management, 43(15), 1953-1968.

[11] Cohen, J. P., & Coughlin, C. C. (2008). Spatial hedonic models of airport noise, proximity, and housing prices. Journal of Regional Science, 48(5), 859-878.

[12] Miljković, D., Ivošević, J., & Bucak, T. (2013, January). Psycho-acoustical Ergonomics in a light Aircraft Interior. In 5th International Ergonomics Conference" Ergonomics 2013".

[13] Morrell, P., & Lu, C. H. Y. (2000). Aircraft noise social cost and charge mechanisms–a case study of Amsterdam Airport Schiphol. Transportation Research Part D: Transport and Environment, 5(4), 305-320.

[14] NASA. Long-Term Warming Trend Continued in 2017: NASA, NOAA `https://www.giss.nasa.gov/research/news/20180118/`, March 2018.

[15] Kallas, S., Geoghegan-Quinn, M., Darecki, M., Edelstenne, C., Enders, T., Fernandez, E., & Hartman, P. (2011). Flightpath 2050 Europe's Vision for Aviation. Report of the High Level Group on Aviation Research, European Commission, Brussels, Belgium, Report No. EUR, 98.

[16] Ashcraft, S. W., Padron, A. S., Pascioni, K. A., Stout Jr, G. W., & Huff, D. L. (2011). Review of propulsion technologies for N+ 3 subsonic vehicle concepts. Glenn Research Center, Cleveland, Ohio

[17] Lorenz, L., Seitz, A., Kuhn, H., & Sizmann, A. (2014). *Hybrid power trains for future mobility*. Deutsche Gesellschaft für Luft-und Raumfahrt-Lilienthal-Oberth eV.

[18] Emadi, A., Lee, Y. J., & Rajashekara, K. (2008). *Power electronics and motor drives in electric, hybrid electric, and plug-in hybrid electric vehicles*. IEEE Transactions on industrial electronics, 55(6), 2237-2245.

[19] Rosero, J. A., Ortega, J. A., Aldabas, E., & Romeral, L. A. R. L. (2007). Moving towards a more electric aircraft. IEEE Aerospace and Electronic Systems Magazine, 22(3), 3-9.

[20] Pipistrel. First Pipistrel's Alpha Electro took flight in Australia, `http://www.pipistrel.si/news/first-pipistrels-alpha-electro-took-flight-in-australia`, March 2018

[21] Wikipedia. Tesla Model S Battery, `http://enipedia.tudelft.nl/wiki/Tesla_Model_S_Battery`, March 2018

[22] Wall, T. J., & Meyer, R. (2017). *A Survey of Hybrid Electric Propulsion for Aircraft*. In 53rd AIAA/SAE/ASEE Joint Propulsion Conference (p. 4700).

[23] Harmon, F. G., Frank, A. A., & Chattot, J. J. (2006). Conceptual design and simulation of a small hybrid-electric unmanned aerial vehicle. Journal of Aircraft, 43(5), 1490-1498.

[24] Mi, C., & Masrur, M. A. (2017). Hybrid electric vehicles: principles and applications with practical perspectives. John Wiley & Sons.

[25] Koster, J., Velazco, A., Munz, C. D., Kraemer, E., Wang, K. C., & Verstraete, D. (2012). HYPERION UAV: an international collaboration. In 50th AIAA Aerospace Sciences Meeting Including the New Horizons Forum and Aerospace Exposition (p. 1223).

[26] Glassock, R., Hung, J. Y., Gonzalez, L. F., & Walker, R. A. (2008). Design, modelling and measurement of a hybrid powerplant for unmanned aerial systems. Australian Journal of Mechanical Engineering, 6(2), 69-78.

[27] Ausserer, J., & Harmon, F. (2012, July). Integration, Validation, and Testing of a Hybrid-Electric Propulsion System for a Small Remotely Piloted Aircraft. In 10th International Energy Conversion Engineering Conference (p. 4239).

[28] Diamond Aircraft. Diamond Aircraft proudly presents the world's first serial hybrid electric aircraft "DA36 E-Star", http://www.diamond-air.at/en/media-center/press-releases/news/article/diamond-aircraft-proudly-presents-the-worlds-first-serial-hybrid-electric-aircraft-da36-e-star/. March 2018

[29] Rolls Royce. Rolls-Royce works with EADS on advanced hybrid distributed propulsion concept for future airliners, https://www.rolls-royce.com/media/press-releases/yr-2013/18062013-works-with-eads.aspx. March 2018

[30] Wikipedia. Airbus E-Fan, https://en.wikipedia.org/wiki/Airbus_E-Fan. March 2018

[31] Airbus. Airbus, Rolls-Royce, and Siemens team up for electric future Partnership launches E-Fan X hybrid-electric flight demonstrator, http://www.airbus.com/newsroom/press-releases/en/2017/11/airbus--rolls-royce--and-siemens-team-up-for-electric-future-par.html. March 2018

[32] Bradley, T. H., Moffitt, B. A., Mavris, D. N., & Parekh, D. E. (2007). Development and experimental characterization of a fuel cell powered aircraft. Journal of Power sources, 171(2), 793-801.

[33] Zunum Aerospace, zunum.aero. March 2018

[34] Pipistrel, http://www.pipistrel.si. March 2018

[35] MAHEPA, https://mahepa.eu/the-project/. March 2018

[36] Corriere della sera. L'aerotaxi del Politecnico di Milano che ha conquistato New York, http://www.corriere.it/tecnologia/cyber-cultura/15_novembre_22/aerotaxi-politecnico-milano-che-ha-conquistato-new-york-839af3f6-9138-11e5-bbc6-e0fb630b6ac3.shtml. March 2018

[37] Politecnico di Milano. Politecnico flies high thanks to the team Hybris, https://www.polimi.it/nc/en/storie-polimi/il-politecnico-vola-in-alto-grazie-al-team-hybris/. March 2018

[38] De Soto, W., Klein, S. A., & Beckman, W. A. (2006). Improvement and validation of a model for photovoltaic array performance. Solar energy, 80(1), 78-88.

[39] Brano, V. L., Orioli, A., Ciulla, G., & Di Gangi, A. (2010). An improved five-parameter model for photovoltaic modules. Solar Energy Materials and Solar Cells, 94(8), 1358-1370.

[40] Pornet, C., & Isikveren, A. T. (2015). *Conceptual design of hybrid-electric transport aircraft*. Progress in Aerospace Sciences, 79, 114-135.

[41] Paolo Romagnolli (2017), *DLR-HY4 Flight Test Campaign*. In 28th Society of Flight Test Engineers, 2017.

[42] Mathworks. Bus Selector, https://it.mathworks.com/help/simulink/slref/busselector.html. February 2018.

[43] Mathworks. Enabled Subsystems, https://it.mathworks.com/help/simulink/ug/enabled-subsystems.html. February 2018.

[44] Mathworks. Struct, https://it.mathworks.com/help/matlab/ref/struct.html?s_tid=doc_ta. February 2018.

[45] Tremblay, O., & Dessaint, L. A. (2009). *Experimental validation of a battery dynamic model for EV applications*. World Electric Vehicle Journal, 3(1), 1-10.

[46] Dürr, M., Cruden, A., Gair, S., & McDonald, J. R. (2006). *Dynamic model of a lead acid battery for use in a domestic fuel cell system*. Journal of power sources, 161(2), 1400-1411.

[47] Kuhn, E., Forgez, C., Lagonotte, P., & Friedrich, G. (2006). *Modelling Ni-mH battery using Cauer and Foster structures*. Journal of power sources, 158(2), 1490-1497.

[48] Tremblay, O., Dessaint, L. A., & Dekkiche, A. I. (2007, September). *A generic battery model for the dynamic simulation of hybrid electric vehicles*. In Vehicle Power and Propulsion Conference, 2007. VPPC 2007. IEEE (pp. 284-289). Ieee.

[49] Mathworks. Powertrain Blockset, https://it.mathworks.com/products/powertrain.html. February 2018.

[50] Mathworks. Algebraic Loops, https://it.mathworks.com/help/simulink/ug/algebraic-loops.html#bsn4zj6. February 2018.

[51] Mathworks. Unit Delay, https://it.mathworks.com/help/simulink/slref/unitdelay.html?s_tid=doc_ta. February 2018.

[52] Mathworks. Datasheet Battery, https://it.mathworks.com/help/autoblks/ref/datasheetbattery.html. February 2018.

[53] Vratny, P. C., Gologan, C., Pornet, C., Isikveren, A. T., & Hornung, M. (2013, September). *Battery pack modeling methods for universally-electric aircraft*. In 4th CEAS Air & Space Conference (pp. 525-535). Linköping, Sweden: Linköping Univ. Electronic Press.

[54] Mathworks. Bidirectional DC-DC, https://it.mathworks.com/help/autoblks/ref/bidirectionaldcdc.html. February 2018.

[55] Mathworks. Variant Subsystems https://it.mathworks.com/help/simulink/slref/variantsubsystem.html. March 2018.

[56] Burlamaqui Filho, F. D. A. C., Góes, L. C. S., Oliveira, A. B. V., Bosa, R. W., & Fernandes, G. S. (2012). *Dynamic modeling nonlinear and control system for a turboshaft*. In 12th Pan-American Congress of Applied Mechanics.

[57] Cappuccilli, M. (2012). *Modellazione e implementazione numerica di un motore a turbina per elicottero*.

[58] Ailer, P., Santa, I., Szederkényi, G., & Hangos, K. M. (2001). *Nonlinear model-building of a low-power gas turbine*. Periodica Polytechnica. Transportation Engineering, 29(1-2), 117.

[59] Jiao, Y. K., Kou, K. H., & Chen, Y. (2016, August). *Modeling and simulation for piston engine towards flight simulator (IEEE CGNCC)*. In Guidance, Navigation and Control Conference (CGNCC), 2016 IEEE Chinese (pp. 238-240). IEEE.

[60] Mathworks. Mapped SI Engine, `https://it.mathworks.com/help/autoblks/ref/mappedsiengine.html`. March 2018.

[61] Mathworks. Mapped CI Engine, `https://it.mathworks.com/help/autoblks/ref/mappedciengine.html`. March 2018.

[62] Mathworks. Bus Creator, `https://it.mathworks.com/help/simulink/slref/buscreator.html`. March 2018.

[63] Galfetti L. *Notes of aerospace propulsion course*. Politecnico di Milano

[64] Pillay, P., & Krishnan, R. (1989). Modeling, simulation, and analysis of permanent-magnet motor drives. II. The brushless DC motor drive. IEEE transactions on Industry applications, 25(2), 274-279.

[65] Masarati P. *Dinamica dei Sistemi Aerospaziali*. Politecnico di Milano

[66] Pillay, P., & Krishnan, R. (1988). *Modeling of permanent magnet motor drives*. IEEE Transactions on industrial electronics, 35(4), 537-541.

[67] Conte, G. (2009). *Corso di elettrotecnica e macchine elettriche*. Hoepli.

[68] Gohardani, A. S., Doulgeris, G., & Singh, R. (2011). *Challenges of future aircraft propulsion: A review of distributed propulsion technology and its potential application for the all electric commercial aircraft*. Progress in Aerospace Sciences, 47(5), 369-391.

[69] Gokul, R., & Baliga, R. (2012). *Continuously Variable Transmission*. NMAM Institute of Technology.

[70] Mathworks. Gear box, `https://it.mathworks.com/help/physmod/simscape/ref/gearbox.html`. March 2018.

[71] Mathworks. From Workspace, `https://it.mathworks.com/help/simulink/slref/fromworkspace.html`. March 2018.

[72] Mathworks. Sigmf, `https://it.mathworks.com/help/fuzzy/sigmf.html`, March 2018.

[73] Mathworks. ISA Atmosphere Model, `https://it.mathworks.com/help/aeroblks/isaatmospheremodel.html`. March 2018.

[74] Salmasi, F. R. (2007). Control strategies for hybrid electric vehicles: Evolution, classification, comparison, and future trends. IEEE Transactions on vehicular technology, 56(5), 2393-2404.

[75] Sciarretta, A., & Guzzella, L. (2007). Control of hybrid electric vehicles. IEEE Control systems, 27(2), 60-70.

[76] Mathwork. PID Controller, Discrete PID Controller, `https://it.mathworks.com/help/simulink/slref/pidcontroller.html`. March 2018.

[77] Mathworks. If, `https://it.mathworks.com/help/simulink/slref/if.html`. March 2018.

[78] Arditi, M., D'ascenzo, A., Montorfano, G., Poiana, G., Rossi, N., Spada, C., & Sesso, M., (2017), Project A: Progetto di velivoli A.A. 2016-2017. Course report.

[79] Bernasconi, A., Capoferri, L., Riboldi, C. E., & Trainelli, L. (2017). Hybris–An Innovative Concept for Future General Aviation. In 13th Pegasus-AIAA Student Conference (pp. 1-11).

[80] Bernasconi, A., Biondani, F., Capoferri, L., Favier, A., & Velarde, C. (2016). Hybris: Progetto di velivoli A.A. 2015-2016. Course report.

[81] Bosque, R. A., Bona, G. E., Bucari, M., Castagnoli, A., & Casado, A. G. (2013). Flybrid, the next step for a greener aviation. Course report.